IMPROVED DELAMINATION RESISTANCE OF THIN-PLY BASED LAMINATES: AN EXPERIMENTAL AND NUMERICAL STUDY

Gerard Guillamet Busquets

Universitat de Girona

Doctoral Thesis

IMPROVED DELAMINATION RESISTANCE OF THIN-PLY BASED LAMINATES: AN EXPERIMENTAL AND NUMERICAL STUDY

by
Gerard Guillamet Busquets

2016

Universitat de Girona

Doctoral Thesis

IMPROVED DELAMINATION RESISTANCE OF THIN-PLY BASED LAMINATES: AN EXPERIMENTAL AND NUMERICAL STUDY

by
Gerard Guillamet Busquets

2016

Doctoral Programme in Technology

supervised by
Dr. Albert Turon Travesa and Dr. Josep Costa Balanzat

Thesis submitted to the University of Girona for the degree of Doctor of Philosophy

Preface and Acknowledgements

The work presented in this thesis was conducted under the auspices of the AMADE research group (Dept. of Mechanical Engineering and Industrial Construction at University of Girona). The thesis was carried out under the pre-doctoral grant nº 2013FI_B 01062 with the support of *Generalitat de Catalunya*. The activity was partially funded by the Spanish government through the contracts DPI2012-34465 and MAT2012-37552-C03-03; and by Airbus under the project 2^{nd} generation of Composites (2genComp). Additionally, part of the research presented in this thesis was developed during a research stay at Aalborg University (Denmark) funded by the University of Girona through the grant MOB2015.

First of all, I would like to thank my advisors, Albert Turon and Josep Costa, for their competent supervision and their infinite patience. They were always there to support and guide me during all stages of my Ph.D. I have to really appreciate their input and contribution to the many useful discussions we had, all of which have helped to enrich the content of this thesis. During my Ph.D. I visited Esben Lindgaard and Brian Bak at Aalborg University in Denmark for almost four months. I learned a lot from them and we had many good discussions on numerical modeling of composite laminates.

My deepest gratitude goes to my family for their unflagging love and support throughout my life, they were always there to support me.

Last but not least, I am also grateful to my current and former colleagues in AMADE for creating such an enjoyable working atmosphere.

Gerard Guillamet Busquets
University of Girona, May 26, 2016

Publications

The present Ph.D. thesis has been prepared as a compendium of peer-reviewed journal papers in accordance with the regulations of the University of Girona, parts of which are used directly or indirectly throughout the thesis. As part of the assessment, co-author statements have been made available to the assessment committee and are also available at the Faculty.

Publications in refereed journals

The main body of this thesis consists of the following papers:

A) G. Guillamet, A. Turon, J. Costa, J. Renart, P. Linde, J.A. Mayugo, "Damage occurrence at edges of non-crimp-fabric thin-ply laminates under off-axis uniaxial loading" *Composites Science and Technology*, vol. 98, pp. 44–50, 2014. doi: 10.1016/j.compscitech.2014.04.014

ISSN: 02663538, Impact factor: 3.569, ranked 1/24 in category *Materials Science, Composites*, Q1.[a]

B) G. Guillamet, A. Turon, J. Costa, P. Linde, "A quick procedure to predict free-edge delamination in thin-ply laminates under tension," *Engineering Fracture Mechanics*, (article in press), 2016.
doi: 10.1016/j.engfracmech.2016.01.019

ISSN: 00137944, Impact factor: 1.767, ranked 40/137 in category, *Mechanics*, Q2.[a]

C) G. Guillamet, J. Costa, A. Turon, J.A. Mayugo, P. Linde, "In search of the quasi-isotropic laminate with optimal delamination resistance under off-axis loads. Effect of the ply sequence and of using thin plies," *Submitted to Composites Part A: Applied Science and Manufacturing*, 2016.

ISSN: 1359-835X, Impact factor: 3.071, ranked 4/24 in category, *Materials science, Composites*, Q1.[a]

[a] According to the *2014 Journal Citation Reports (JCR)*

Other publications that have been derived from this thesis but are not included in this document are listed below:

Magazine article

- P.P. Camanho, A. Arteiro, A. Turon, J. Costa, G. Guillamet, E.V. González, "Structural integrity of thin-ply laminates," *JEC Composites Magazine*, vol. 49, no. 71, pp. 91–92, 2012.

Journal article

- Y. Liv, G. Guillamet, E.V. González, L. Marín, J. Costa, J.A. Mayugo, "Experimental study of compression after impact strength of tailored non-conventional laminates," *(pending submission)*, 2016.

Conference proceedings

- G. Guillamet, A. Turon, E.V. González, J. Renart, J. Costa, "Damage resistance and damage tolerance of thin-ply NCF thin laminates,". *V ECCOMAS Thematic conference on the Mechanical Response of Composites (COMPOSITES 2015)*, Bristol, England, 7-9 September 2015.

- G. Guillamet, Y. Liv, A. Turon, L. Marín, J. Costa, J.A. Mayugo, "Design of non-conventional CFRP laminates for improved damage resistance and damage tolerance," *16th European Conference on Composite Materials, ECCM 2014*, Seville, Spain, 22-26 June 2014.

- G. Guillamet, A. Turon, J. Costa, J. Renart, "Damage evolution in thin and thick-ply regions of NCF thin-ply laminates under off-axis uniaxial loading," *16th European Conference on Composite Materials, ECCM 2014*, Seville, Spain, 22-26 June 2014.

- L. Zubillaga, N. Carrère, A. Turon, G. Guillamet, "Experimental validation of stress/energy models to predict the onset of delamination from free-edges," *IV ECCOMAS Thematic Conference on the Mechanical Response of Composites, COMPOSITES 2013*, S. Miguel - Azores, Portugal, 25-27 September 2013.

- G. Guillamet, A. Turon, J. Costa, "Predicción de la deslaminación en los bordes libres en composites laminados mediante elementos finitos," *X Congreso Nacional de Materiales Compuestos, MATCOMP13*, Algeciras, Spain, 2-5 July 2013.

- L. Zubillaga, A. Turon, N. Carrère, G. Guillamet, I. Urresti, "Validación del criterio basado en tensión/energía para la deslaminación por efecto

de borde," *X Congreso Nacional de Materiales Compuestos, MATCOMP13*, Algeciras, Spain, 2-5 July 2013.

- G. Guillamet, A. Turon, P.P. Camanho, "Ply thickness influence on free-edge delamination in laminated composites," *I International Conference on Mechanics of Nano, Micro and Macro Composite Structures, ICNMMCS 2012*, Torino, Italy, June 18-20 2012.

- P.P. Camanho, A. Arteiro, A. Turon, J. Costa, G. Guillamet, E.V. González, "Structural integrity of thin-ply laminates," *Composites Design Conference, JEC Europe 2012 Composites Show & Conferences*, Paris, France, March 27-29 2012.

Universitat de Girona

Dr. Albert Turon Travesa, Assoc. Prof. at University of Girona, and Dr. Josep Costa Balanzat, Full Prof. at University of Girona

hereby CERTIFY that:

The thesis entitled *Improved delamination resistance of thin-ply based laminates: an experimental and numerical study*, submitted for the degree of Doctor of Philosophy by Gerard Guillamet Busquets, has been conducted under our supervision and fulfills the requirements for the *International Doctorate*.

Albert Turon Travesa
Assoc. Prof. at University of Girona

Josep Costa Balanzat
Full Prof. at University of Girona

Girona, May 26, 2016

List of Figures

List of Tables

Contents

Abstract

Delamination is one of the most feared failure modes in laminated composites because it can compromise the structural integrity of the laminate. In a literature review, it has been demonstrated that the ply thickness plays a key role in the onset of damage mechanisms such as delamination, and so it is of particular interest to re-examine this effect when using much thinner plies. Thus, departing from an emerging technology such as tow-spreading thin-ply production as starting point, the overall purpose of this Ph.D thesis is motivated by the industry need to better understand the potential benefits of thin-ply laminates in terms of delamination resistance and to propose predictive tools for their design.

First, the ply thickness effect is studied in a thin-ply non-crimp-fabric (NCF) laminate under different tensile loading directions. Damage occurrence and its development at free-edges is analyzed experimentally for a quasi-isotropic lay-up with two regions through the laminate thickness: a thick-ply region, where plies are grouped, and a thin-ply region, where the plies are dispersed. The onset of three failure mechanisms (transverse cracking, matrix crack induced delamination and free-edge delamination) are shown to be clearly delayed or even suppressed at the thin-ply region, whereas extensive crack growth is observed at the thick-ply region. Moreover, the effect of the loading direction also plays an important role in the progression of the damage mechanisms at the free-edge. Due to the differences in the ply sequences resulting from the loading directions and the damage occurrence at both regions, the laminate becomes anisotropic in terms of strength while being completely isotropic in in-plane stiffness.

Then, thin-ply based laminates challenge the use of traditional analytical and numerical tools used to predict edge delamination. This thesis predicts delamination at free-edges by assuming two delamination sources: matrix crack induced delamination which is accounted for by an analytical model using classical lamination theory and a failure criteria; and free-edge delamination with a finite element model using cohesive elements. Both approaches are demonstrated as being able to predict edge delamination by taking into account the effect of ply thickness, ply location and the mixed mode ratio at

interfaces. In addition, these approaches provide good equilibrium between predictive capabilities and computational effort, resulting in useful and rapid tools for laminate design in future optimization exercises.

Finally, an optimization procedure is proposed to find quasi-isotropic laminates with optimal delamination resistance. Four domains of stacking sequences with different loading directions, ply thickness and ply orientations are studied. The optimal lay-ups found using the proposed methodology are compared with a well-known baseline lay-up in the literature. The methodology succeeds in improving the delamination resistance of the baseline lay-up when thin plies are used over the traditional standard ply thicknesses. Furthermore, the results show that the use of thin plies enlarges the design domain and generates a safe space practically isotropic in any loading direction.

Resum

La delaminació és un dels mecanismes de fallada més temuts en materials compòsits ja que pot comprometre la integritat estructural del laminat. La revisió bibliogràfica demostra que el gruix de capa té un paper clau en l'aparició dels mecanismes de dany, entre ells la delaminació, i és interessant tornar a examinar aquest tipus de dany quan s'utilitzen capes molt més primes que les convencionals. Per tant, partint d'una tecnologia emergent com la dispersió de fibres (en anglès, *spread tow technology*), la motivació per dur a terme aquesta tesi doctoral prové del desig, per part de la indústria, de comprendre millor els beneficis dels laminats de capes primes en termes de resistència a la delaminació i proposar eines de predicció per al seu disseny.

En primer lloc, l'efecte de gruix de capa s'estudia en un laminat quasi-isòtrop de capes primes fabricat amb un tipus de teixit de trama no entrellaçada (en anglès, *Non-Crimp-Fabric* (NCF)). Aquest laminat està sotmès a diferents direccions de càrrega a tracció i consta de dues regions amb gruixos de capes diferenciades: un regió on s'agrupen capes amb la mateixa direcció (capes gruixudes) i una regió de capes primes. L'aparició del dany i el seu desenvolupament és observat experimentalment a la vora lliure del laminat. Es demostra que l'aparició de tres mecanismes de fallada (esquerdes a la matriu, delaminació induïda per esquerdes a la matriu i delaminació produïda per efecte de vora) estan clarament endarrerits o fins i tot suprimits a la regió de capes primes. D'altra banda, l'efecte de la direcció de càrrega també té un paper important pel que fa a la progressió dels mecanismes de dany en aquestes regions. Degut a les diferents seqüències de capes, resultants de les direccions de càrrega, i l'aparició del dany a les dues regions, el laminat resulta ser anisòtrop en termes de resistència tot i ser elàsticament isòtrop en el pla.

En segon lloc, dues formulacions existents per predir la delaminació a la vora del laminat són avaluades utilitzant aquest tipus de material. En aquesta tesi, la delaminació a la vora del laminat es prediu segons dues fonts demostrades experimentalment: delaminacions induïdes per una esquerda a la matriu, mitjançant un model analític (teoria clàssica de laminats amb un criteri de falla); i delaminacions produïdes per efecte de vora mitjançant

un model d'elements finits amb elements cohesius. Es demostra que les dues formulacions són capaces de predir la delaminació a la vora del laminat tenint en compte l'efecte del gruix de la capa, posició de la capa i el mode mixt de delaminació a les interfícies. A més, aquestes formulacions proporcionen un bon equilibri entre la capacitat de predicció i l'esforç computacional i per tant, resulten ser eines útils i ràpides pel disseny de laminats en exercicis futurs d'optimització.

Finalment, es proposa una metodologia per obtenir laminats quasi-isòtrops amb una resistència a la delaminació òptima. S'estudien quatre dominis de laminats quasi-isòtrops utilitzant dos tipus de materials i orientacions diferents. Els laminats òptims són comparats amb un laminat de referència que ha estat àmpliament estudiat a la literatura. La resistència a la delaminació és significament millorada quan els laminats són fabricats amb capes primes. A més, els resultats mostren que l'ús d'aquestes capes augmenta l'espai de disseny i genera un zona de seguretat pràcticament isòtropa.

Resumen

La deslaminación es uno de los mecanismos de daño más temidos en materiales compuestos ya que puede comprometer la integridad estructural del laminado. La revisión bibliográfica demuestra que el espesor de capa tiene un papel clave en la aparición de los mecanismos de daño, entre ellos la deslaminación, y es interesante examinar este tipo de daño cuando se utilizan capas mucho más delgadas que las convencionales. Por lo tanto, partiendo de una tecnología emergente como la dispersión de fibras (en inglés, *spread tow technology*), la motivación para llevar a cabo esta tesis doctoral proviene del deseo, por parte de la industria, en comprender mejor los beneficios de los laminados de capas delgadas en términos de resistencia a la deslaminación y proponer herramientas de predicción para su diseño.

En primer lugar, el efecto del espesor de capa se estudia en un laminado cuasi-isótropo de capas delgadas fabricado con un tejido no entrelazado (en inglés llamado *Non-Crimp-Fabric* (NCF)). Este laminado esta sometido a diferentes direcciones de carga a tracción y consta de dos regiones con espesores de capas diferenciadas: una región donde se agrupan capas con la misma dirección (capas gruesas) y una región de capas delgadas. La aparición del daño y su desarrollo es observada experimentalmente al borde libre del laminado en las dos regiones. Se demuestra que la aparición de tres mecanismos de daño (grietas en la matriz, deslaminación inducida por grietas en la matriz y deslaminación producida por efecto de borde) están claramente retrasados u incluso suprimidos en la región de capas delgadas respeto a la de capas gruesas. Por otra parte, el efecto de la dirección de la carga también tiene un papel importante en la progresión de los mecanismos de daño. Debido a las diferencias entre las secuencias de capas, resultantes de las direcciones de carga, y la aparición del daño a las dos regiones, el laminado resulta ser anisótropo en términos de resistencia a pesar de ser elasticamente isótropo en el plano.

En segundo lugar, dos formulaciones existentes para la predicción de la deslaminación al borde libre del laminado son evaluadas utilizando este tipo de material. En esta tesis, la deslaminación al borde del laminado se predice según dos fuentes de deslaminación demostradas experimental-

mente: deslaminaciones inducidas por una grieta en la matriz, mediante un modelo analítico (teoría clásica de laminados con un criterio de falla); y deslaminaciones producidas por efecto de borde mediante un modelo de elementos finitos con elementos cohesivos. Se demuestra que las dos formulaciones son capaces de predecir la delaminación al borde del laminado teniendo en cuenta el efecto del espesor de la capa, posición de la capa y el modo mixto de deslaminación en las interfaces. Además, estas formulaciones proporcionan un buen equilibrio entre la capacidad de predicción y el esfuerzo computacional, y por lo tanto, resultan herramientas útiles y rápidas para el diseño de laminados en ejercicios futuros de optimización.

Finalmente, se propone una metodología para obtener laminados cuasi-isótropos con una resistencia a la deslaminación óptima. Se estudian cuatro dominios de laminados cuasi-isótropos utilizando dos tipos de materiales y orientaciones diferentes. Los laminados óptimos son comparados con un laminado de referencia ampliamente estudiado en la literatura. La resistencia a la deslaminación es considerablemente mejorada cuando los laminados son fabricados con capas delgadas. Además, los resultados demuestran que el uso de estas capas aumenta el espacio de diseño y genera una zona de seguridad prácticamente isótropa.

Chapter 1

Introduction to the Ph.D. thesis

This work is the result of a collaboration with Airbus under the project 2^{nd} generation of Composites, *2genComp*. The work was initiated at the wish of the industry to improve understanding the delamination resistance of thin-ply NCF laminates. This Ph.D. thesis was undertaken with the following overall purpose:

To demonstrate the potential benefits of thin-ply laminates in terms of delamination resistance and to propose predictive tools for their design.

In the following sections of this chapter, the contextual background and the motivation of this thesis is presented. Next, a review on the delamination resistance and the ply thickness effect in laminated composites is analyzed and discussed. Following that, another review but on thin-ply laminates is provided and the yet unsolved challenges are identified. Finally, the objectives of the present work are described.

1.1 Contextual background

Unlike many materials, whose applications are discerned only after they have been discovered or invented, composites are often carefully designed with a particular application in mind. Originally developed as light and strong materials for the aerospace industry in the late 20th century, they have now found their way into many industries such as the automotive or marine industry, wind energy, civil infrastructure or even sports.

Composite materials are made by combining two or more materials into one with better properties than its individual components. One of the most

widely-used composites are the Fiber Reinforced Polymers (FRP), which consist of layers of long continuous fibers, e.g. carbon, glass and aramid, with a polymer matrix such as epoxy. By assembling different oriented layers of fibrous composite materials (laminae/plies) and joining them, a laminated composite is created. Fig. 1.1 illustrates the schematic of a laminated composite.

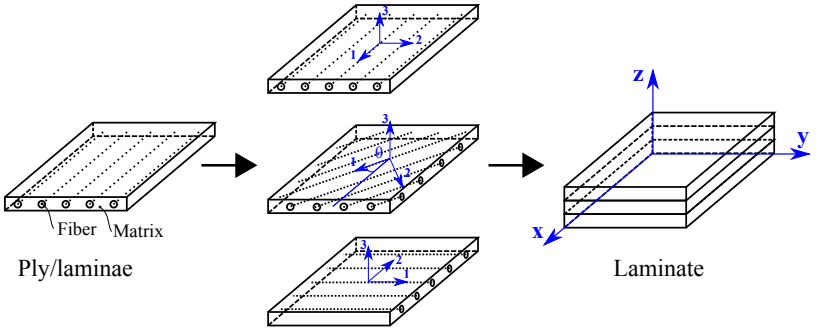

Fig. 1.1: Schematic of a laminated composite.

This type of composite material has excellent stiffness-to-weight and strength-to-weight ratios producing very lightweight structures. Furthermore, they give designers and engineers tremendous freedom in terms of both form and function for a particular application in mind.

Nowadays, composite materials are widely used in many markets and products. For instance, composite material consumption has increased significantly in the commercial aeronautical sector, from a mere five to six percent in the 1990s to more than 50 percent in today's advanced aircraft programs, such as the Boeing 787 Dreamliner and the Airbus 350 XWB. Fig. 1.2 shows the material percentage and its location in the Airbus A350 XWB.

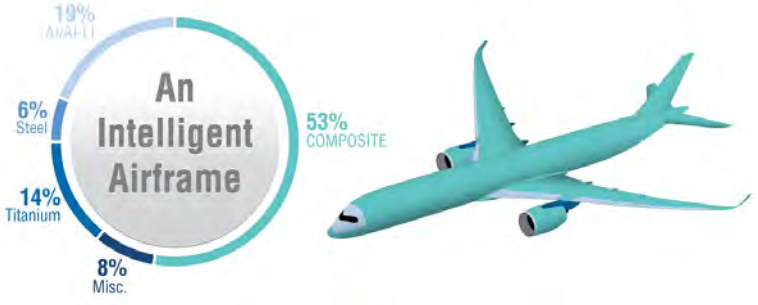

Fig. 1.2: Materials used in the construction of the A350-XWB aircraft. Picture from Airbus website.

On the other hand, composite materials exhibit complex failure mechanisms that are challenging to predict due to the strong heterogeneity and anisotropy of the material. Two types of damage can develop in a laminated composite: interlaminar or intralaminar. Intralaminar damage is mainly related to the presence of matrix cracking, fiber breakage and/or fiber matrix debonding, whereas delamination (interlaminar damage) is mainly related to the loss of adhesion between plies due to their relatively weak interlaminar strength.

Typically, matrix cracking occurs as the first-ply failure, delamination damage follows and fiber breakage usually happens at the last stage of the failure. Fig. 1.3 shows the damage development in form of matrix cracking and delamination at the edge of a composite laminate loaded in tension. It can be seen that only the occurrence of matrix cracking and delamination and the interaction between them (without fiber breakage) can compromise the integrity of the whole laminate. Therefore, delamination resistance is particularly important for the structural integrity of a composite structure and it is the damage mechanism this Ph.D. project focuses on.

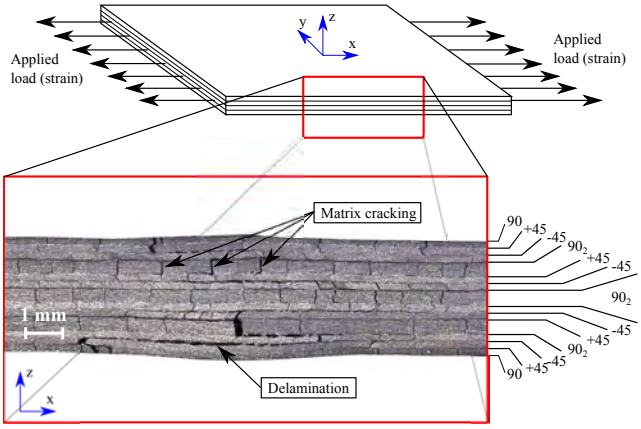

Fig. 1.3: Damage occurrence at edges of a laminated composite loaded in tension.

1.2 Thesis motivation

Although composite materials have successfully penetrated in various market segments, continuous innovation is required to address needs that are constantly appearing in the industry, such as the need for light-weights and cost reduction.

One of the new technologies in the composites industry is the *spread tow technology*, in which laminates can be produced by stacking completely flat

plies with thicknesses as little as 0.02 mm. The reader is referred to Section 1.4 for a complete description of this technology. When these innovations appear, industrial manufacturers try to follow their development aiming to improve the performance of their own composite structures. Thus, understanding the potential benefits and drawbacks of these new materials, with respect to manufacturing, processing, characterization, design and cost-effectiveness, is extremely important in order to guarantee their successful introduction onto the market.

The use of thin-ply laminates, with plies much thinner than current conventional plies, aims to improve the performance of laminated composite structures. For a given total laminate thickness, the use of thin-plies in the design entails, as opposed to conventional plies, a higher number of plies. Consequently, the design space expands dramatically, opening the door to a wide range of new design opportunities. In a pioneering work conducted by Sihn et al. [1], it was shown that thin-ply based laminates delay the onset of matrix cracking and delamination and increase the failure loads.

In fact, several studies in the literature show an improvement on the damage resistance of laminated composites when dispersed orientations are used (also known as sublaminate scaling) instead of grouping layers (ply clustering or ply blocking). However, the use of much thinner plies was not studied in detail in an industrial context because of the lack of technology available to produce the aforementioned materials.

Therefore, the effect of ply thickness on damage occurrence should be re-examined when dealing with thin-plies, as current design theories would predict asymptotic ply strength as the thickness decreases [2]. The interaction between failure mechanisms, i.e. delamination triggered by matrix cracks, should also be accounted for by using failure criteria sensitive to the ply thickness, ply orientation and location. Furthermore, the applicability of quick design tools for the onset of delamination and strength of thin-ply based laminates has yet to be assessed and constitute a computational challenge due to the large number of stacking sequences when thin-plies are used for a laminate of useful thickness.

1.3 Delamination resistance and ply thickness effect

Different failure mechanisms, such as matrix cracking, delamination or fiber breakage, may develop in laminated composite structures. Within these distinctive failure mechanisms, delamination is a major failure mechanism because the low fracture toughness and interlaminar strength between plies may expose the laminated composite structure to delamination damage and compromise its structural integrity. Moreover, this form of damage is not vis-

ible on the surface or even at free edges making it difficult to detect during inspection.

On the other hand, it is known that the onset and growth of delamination depend upon the following variables: ply orientation, ply thickness, stacking sequence, temperature, nature of loading, etc. Among them, the ply thickness effect strongly influences laminate strength and the initiation and growth of delamination.

This section reviews the effect of the ply thickness on delamination resistance. Firstly, typical sources of delamination are presented. Then, the initiation of delamination and growth from two different sources: free edges and matrix cracks is analyzed and discussed.

1.3.1 Sources of delamination

There are circumstances in which interlaminar stresses between plies of laminated composite arise and may cause delamination. According to their location, delamination sources can generally be grouped into two categories: at geometric or material discontinuities. Fig. 1.4 illustrates typical sources of delamination in laminated composites.

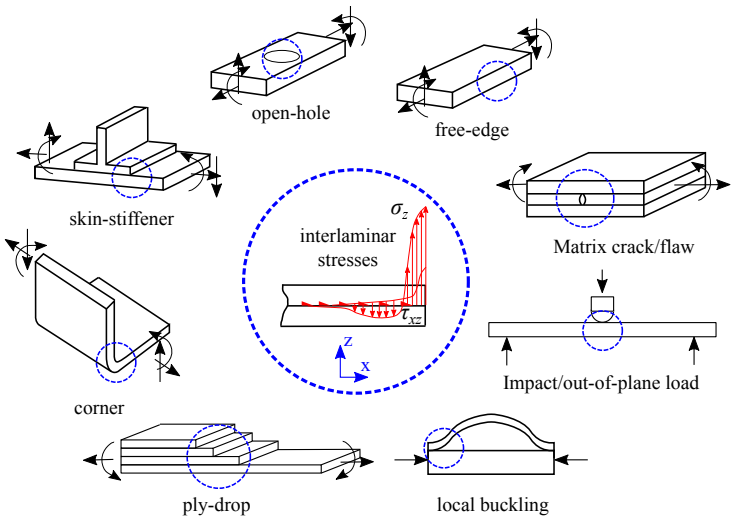

Fig. 1.4: Typical sources of delamination in laminated composites.

Geometric discontinuities are commonly encountered in various engineering applications, for example internal/external ply drop terminations, corners, tubular sections, skin stiffener terminations and flanges, etc. Forces and moments are transferred to the continuous plies through interlaminar normal and shear stresses and may provoke delaminations.

Material discontinuities are present at interfaces between plies of different orientation due to the mismatch of mechanical properties. When bonded, interlaminar normal and shear stresses are induced at free edges, at holes and notches. Moreover, the orientation of the fiber results in a mismatch of coefficients of thermal and moisture expansion. For this reason the curing process or the working environment once the laminated composite is in service needs to be considered in the design to avoid interlaminar damage growth.

As highlighted in [3], delamination can occur due to the presence of intralaminar damage such as a matrix crack. Because of the low transverse strength, delamination can initiate at relatively low loads.

Another source of delamination occurs when the laminated composite is subjected to out-of-plane loading. One scenario that is especially important in the aircraft industry are the impact events that may occur due to a bird strike or a tool-drop during inspection. Since delamination is known to severely reduce the compressive strength of the laminate, the research community has devoted much effort to characterizing the compression after impact strength.

1.3.2 Free-edge delamination

One of the most common source of delamination appears at the laminate edge - *free-edge delamination* - where interlaminar normal and shear stresses arise due to the mismatch in Poisson contraction of the individual plies with different orientations. Fig. 1.5 shows two examples of the free-edge effects along the straight edges of laminated composites under in-plane uniaxial loading. It is clearly seen that, depending on the stacking sequence and its ply orientations, effects of Poisson's ratio or shear coupling mismatch induce interlaminar stresses at the free-edge.

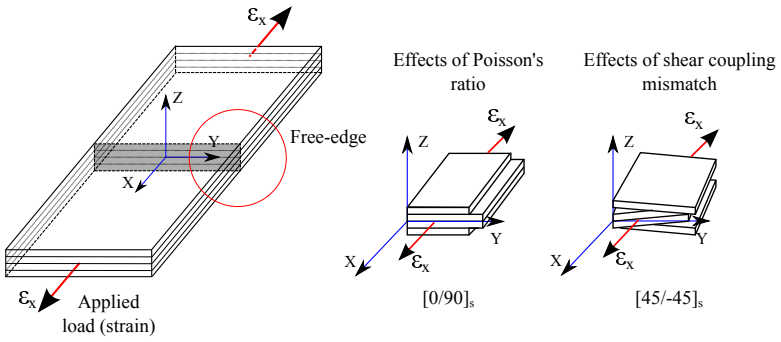

Fig. 1.5: Free-edge effects of a laminated composite under uniaxial loading.

The free-edge problem has been a subject of study since the early 1970s [4, 5]. Since then, a great amount of work has been reported on the free-edge problem indicating that free-edge delamination is attributed to the existence

of interlaminar stresses; the interested reader should refer to this review work [6]. This interlaminar stress distribution at the free-edge depends on many parameters, such as ply orientations, stacking sequence, ply thickness, test temperature, nature of loading, etc. Among them, ply thickness plays an important role in the occurrence of delamination. Even delamination at free edge usually interplays with other failure modes, in particular matrix cracking, a more detailed description of this delamination source is described in the following section.

Experimental evidence

In a given laminate under tensile load, it is possible that transverse cracking occurs before free-edge delamination, or vice versa. In this section, experimental evidence is strictly given only for those cases where delamination occurs before matrix cracking.

One pioneering work with a detailed description of the observed damage mechanisms at the free-edge was conducted by Crossman et al. [3,7]. In this work, they observed pure edge delamination in a $[\pm 25/90_{n/2}]_s$ when $n = 1$ and about 2. The delamination was located at the midplane of the lay-up (90/90 interface). A visual depiction of this edge delamination and an X-ray of the specimen was performed later by Lorriot et al. [8] in a similar lay-up, as shown in Fig. 1.6.

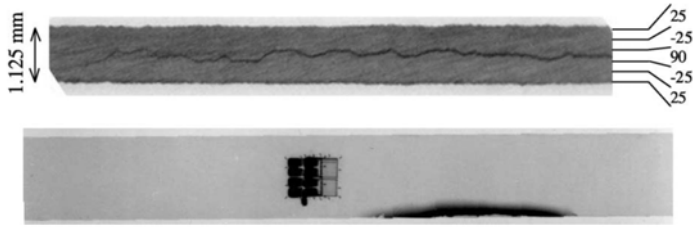

Fig. 1.6: Free-edge and X-ray of $[\pm 25_2/90]_s$ laminated specimen after delamination [8].

Fig. 1.7 shows the onset strains for each damage mechanism and the laminate failure with respect to thickness of the 90° layer. An interesting trend observed in this figure is that the laminate strain applied for delamination onset is decreased when n is increased.

Some years later, Johnson and Chang [10] performed an extensive experimental campaign with a wide variety of stacking sequences. Only for a few lay-ups, such as $[90/30/-30]_s$ or $[90/45/-45]_s$, did the initial damage consist of mode I edge delamination. For the remainder of the lay-ups the initial damage was matrix cracking followed by delamination or matrix cracking accumulation during the loading.

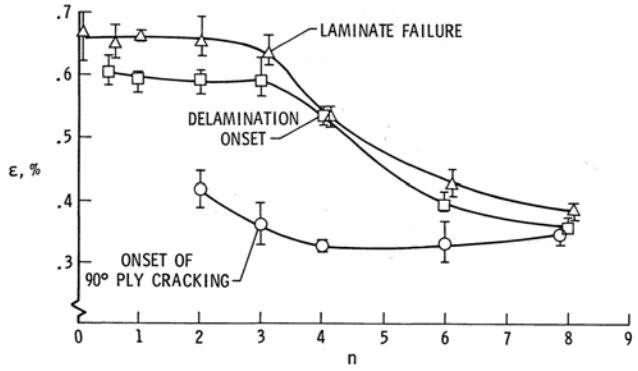

Fig. 1.7: Strain at onset of 90° ply cracking, delamination, and laminate failure from $[\pm 25/90_{n/2}]_s$ laminates. This figure belongs from a work conducted by O'brien [9] reporting the results from Crossman and Wang [7].

In other studies, the free-edge delamination problem has focused on angle-ply laminates in the form of $[\pm\theta_n]$, where n is the repeated layers. According to several authors [8,11], in lay-ups with slightly disoriented angles with respect to the load direction (ply orientations smaller than 30°), delamination initiates in mode III at the interface between layers, without the interaction with other failure modes such as matrix cracking. Furthermore, these works conclude that the onset stress for delamination increases when the ply thickness decreases, thus, following the same trend observed in previous studies using different stacking sequences.

Therefore, a general conclusion from the previous studies is that the initiation of delamination strongly depends on the ply thickness and all the results show the same trend: the onset stress or strain for delamination decreases when the ply thickness is increased.

Predictions

Two types of methods can be used for predicting delamination initiation and propagation at free edges: stress-based formulations for initiation and energy-based (energy release rate) for initiation and/or propagation.

The stress-based methods require interlaminar stresses at each interface to be determined and then, their comparison with the material's strength characteristics made. However, they are mesh size dependent due to the singularity near the crack tip. Some analytical studies are able to calculate the full stress tensor near the edges and determine the onset of delamination by using a stress criterion [8,11,12]. To predict delamination onset, a stress criterion involving the average of the interlaminar stresses over a characteristic length from the edge is often proposed in order to overcome the difficul-

ties resulting from the presence of a singularity. It is worth mentioning that these methods are formulated for specific delamination mode cases and different assumptions are made to select the characteristic length. Other works combine a stress condition with an energy analysis. For instance, the model proposed by Martin et al. [13] requires a generalized plane strain model to determine the stress distribution near the free-edge and then, the delamination onset can be predicted using the interlaminar fracture energy and the interlaminar shear strength of the material.

Other types of methods are those using the finite element method in combination with the virtual crack closure technique (VCCT) [14] and the cohesive zone or interface element technique [15–18]. The main difference between them is that the VCCT requires a pre-existing crack and cohesive elements do not. For instance, O'Brien [18] used the VCCT to compute the energy release rates associated with delamination growth. Based on the energy-based formulations, he also proposed a closed-form equation for the energy release rate associated with delamination growth in a laminate. This equation was used to predict the critical strain for free-edge delamination of $[\pm 45_n/0_n/90_n]$ with $n = 1, 2, 3$ laminates. Fig. 1.8 show the predictions on the onset of delamination and the effect of the ply thickness.

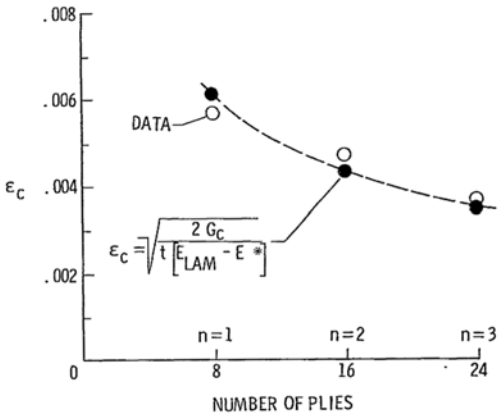

Fig. 1.8: Edge delamination onset prediction compared with $[\pm 45_n/0_n/90_n]$ ($n = 1, 2, 3$) data [18].

Another use of VCCT on the free-edge problem was made by Hallet et al. [19]. In this work they computed the critical strain for delamination on $[45_m/90_m/-45_m/0_m]$ laminates with $m = 1, 2, 4, 8$. In this case, the use of VCCT was applied as a preliminary analysis to show the limitations of this technique when other failure mechanisms, such as matrix cracking, interact. However, the ply thickness effect on the predictions was well captured, showing an increase of the critical strain when the ply thickness decreases.

The main limitation to the use of the VCCT is the location of one or various critical interfaces and the definition of a pre-existing crack. Instead, the use of cohesive elements does not require a pre-existing crack. One of the first studies using interface elements for predicting the onset of free-edge delamination was conducted by Schellekens and De Borst [15]. In this work $[\pm 25_n/90_n]_s$ and $[\pm 45_n/0_n/90_n]$ with $n = 1, 2, 3$ laminates were simulated and then, the predictions were compared with the experimental results from Crossman and Wang [7] and O'Brien [9,18]. Despite the occurrence of matrix cracks followed by delamination observed in the experiments, the predictions on the free-edge delamination by Schellekens and De Borst were in agreement with the experiments and the same trend was obtained for the ply thickness dependence. In most of the cases, transverse cracking and delamination occurred simultaneously.

More recently, Turon et al. [17] predicted the initiation and propagation of free-edge delamination of the $[\pm 25/90]_s$ investigated by Crossman and Wang [7] and they conducted a sensitivity analysis with different element sizes and interface strengths. Fig. 1.9 shows the evolution of stresses during the delamination onset and propagation and Fig. 1.10 shows the force-displacement curves with different element sizes.

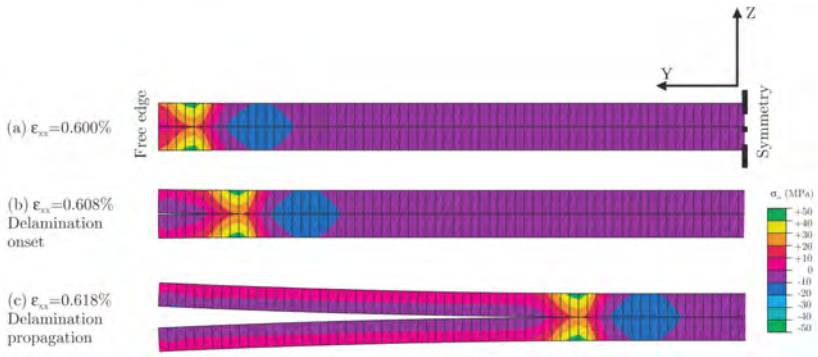

Fig. 1.9: Evolution of stresses during delamination onset and propagation of the two interior layers of $[\pm 25/90]_s$ laminate [17].

The predictions were in agreement with the experiments with differences of 3% when the mesh was refined sufficiently. Some advantages to the use of cohesive zone models are their applicability to any structure with multiple loads and the fact that they do not require the presence of an initial crack. However, it is necessary to define a small element size in order to obtain accurate results, when the mesh is refined enough, the finite element model becomes non-mesh dependent [17].

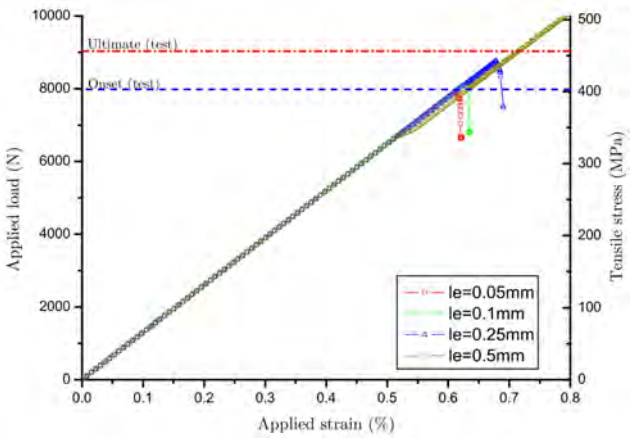

Fig. 1.10: Load-displacement curves obtained for a free-edge test with different mesh sizes [17].

1.3.3 Matrix crack induced delamination

Another source of delamination is from a matrix crack. Interlaminar stresses that develop in the ply interface at matrix crack tips may cause local delamination to form and grow. Fig. 1.11 illustrates a matrix crack triggering a delamination of a laminated composite under uniaxial loading. Some experimental evidence and numerical models to predict this phenomenon have been reported in the literature [3, 9, 10, 19, 20].

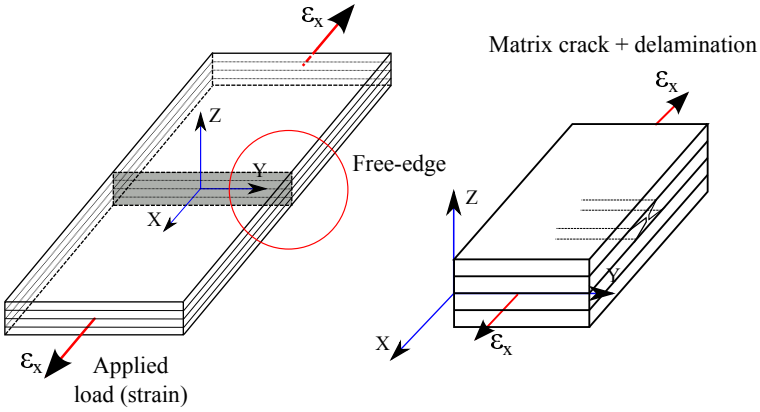

Fig. 1.11: Matrix crack induced delamination in a laminated composite under uniaxial loading.

Experimental evidence

As mentioned before, some lay-ups with specific ply orientations and thicknesses exhibit matrix cracking before free-edge delamination. For instance, the initiation of transverse cracking at the 90° from the $[\pm 25/90_n]_s$ lay-up was found to depend on the thickness of this layer, as shown in Fig. 1.7. For example, the occurrence of one or various matrix cracks can trigger a delamination at the adjacent interfaces. The sequence of failure mechanisms which occurred at the free-edge are shown in Fig. 1.12 for (a) just before the onset of delamination (b) just after delamination and (c) just before final failure. The sequence illustrated in column (b) shows that for $n \geq 4$ transverse cracks trigger delaminations, whereas for $n \leq 3$, delaminations grow due to high interlaminar stresses. Moreover, the delamination shape changes from a thumbnail-shape ($n = 3$) to a delamination following a matrix crack ($n = 4$).

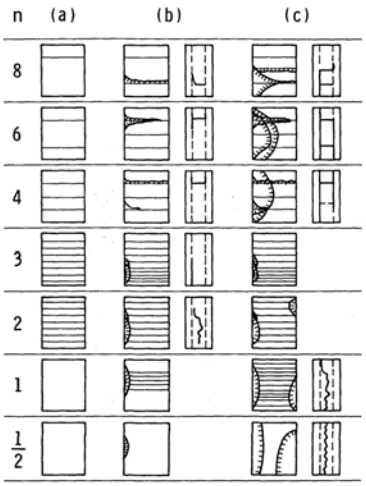

Fig. 1.12: Schematic of fracture sequences in $[\pm 25/90_n]_s$ laminates. (a) just before the onset of delamination (b) just after delamination and (c) just before final failure [9].

Some years later, Johnson and Chang [10] performed a very extensive campaign with different laminates and material systems and analyzed the failure mechanisms observed during the tests. Tensile tests were stopped periodically to make an X-ray to the specimens. Among the failure modes between specimens, they observed that matrix crack induced delamination was present in many laminate configurations, especially in those containing higher ply clustering and larger angle-ply orientations.

Hallett et al. [19] also reported interaction between matrix cracks and delamination damage. In this case, the influence of scaling the ply thickness on the failure mode was analyzed in a quasi-isotropic lay-up $[45_m/90_m/-45_m/0_m]_s$ with $m = 1, 2, 4, 8$. It was observed that for those cases where the

scaling factor was greater than or equal to 2, matrix cracks were observed, followed by delamination in the form of triangular regions. Instead, for the baseline or $m = 1$ case, no matrix cracking or delamination could be observed during the loading and the ultimate failure occurred by fiber breakage. The main conclusion of this work, which follows the same trend as previous studies, is that large ply clustering decreases the failure strain of the laminate and that matrix cracking exerts a strong influence on delamination.

More recently, Zubillaga et al. [20] performed an experimental campaign to analyze the occurrence and progression of transverse cracks and delaminations induced by matrix cracking from five different stacking sequences. The effect of the ply clustering was studied in one lay-up $[60_n/-60_n]_s$, $n = 3, 4$, which was also studied by Johnson and Chang [10]. In both lay-ups, it was observed that the initial damage consisted of matrix cracks followed immediately by delamination at the adjacent interfaces. Moreover, the laminate failure stress measured in the lay-up with $n = 3$ was greater than the lay-up with $n = 4$; in agreement with the results in Ref. [10]. A visual depiction at the free-edge of the $[60_3/-60_3]_s$ laminate before and after failure is shown in Fig. 1.13.

Fig. 1.13: Matrix crack induced delamination in $[60_3/-60_3]_s$ specimen. (a) before crack growth and (b) after failure [20].

Therefore, the occurrence of matrix cracking depends on thickness and consequently, the initiation of delamination has solid experimental evidence. It has been shown that matrix cracking can occur before free-edge delamination and that the interaction between them is extremely important.

Predictions

This review evidences that models and failure criteria for delamination induced by matrix cracking should account for the ply thickness effect. Most of the criteria dealing with delaminations triggered by matrix cracks are formulated based on Fracture Mechanics [9, 10, 21, 22] and they account for the observed thickness dependence. All of these approaches consider an initial crack at the interface between two plies which might propagate in a self-similar way. The criterion compares the energy release rate available to pro-

mote delamination at the interface to its fracture toughness in order to satisfy the delamination growth.

Experiments conducted by Crossman et al. [3] were correlated with the energy-based formulations proposed by Wang and Crossman [23]. In this case, two formulations (one for transverse cracking and the other for edge delamination) were developed independently. As both approaches were formulated independently, the predictions were discussed with respect to their occurrence observed in the experiments. The predictions showed the same trend for both failure modes, i.e. as the ply thickness increases the onset stress decreases. Moreover, in the case of the 90° layer from $[\pm 25/90_n]_s$ laminates, it was demonstrated that the threshold stress for the onset of delamination was inversely proportional to the square-root of the thickness of the repeated layer.

There are other computational methodologies which use cohesive elements to model interlaminar damage with pre-existing matrix cracks [19]. The advantage of these methods is that they can predict the onset and propagation of the damage in any structure with different applied loads. For instance, Hallett et al. [19] obtained very accurate results for predicting delamination in $[45_m/90_m/-45_m/0_m]_s$ laminates with $m = 1, 2, 4, 8$. Again, the onset stress predictions for failure decreases as the ply thickness of the repeated layers m increases and, consequently, the ultimate failure of the laminate is also affected by the progress of delamination due to the ply thickness effect (Fig. 1.14).

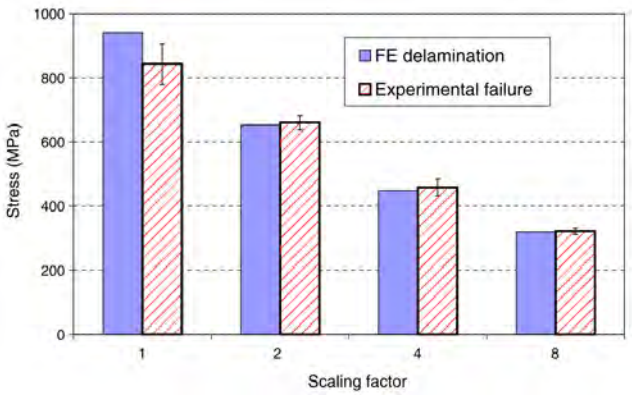

Fig. 1.14: Laminate failure stress on $[45_m/90_m/-45_m/0_m]_s$ laminates (scaling factor refers to m) [19].

Other methods, such as intralaminar progressive damage models [24] or the extended finite element method [25] are able to reproduce the complete sequence of damage events until laminate failure. However, these approaches require high computational costs which make them suitable only for a de-

tailed progressive damage analysis in the final steps of the design.

Recently, Zubillaga et al. [22] proposed a simple failure criterion to predict delamination induced by matrix cracks (MCID). The failure criterion is evaluated at a ply level and applicable to general loading conditions such as the Puck [26] or LaRC [27] failure criteria. The formulation is based on previous work from O'Brien [9] and Maimí et al. [21] and is able to predict mixed mode delamination growth at the interface between a cracked ply and the neighbouring ply. This model was validated by comparing its predictions with available experimental data and analytical models in the literature [7, 9, 19, 21]. Fig. 1.15 shows the comparison between the MCID failure criterion and experimental data obtained by Hallett et al [19]. It can be clearly seen that, the thickness dependence at the onset of delamination is in agreement with the experiments when delaminations are initiated by matrix cracking.

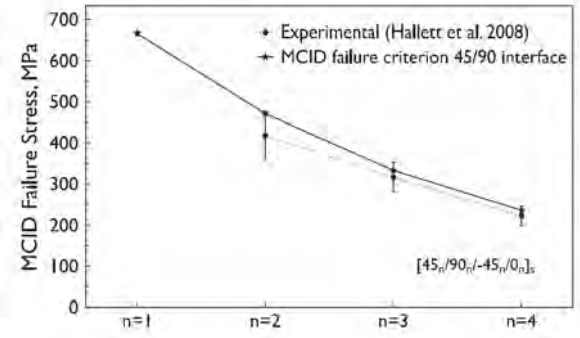

Fig. 1.15: Laminate MCID failure stress on $[45_m/90_m/-45_m/0_m]_s$ laminates [22].

1.3.4 Summary and general considerations

All the previous works has proved that ply thickness plays an important role in the occurrence of delamination triggered either by high interlaminar stresses or by the presence of a transverse crack. Thus, in order to delay or even suppress these damage mechanisms, the design of the stacking sequence is extremely important.

Herakovich, in a historical review into the mechanics of composites [28], showed the significant effects of the stacking sequence for tensile tests on angle-ply laminates. When the $+\theta$ and $-\theta$ layers are stacked in an alternating fashion, $[\pm\theta]_{ns}$, the mode of failure is primarily due to fiber breakage. In contrast, when the $+\theta$ and $-\theta$ layers are grouped together ($[+\theta_n/-\theta_n]_s$), edge effects and interlaminar shear stresses dominate and the specimen fails due to delamination at a much lower axial stress. For example, according to

Herakovich [28], alternating the layers of a $[\pm 30]_s$ specimen resulted in a 48% increase in strength, or quasi-sotropic laminates such as $[\pm 45/0/90]_{ns}$ will be better damage-resistant laminates than $[\pm 45_n/0_n/90_n]_s$.

As one can see, making laminates which are resistant to matrix cracking and delamination damage requires distributing (rather than grouping) the plies through the laminate thickness, so that the thickness of the same kind of plies becomes thin. In fact, it would be even more desirable to use thinner plies whose thickness is a fraction of conventional plies.

1.4 Spread tow thin-ply technology

1.4.1 Technology development

With the increasing demands from the aircraft industry to design structures with the best mechanical behavior and low weight, new manufacturing technologies to produce composite laminates are being developed. One of these technologies - *the spread tow technology* - is able to produce completely flat and straight plies capable of reaching a dry ply thickness as little as 0.02 mm. The laminates made of such thin plies, hereafter referred to as *thin-ply laminates*, are similar to conventional plies (from now on referred to as standard-ply laminates) but with some potential benefits.

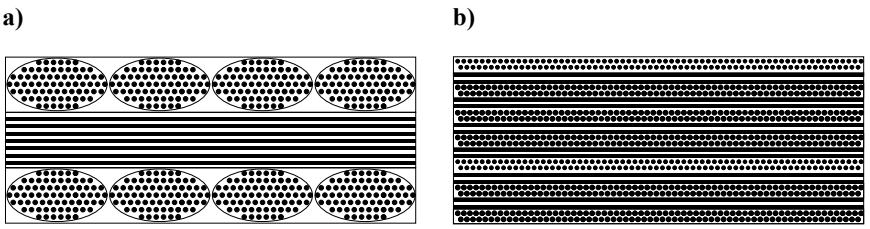

Fig. 1.16: Ply thickness morphology at lamina scale between a standard-ply laminate and a thin-ply laminate. (a) Standard-ply laminate. (b) Thin-ply laminate.

Figure 1.16, illustrates the morphology of standard and thin-ply laminates. It is well appreciated that to reach the same total laminate thickness more plies are needed. It is interesting that in the thin-ply structure the fiber bundles are smaller and better scattered over the laminate width which, in turn, results in a more uniform structure. According to some manufacturers, the thin pre-impregnated unidirectional tapes show a better fiber wet-out than conventional prepreg material. The resin flows in between each and every filament during the impregnation process resulting in a well controlled resin-fiber distribution and improved mechanical properties when compared to conventional composites [29].

The common way to refer to the thickness of a certain ply is through the fiber areal weight of the ply of which the units are g/m^2 (or commonly referred to as gsm). For instance, a standard composite structure can be made of plies between 125 to $200g/m^2$, whereas a typical thin-ply structure could have plies around $50g/m^2$ or even thinner (ultra-thin) plies $25g/m^2$.

As explained above, to obtain a thin-ply the process consist of spreading the fiber tow. Several methods can be found in the literature for spreading tows. Depending on the desired ply thickness and width, some of these methods use pneumatic systems, while other methods are based on mechanical systems or even on ultrasonic propagation waves for spreading.

The pneumatic spreading method was first proposed by Kawabe et al. [30] in 1998, in an attempt to open various reinforcing fiber tows by means of a machine with an airflow system. According to Kawabe et al., this process was successfully applied to carbon and glass fibers and they were able to obtain a wider spread tow. In a more recent work, Sihn et al. [1] used this tow spreading method to produce thin plies. This method was developed in the Industrial Technology Center in Fukui Prefecture, Fukui-city (Japan), and marked a new trend in the development of new processing techniques for manufacturing laminated composites. In this work, Sihn et al. show a conventional tow with 12K filament, usually in a circumferential shape, being transformed into a spread flat shape using airflow, as shown in Fig. 1.17a.

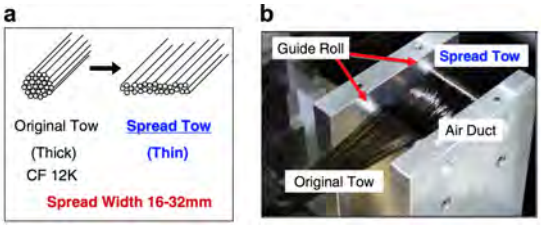

Fig. 1.17: Schematic of the pneumatic tow spreading machine [1].

Fig. 1.17b shows how the tow passes through the machine perpendicularly to an air duct and a vacuum that sucks the air downward. Two guide rolls hold the tow and with a variation of the air speed, the tow sags downward toward the air flow direction so that it loses tension and results in a tension-free state. With a uniform airflow, the tow can be spread continuously and stably, see Fig. 1.18. The wider the tow is spread, the thinner the tow becomes. According to Sihn et al., the airflow does not usually cause any damage to the fiber filaments during this processing because it can be easily adjusted and is fairly low.

Another method consists of spreading fibrous tows mechanically by means of a rotating wheel with teeth placed at perpendicular angle or radial to the wheel (e.g. simulating a comb). The pins enter into the filaments of the tow,

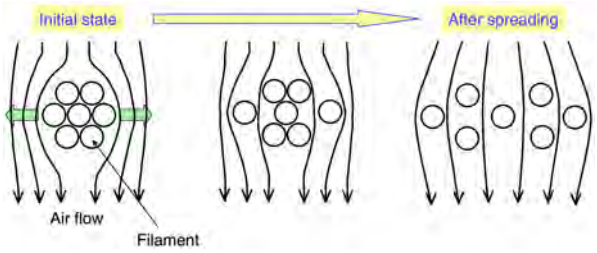

Fig. 1.18: Airflow tow spreading process [1].

thus increasing the space between them and obtaining a wider spread tow. Fig. 1.19 shows and schematic representation of the patented tow spreading machine by Krueger et al. [31].

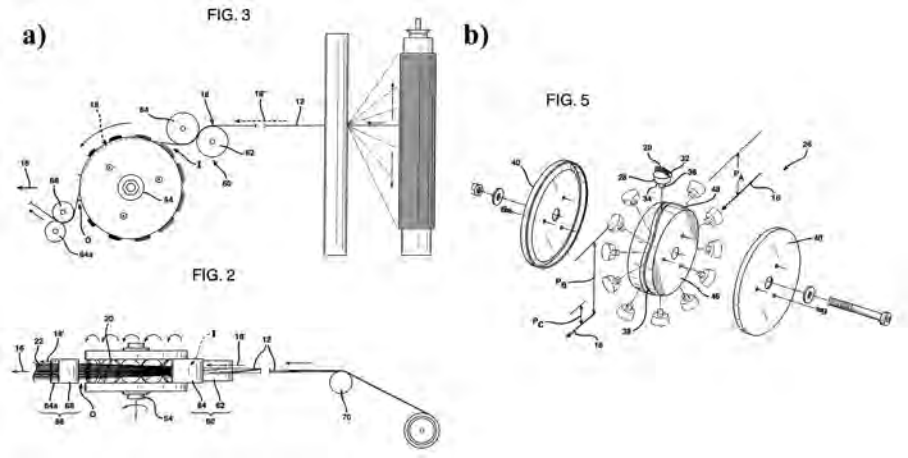

Fig. 1.19: Schematic of the mechanical tow spreading machine [31]. (a) Side and top views (b) Detail of the rotation wheel with teeth.

Another way to spread fiber tows is based on ultrasonic waves [32]. Since 1996, several efforts were made to obtain satisfactory results in the fiber spreading, but it was not until 2005 that a machine was completed and presented by Technomas Corp. A schematic of the ultrasonic fiber-spreading machine is shown in Fig. 1.20. This machine pulls the tow bundle into an ultrasonic bath, which by means of ultrasonic waves, spreads the tow bundles to obtain a flat spread tow.

With the acquisition of skills in fiber spreading from the aforementioned techniques, a number of companies, such as Chomarat in Ardèche (France), North Thin Ply Technology (NTP) in Penthalaz-Cossonay (Switzerland), Oxeon AB, in Borås (Sweden) or Sakai Ovex in Hanandoh Naka Fukui-city

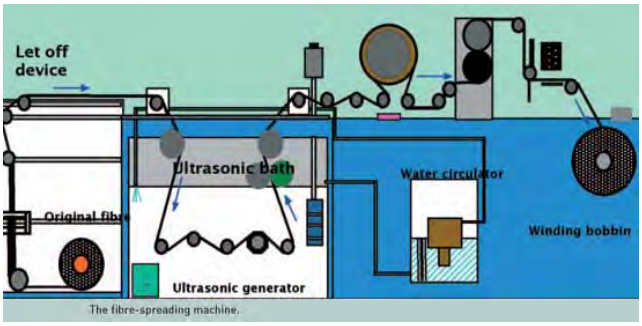

Fig. 1.20: Schematic of the ultrasonic tow spreading machine [32].

(Japan), have adopted the *spread tow technology* to produce thin plies. One of the first manufacturers to do so was Chomarat, who extended their range of carbon multiaxial products, also known as Non-Crimp-Fabrics (NCFs), by developing new reinforcements with low areal weights. The bi-angle thin-ply NCF manufactured by Chomarat is the material used in the studies included in this thesis.

1.4.2 Bi-angle thin-ply Non-Crimp-Fabric (NCF)

Chomarat, in collaboration with Stanford University, was one of the first manufacturers to apply the spread tow thin-ply technology. A team of companies and academics mobilized to launch an unbalanced multiaxial non-crimp-fabric with thin-plies under the brand C-Ply™.

C-Ply™ is a multiaxial or Non-Crimp-Fabric (NCF) composed of thin plies of carbon fibers stacked in two or more angles and stitched together by thin polyester fibers. Fig. 1.21 illustrates the surface appearance of the NCF material.

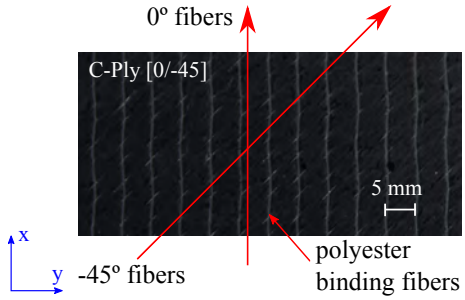

Fig. 1.21: The appearance of a thin-ply C-ply [0/-45].

The thin-ply NCF manufacturing process from Chomarat consists of three

basic steps [33]:

Step 1: *Spreading*. Achieving lower ply weight than $150g/m^2$, the spreading process converts the conventional tows into a finely aligned unidirectional thin sheet using, as described previously, a pneumatic device. Nowadays, Chomarat offers a wide range of fibers including carbon, E-glass, S2-glass, aramid and hybrid combinations with areal weight as low as $50g/m^2$. Fig. 1.22 shows a UD carbon T800 with 24K filament before spreading and after spreading.

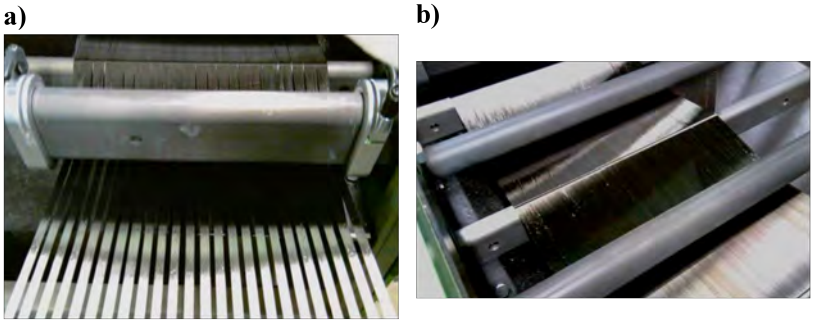

Fig. 1.22: Spreading process of a UD carbon T800 with 24K filament [34]. (a) Before spreading. (b) After spreading ($50g/m^2$) .

Step 2: *Ply forming*. This is carried out in a multiaxial machine laying down the yarns as in the standard technique, UD plies are placed on top of one another in the desired directions. Today, the kinematics of the machine allows to obtain a wide range of angles as low as 20 degrees. Fig. 1.23 shows the NCF machine from Chomarat.

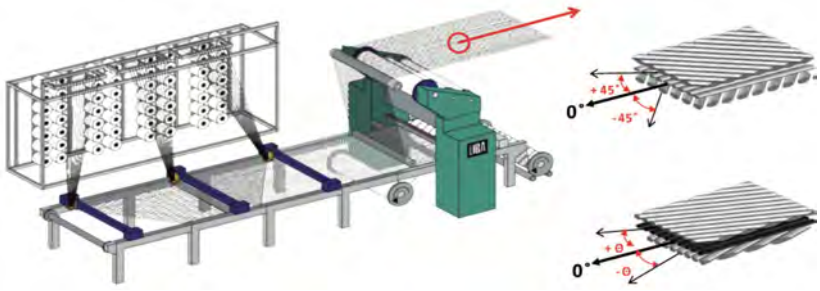

Fig. 1.23: Computer-controlled NCF manufacturing machine at Chomarat. A shallow angle is possible up to 20 degrees [35].

Step 3: *Combining*. This last step of the manufacturing process ties the multiaxial plies together and consolidates the laminate. The plies are stitched together by a very fine thread to reduce, as much as possible, the impact of foreign materials and the creation of voids.

According to the manufacturer, the final product is suitable for all lamination techniques, including prepreg, hand lay-up (HLU), liquid resin infusion (LRI), resin film infusion (RFI), resin transfer molding (RTM) and vacuum assisted resin transfer molding (VARTM).

Advantages

The thin-ply NCF is seen as an innovative material that can potentially lead to major changes in how composite laminates will be designed and manufactured in the near future. Several advantages regarding the use of this material are listed below:

- Greater freedom in laminate design. Per given laminate thickness, more plies can be accommodated when thin-plies are used.
- Delay in the onset of damage mechanisms. As a result of the decrease in the thickness of the ply, failure mechanisms such as matrix cracking and delamination can be delayed close to the fiber failure [36].
- Manufacturing cost reduction. The multi-axial structure reduces the cost of manufacturing during the lamination process and has the added advantage of ease-of-handling [33].
- Less resin areas. The spread tow plies display improved fiber distribution resulting in fewer resin rich areas or weaker zones in comparison to standard-ply NCF configurations.
- Homogenization. When the number of plies is very large, i.e. by using thin plies, it is possible to achieve a null, or close to null, coupling matrix without imposing symmetry [37].

1.5 Damage occurrence on thin-plies

If a ply distribution through the laminate thickness is better than grouping plies, as discussed previously in section 1.3, one can envisage a remarkable improvement to the onset of the microcraking and delamination damage if the ply thickness is reduced below standard values. During the last decade, with the acquisition of skills in fiber spreading (section 1.4), producing thin-ply laminates with ply thickness's as little as 0.02 mm has become feasible.

Until very recently, few research works can be found in the literature on the use of thin-ply based laminates. In this section, only information related to the damage occurrence and laminate strength of thin-ply laminates is summarized. The available studies are divided in two categories: experimental and numerical/analytical works.

1.5.1 Experimental work

One pioneering work related to thin plies was carried out by Sihn et al. [1], who performed an extensive experimental campaign to study the thickness effect of laminate composites with dispersed and grouped plies, in which the plies were designed as THIN-ply and THICK-ply, respectively. The ply thickness studied was 0.04 mm for the THIN-ply laminate and 0.2 mm (5×0.04) for the THICK-ply layup. Uniaxial tension static and fatigue loading were applied on both un-notched and open-hole specimens. Impact and compression after impact tests were also conducted. In general terms, the results indicated suppression and/or delay of microcracking, delamination and splitting damage on both un-notched and open-hole THIN-ply specimens. In both configurations, THICK-ply specimens showed a noticeable decrease in the ultimate strain, which indicates severe damage due to microcracks and delamination, see Figure 1.24 for (a) un-notched and (b) open-hole specimens. On the contrary, THIN-ply specimens retained linearity nearly up to the ultimate failure stress.

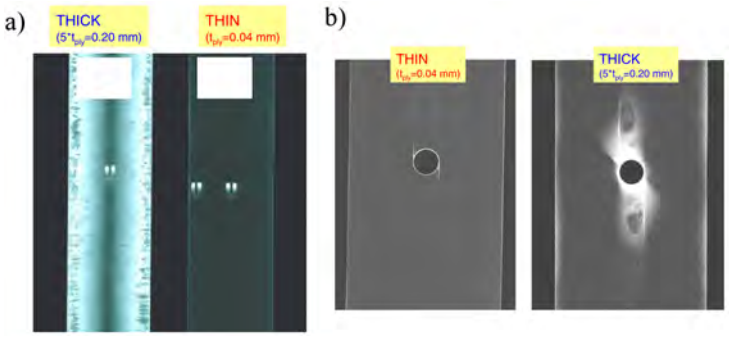

Fig. 1.24: X-ray images of the internal damage for (a) un-notched and (b) open-hole specimens in fatigue loading [1].

A similar work, albeit using different grade materials, was conducted by Yokozeki et al. [38]. In this study, they investigated the properties of several strengths, as well as the damage resistance of thin-ply laminates. Specifically, uni-axial tension in static and fatigue loading, static compression, open-hole and compression after impact tests were investigated by comparing results between laminates manufactured from thin-plies of $75g/m^2$ and standard-

plies of $145g/m^2$. It is worth mentioning that the in-plane stiffness, total thickness and lay-up ratio of orientation angles of the thin-ply laminate were the same as the standard-ply laminate. The results showed a substantial improvement in terms of ultimate strength of the thin-ply laminate with respect to the standard-ply laminate. About 10% in compression tests without hole, open-hole compression and compression after impact and 20% in the tension test. Similar results were obtained in Ref. [1].

More recently, Amacher et al. [29] carried out a broader experimental campaign in order to study the influence of ply thickness on the ultimate strength and the onset of damage at lamina, laminates and components. In this work, three different ply thickness were studied: $30g/m^2$, $100g/m^2$ and $300g/m^2$. Uni-axial tension, open-hole compression and open-hole tensile fatigue tests showed very significant improvements in terms of the onset of damage and ultimate strength when decreasing the ply thickness; in agreement with the previous studies available [1,38]. For instance, Fig. 1.25 shows the ultimate strength and onset of damage with respect to ply thickness in unnotched quasi-isotropic tensile tests. It is demonstrated that using ultra-thin plies ($30g/m^2$), damage mechanisms can be delayed until the ultimate failure strain of the laminate. In this case, the specimen fails in a quasi-brittle manner with a clear net section, while the remaining failed laminates (with thicker plies) show extensive matrix cracking and delamination.

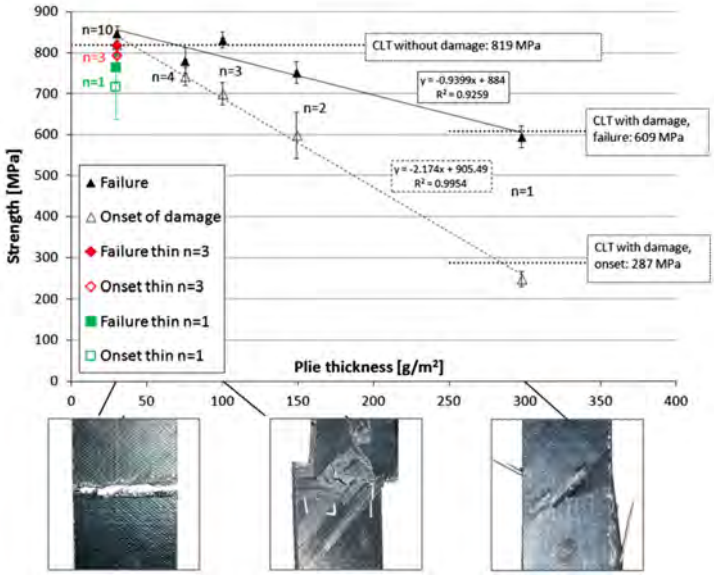

Fig. 1.25: Ultimate strength and onset of damage with respect to ply thickness in unnotched quasi-isotropic tensile tests [29].

In other studies, such as Yokozeki et al. [39], the damage resistance of carbon fiber/toughened epoxy thin-ply laminates subjected to out-of-plane loading was analyzed. Quasi-isotropic laminates were manufactured with standard-ply and thin-ply prepreg with the same ply thickness as used in Ref. [38]. The main objective of this work was to examine the effect of ply thickness on the damage accumulation process under indentation. During the transverse loading the sequence of damage events was quite different between both configurations: accumulation and growth of matrix cracks and delaminations were observed in the standard laminate, whereas sudden fiber fracture occurred in thin-ply laminates, see Figure 1.26.

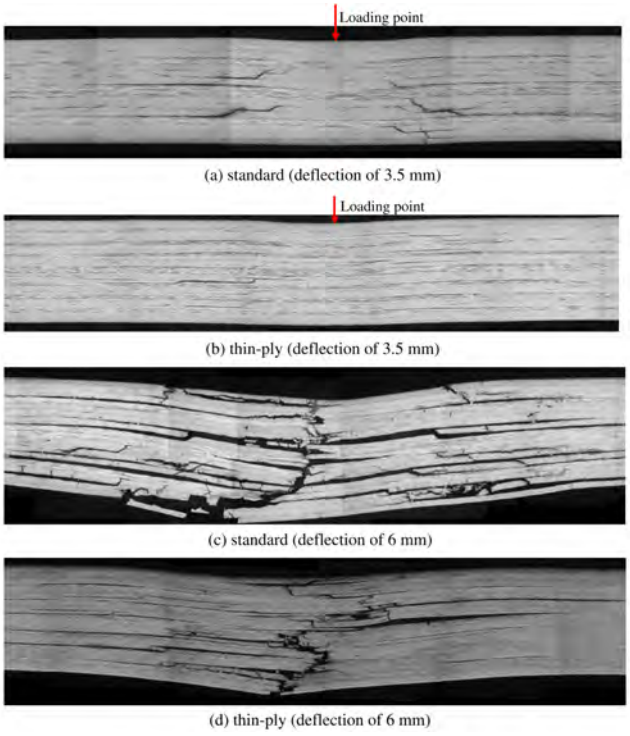

Fig. 1.26: Cross-sectional images of different indentation loads for the standard and thin configurations [39].

One year later, Saito et al. [40] studied the effect of ply thickness on impact damage morphology. Quasi-isotropic laminates were manufactured with 0.038 mm and 0.147 mm ply thicknesses, in this article designated as thin-ply and thick-ply laminates, respectively. Impact tests were carried out and the damage inside the laminates was evaluated by using ultrasonic scanning and sectional fractrography. After that, compression after impact was also conducted. The results obtained in this study showed that transverse

cracks decreased drastically in thin-ply laminates, and localized delaminations were largely extended, in agreement with Refs. [1, 39]. However, the compressive strength after impact for the thin-ply laminates was 23% higher than thick-ply laminates.

On the other hand, thin-ply configurations in a multi-axial form, e.g. thin-ply Non-crimp-Fabrics (NCFs), have received special attention thanks to their ease of handling an low manufacturing costs. One pioneering work using thin-ply NCF laminates was carried out by Arteiro et al. [41], who conducted an extensive experimental test program to investigate the mechanical performance of thin-ply NCF laminates with and without notches. Two different thin-ply NCF laminates were tested, the first with an asymmetric laminate and the second with a symmetric laminate with blocked plies or with ply clustering. The results showed that thin-ply laminates loaded in tension exhibit an approximately linear behavior up to final failure and without severe damage such as extensive matrix cracking and delamination, in agreement with Refs. [1, 29]. This behavior was clearly observed in the lay-up without ply clustering (asymmetric configuration) which exhibited a brittle type of net-section failure mode, dominated by fiber breakage, as shown in Fig. 1.27.

(a) Lay-up 1 (asymmetric) laminate.

(b) Lay-up 2 (symmetric) laminate.

Fig. 1.27: Representative unnotched tension thin-ply NCF specimens after testing [41].

With regards to those specimens with notches, this ability to suppress damage development was able to get a low notch sensitivity. Additionally,

a remarkable improvement was observed in bolt-bearing configurations over traditional composite materials and which is in agreement with the thin-ply UD material studied in Ref. [29].

Furthermore, as the previous study [41] was restricted to the notched response of small scale samples, Arteiro et al. [42] studied the large damage capability of the same material. The residual strength of thin-ply NCF laminates with large through-the-thickness cracks was investigated. These experiments show that thin-ply NCFs also exhibit high resistance to propagation of large cracks. Fig. 1.28 shows the fractured center-notched plate after testing.

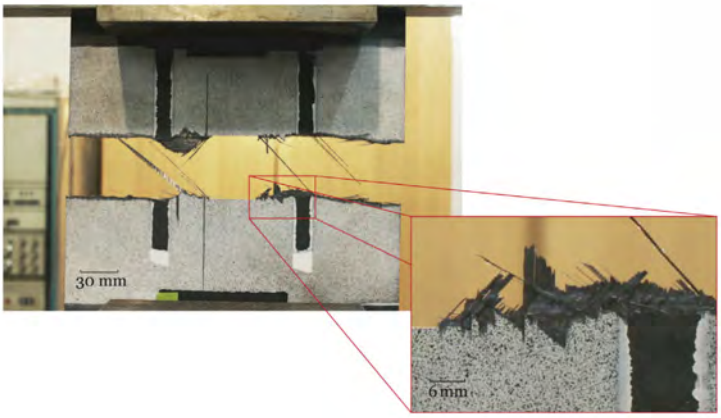

Fig. 1.28: Fracture center-notched thin-ply NCF plate after testing [42].

1.5.2 Numerical and analytical works

Based on the experimental works described in the previous section, there is a clear difference on the initiation of the damage mechanisms between standard-ply and thin-ply materials, and their evolution until the laminate failure. To summarize the aforementioned experimental results, Fig. 1.29 provides a qualitative description of how thin-ply based laminates modify the sequence of damage events with respect to standard thickness plies.

The question arises whether current design procedures (analytical or numerical models) can capture the particular phenomenology of thin-ply composite materials, which is an obvious requirement if these new materials are to be introduced into an industrial context. Due to the novelty of this material little research is available in the literature.

For instance, Arteiro et al. [44] assessed the validity of three current analytical tools when predicting the residual strength of thin-ply Non-Crimp-Fabrics. In this study, point-stress and average-stress models [45], and a finite fracture mechanics model [46] were used to predict the notched response of

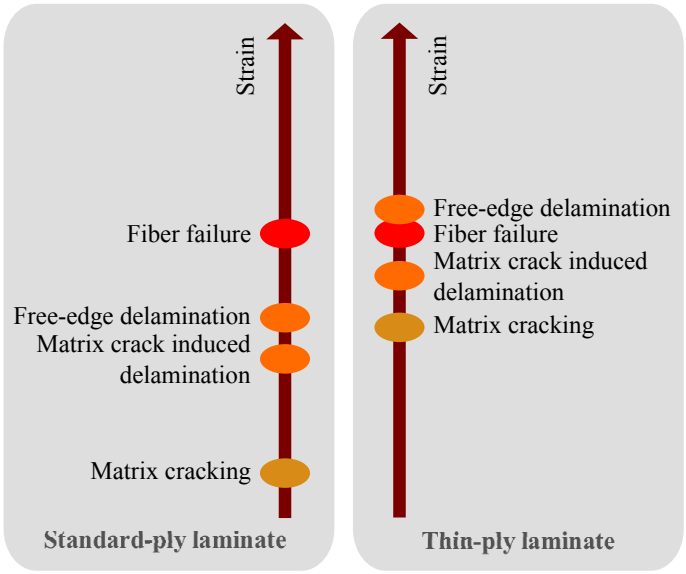

Fig. 1.29: Qualitative depiction of the sequence of damage mechanisms between standard-ply and thin-ply laminates [43].

thin-ply laminates. The experimental results obtained in Ref. [41] were compared with the predictions from the aforementioned models. It was demonstrated that, these models reasonably predict both tensile and compression notched strength and they account for the effect of the ply thickness.

As the previous study was restricted to the notched response of small scale samples [44], in another work by Arteiro et al. [42], they studied the large damage capability of the same material conducting experiments (as reported in the previous section) and their predictions. The same analysis methods used in Ref. [44] in addition to linear fracture mechanics and inherent flaw were used to predict large damage capability. Classical linear elastic fracture mechanics, inherent flaw, point-stress and average stress failed to predict the residual strength of laminated plates with large through-thickness cracks. Instead, taking into account the R-curve of the material in the finite fracture mechanics analysis, good predictions were obtained. It is worth mentioning, that the previous models did not require the use of finite element analysis or complex methods and they established adequate trends that can be very useful in preliminary studies.

With the prediction of matrix cracking, the current in-situ strength theories [2], which are used in most of the failure criteria such as [27, 47–49], already take into account the effect of ply thickness. However, they are not validated for such low grade materials (thin-plies) and they predict asymptotic behavior for very low thicknesses. In a work conducted by Camanho

et al. [50], the effect of the ply thickness on the in-situ strengths based on fracture mechanics models [2] is discussed. The calculated in-situ strengths are illustrated in Figure 1.30. It is well appreciated that transverse tensile and compression strengths (respectively Y_t and Y_c), and longitudinal and transverse shear strengths (respectively S_l and S_t) increase when the thickness of the ply decreases.

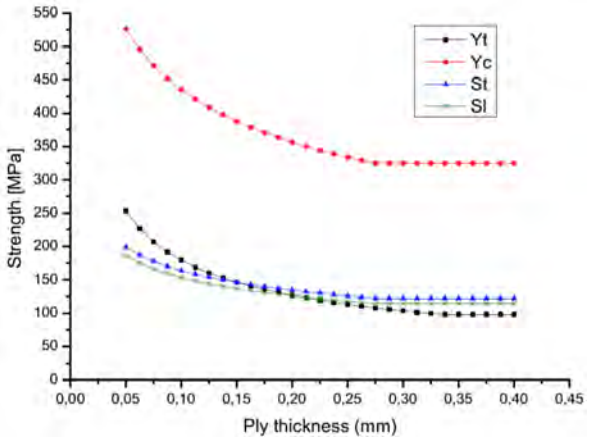

Fig. 1.30: Effect of ply thickness on its in-situ strengths [50].

Amacher et al. [29] used the in-situ strength theory developed by Camanho et al. [2] and they used classical laminate theory to calculate the laminate stresses of a ultra-thin quasi-isotropic unnotched laminate under tensile. However, the predictions obtained in that work did not follow the in-situ strength theory: the measured onsets scaled linearly, whereas the in-situ strength theory leads to an asymptotic relation. These discrepancies suggest that other limiting mechanisms at the free-edge of the laminate might affect the overall scaling observed on the macroscopic level. However, further studies are required to improve and/or validate existing theories, such as the in-situ strength model, for a wider range of thin-ply composites.

More recently, some studies have focused on transverse cracking using micro-mechanical models [51, 52] for a wider range of ply thickness. For instance, Arteiro et al. [52] studied the in-situ effect for ultra-thin plies using a micromechanical model by means of the finite element analysis. Their results showed that thicker transverse laminae trigger cracks that suddenly propagate and lead to stress relaxation, whereas thinner transverse laminae (ultra-thin plies) show a gradual crack extension which does not completely penetrate through the thickness, making stress relaxation much more difficult, as shown in Fig. 1.31.

In another similar work, Saito et al. [51] numerically investigated matrix

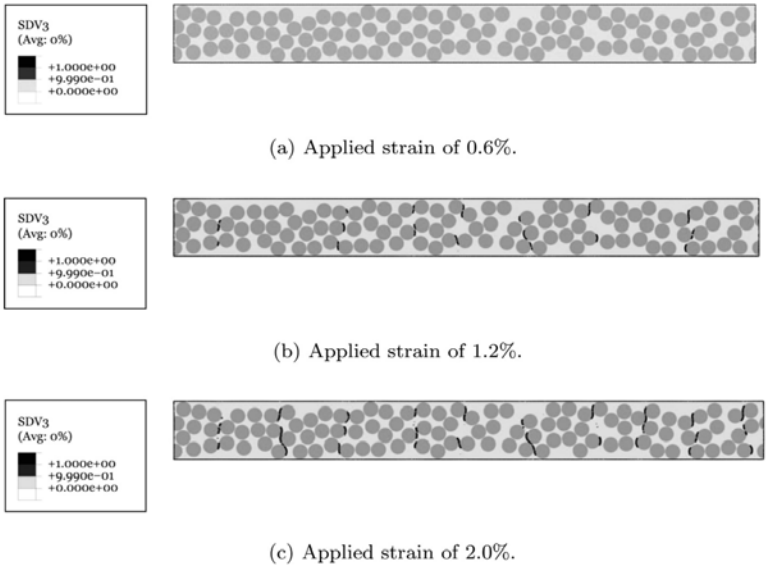

Fig. 1.31: Contour plots of the matrix damage variable for the ultra-thin 90 degree ply with different applied strains [52].

cracking in the inner transverse ply of a thin-ply laminate, and the effect of the stiffness of the adjacent plies, to clarify the mechanisms of transverse damage suppression in thin-ply laminates. The numerical results were consistent with the experiments [53] with drastic penetration of the transverse cracks for the thicker 90° plies. When there were 45° plies adjacent to the inner 90° layer, matrix crack propagation was faster than when there were 0° adjacent plies, confirming the effect of the stiffness of adjacent plies on the constraint imposed to the 90° laminae. These results highlight the importance of the ply location and orientation through the laminate thickness with respect to the load direction.

With regards to other studies, there has been a focus on predicting edge delamination using the finite element method. One of the first numerical works on the prediction of free-edge delamination in thin-ply laminated composites was co-authored by this doctoral candidate in [50]. The numerical model was developed with Abaqus software [54] and it included user-defined cohesive elements at each ply interface, previously developed by Turon et al. [16]. Different quasi-isotropic laminates $[45_n/-45_n/0_n/90_n]_{rs}$ with $n = 1, 2, 3$ and $r = 1, 3, 6$ made of T700/M21 fiber/epoxy system were simulated all the while keeping the total thickness of the laminate constant. Fig. 1.32 illustrates the deformed shapes at the free-edge of two laminates: a lay-up with ply clustering ($n = 3$ and $r = 1$) termed thick-ply laminate (on the left) and a lay-up with sub-laminate repetition ($n = 1$ and $r = 6$) termed

thin-ply laminate. The relative displacement between plies for the thin-ply configuration (Fig. 1.32b) is smaller than that of the thick-ply laminate (Fig. 1.32a), which results in a reduction of the interlaminar stresses at the free-edge. Thus, for an applied strain of 1%, the thick-ply laminate is more prone to delamination at the free-edge than the thin-ply configuration is.

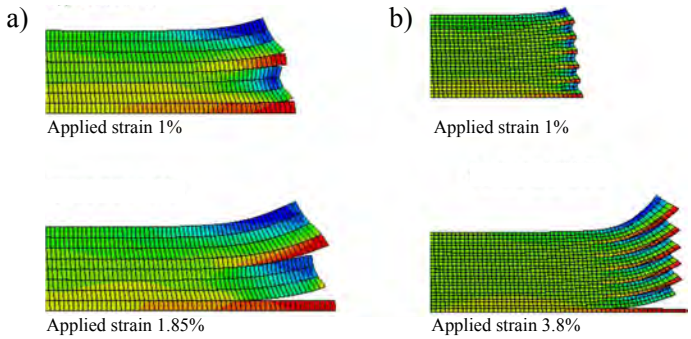

Fig. 1.32: Deformed shapes of the free-edge delamination in (a) thick-ply laminate $[45_3/-45_3/0_3/90_3]_{2s}$ and (b) thin-ply laminate laminate $[45/-45/0/90]_{6s}$ [50].

Fig. 1.33 shows the predicted strain corresponding to the onset of free-edge delamination in terms of the ply thickness. It is clearly seen that delamination onset strain increases considerably when ply thickness is reduced.

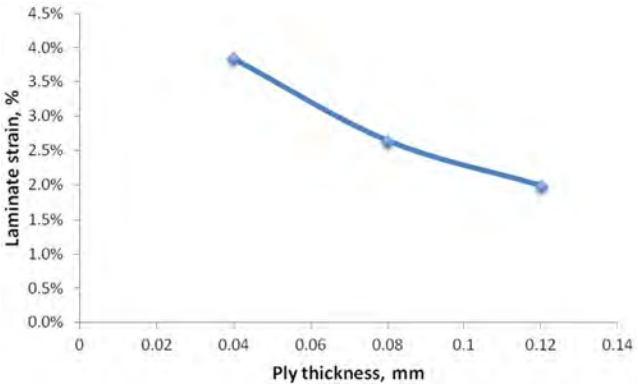

Fig. 1.33: Onset free-edge delamination strain as function of the ply thickness [50].

These numerical results are a good initial step towards understanding the effect of thin plies in delamination resistance at free-edges but further investigations should be conducted. For instance, the presence of matrix cracks at the free-edge may also induce delaminations [10, 20].

1.6 Challenges and research objectives addressed

Departing from an emerging technology like tow-spreading thin-ply production, the aim of this Ph.D. thesis is to improve understanding the delamination resistance of thin-ply NCF laminates and assess the validity of current predictive tools for their design.

Most of the current work is focused on material characterization at the laminate or component level, such as un-notched strength tests, notched tests, open-hole, impact, bolted-joint tests, etc., and the residual strength is the main parameter with which to compare standard grade materials. However, none of them places any particular emphasis on the onset of damage mechanisms and their subsequent development at the laminate edges.

The onset and the progression of damage in a wide range of geometries starts at free-edges, e.g. open-holes, ply drop terminations, skin-stiffeners, etc. The high interlaminar stresses in this region generate delamination which may affect the structural integrity of the laminate. Thus, the case of a composite laminate under tensile loading has become a good benchmark problem for the research community to analyze the sequence of damage events which affect the laminate failure. Then, the effect of ply thickness on damage occurrence at the free-edge should be re-examined when dealing with thin-plies because a different phenomenology has been observed in comparison with standard grade materials. The interaction between failure mechanisms, i.e. delamination triggered by matrix cracks, should also be accounted for by using failure criteria sensitive to ply thickness, ply orientation and location. Moreover, the applicability of quick design tools for the onset of delamination has yet to be assessed and constitutes a computational challenge because of the large number of stacking sequences when thin-plies are used for a laminate of useful thickness.

As advanced composites are frequently used in strength critical applications in which they have to withstand loads in different directions, thus, a laminate under different loading directions is of particular interest to the scientific community. In view of thin-plies being capable of delaying the first-ply failure and improving the ultimate strength over standard-ply laminates, one can envisage an improved laminate strength behavior when the load direction is changed. Nevertheless, the delamination resistance of thin-ply laminates under different loading directions has not yet been investigated.

Therefore, the objectives of this thesis derive from the above challenges. These objectives have been solved systematically and each of them corresponds to a paper:

A. Enhancing the understanding of the damage mechanisms observed at the free-edge of thin-ply NCF laminates under different loading directions.

B. Evaluating the capability of current advanced design procedures to predict the onset of free-edge delamination on laminates made of thin-plies.

C. Establishing a design procedure to search for the quasi-isotropic laminate with optimal delamination resistance under off-axis loads.

Objective A aims to better understand the occurrence and the sequence of damage mechanisms at the free-edge of thin-ply laminates by conducting an experimental campaign on tensile tests. A detailed analysis is performed on the damage development at the edges of a quasi-isotropic laminate made of thin-ply NCF under different off-axis loads. The lay-up studied has two regions or sub-laminates, with and without ply clustering, in order to study the effect of the ply thickness in the same lay-up. Moreover, different off-axis loads are analyzed in order to evaluate the strength of the laminate in each direction.

Objective B aims to evaluate the capability of two current and advanced design procedures (a failure criterion for matrix crack induced delamination and cohesive elements) for predicting the experimental behavior of damage mechanisms observed at the free-edges of thin-ply laminates. Both approaches highlight two different phenomena that could either occur simultaneously or could interact: delamination triggered by transverse cracks and delamination generated by high interlaminar normal and shear stresses. In order to asses the validity of the proposed tools in predicting the onset of delamination of the thin-ply laminates, the results obtained in the experimental test program in objective A are compared with the predictions of these methods.

Objective C aims to define a design procedure for seeking quasi-isotropic lay-ups optimized in terms of free-edge delamination resistance under different off-axis loading directions. Using combinatorics, different domains of quasi-isotropic configurations with different ply thickness and orientations are explored. The optimization procedure has been conducted assuming two states of the material: a laminate with and without flaws. The numerical comparison with typical grade CFRP will define the performance of the thin-ply based laminates in terms of delamination resistance.

Chapter 2

Scope of the publications

In this chapter the scope of the publications is described and the coherence of each paper in the context of the thesis is highlighted. Following that, in Chapters 3 and 4, a general discussion of the results and the conclusions are given as a whole.

2.1 Paper A:*"Damage occurrence ..."*

Paper A entitled *Damage occurrence at edges of Non-crimp-fabric thin-ply laminates under off-axis uniaxial loading* [55], presents an experimental study of the damage mechanisms observed at the free-edge of a thin-ply based laminate.

Numerous studies in the literature prove that laminates with dispersed ply orientations are more damage resistance than those with grouped plies. However, the damage that occurs when low grade materials are used (thin-plies) has not been studied in detail. In this paper, a quasi-isotropic $\pi/4$ non-conventional symmetric laminate is devised so that a THIN region (dispersed thin plies) can be distinguished from a THICK region (clustered plies). Then, this laminate is loaded under tension in five different directions: 0° (L0), 22.5° (L23), 45° (L45), 67.5° (L68) and 90° (L90) in order to evaluate the effect of the load direction on damage initiation and ultimate strength. Fig. 2.1 illustrates how the specimens are cut over the panel, and provides the definition of the two regions through the laminate thickness and the ply sequence resulting from each loading direction.

The onset and progress of three damage mechanisms (matrix cracking, delamination triggered by matrix cracks and free-edge delamination) for both regions and each off-axis load direction are analyzed by optically monitoring the specimen at the free-edge.

This experimental study provides knowledge on the damage occurrence when thin plies are grouped (equivalent to standard-ply thickness) or dis-

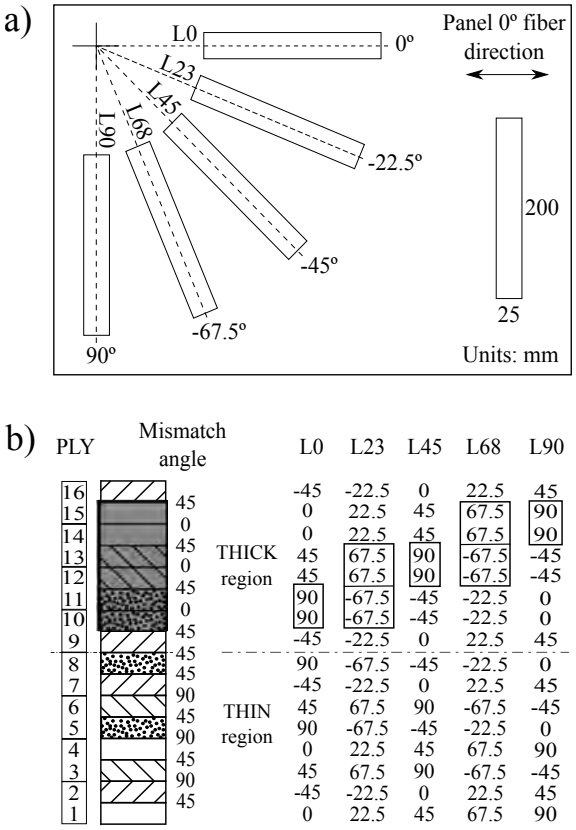

Fig. 2.1: Characteristics of the lay-up and loading conditions. (a) Specimens cut over the panel and (b) Ply configuration for each off-axis load direction [55].

persed (thin plies) in a unique stacking sequence.

2.2 Paper B:*"A quick procedure to predict ..."*

Paper B entitled *A quick procedure to predict free-edge delamination in thin-ply laminates under tension* [43], presents a numerical study on the prediction of edge delamination in thin-ply based laminates.

Delamination at the free-edge of a laminated composite under tension can be triggered by matrix cracks or by high interlaminar stresses. The capability for predicting these phenomena for low grade materials (thin-ply laminates) is particularly challenging because these damage mechanisms are delayed or even suppressed; as observed in the experiments performed in Paper A. Moreover, the use of thin plies increases the number of potential interfaces for delamination and, consequently, the computational cost also increases.

Therefore, developing an efficient modeling approach able to anticipate delamination damage in thin-ply based laminates is of great interest.

In this paper, the initiation of delamination induced by matrix cracks is predicted by means of an existing energy-based failure criterion [22] and classical laminate theory, whereas the onset of free-edge delamination due to interlaminar stresses is predicted by using a finite element model with cohesive elements [16] at ply interfaces. Fig. 2.2 illustrates the free-edge delamination model used in this paper.

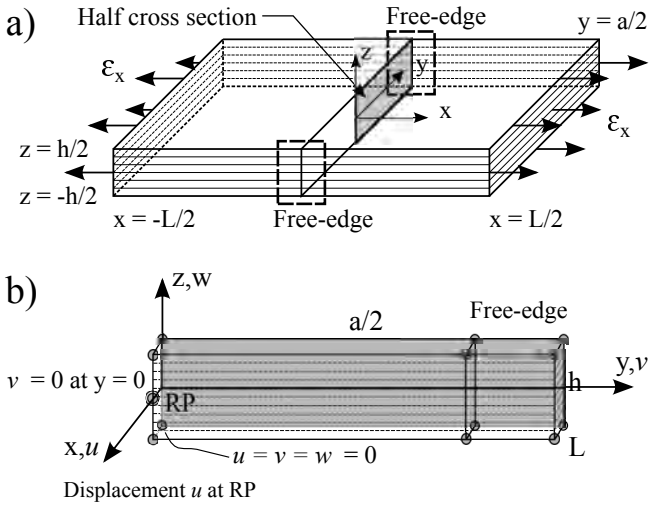

Fig. 2.2: Free-edge delamination model [43]. (a) Composite laminte under tension. (b) Finite element model with cohesive elements at ply interfaces.

This model is first validated by making use of existing published results with standard grade materials (standard-ply laminates) and then, the initiation of delamination is predicted for the thin-ply quasi-isotropic lay-up studied in Paper A.

This numerical study provides knowledge on whether current design procedures (failure criteria and cohesive zone models) can actually capture the particular phenomenology of thin-ply composite materials observed in Paper A, which is an obvious requirement if these new materials are to be introduced into an industrial context.

2.3 Paper C:*"In search of ..."*

Paper C entitled *In search of the quasi-isotropic laminate with optimal delamination resistance under off-axis loads. Effect of the ply sequence and of using thin plies* [56], presents a methodology for determining optimal quasi-isotropic lay-ups

against edge delamination.

Although delamination is one of the most feared failure mechanisms in laminated composites, there is a lack of well established procedures to find the ply configuration with the highest delamination resistance. Nowadays, thin-ply based laminates are gaining interest in the composite community thanks to their ability to delay some failure mechanisms, such as delamination. However, the quantitative estimation of the enlargement on the material design allowable has yet to be quantified.

In this paper, a multi-level methodology is proposed to determine the optimal lay-ups against edge delamination under different off-axis loading directions. Four domains of stacking sequences depending on the ply orientation (quasi-isotropic $\pi/4$ and $\pi/8$ lay-ups) and the type of material (standard UD plies or bi-axial thin-ply NCFs) are explored in order to find the optimal lay-ups against delamination. Tab. 2.1 condenses and exemplifies the characteristics of all the domains considered in this study.

Domain	Potential orientations	Ply thick. (mm)	Num. UD plies	Lay-up rep.	Example
QI4-UD	±45,0,90	0.182	16	1	$[45/-45/90/0/45/-45/90/0]_S$
QI8-UD	±22.5,±45, ±67.5,0,90	0.182	16	1	$[45/22.5/67.5/-45/-67.5/90/0/-22.5]_S$
QI4-NCF	±45,0,90	0.091	32	2	$[(45/90)/(90/-45)/(0/45)/(-45/0)]_{2S}$
QI8-NCF	±22.5,±45, ±67.5,0,90	0.091	32	2	$[(45/90)/(67.5/22.5)/(0/-45)/(-67.5/-22.5)]_{2S}$

Table 2.1: Ply sequence architecture of each of the four domains considered.

The assessment of edge delamination onset for the aforementioned domains establishes two cases: a material with existing flaws equivalent to a matrix crack (delamination can appear at free-edges by high interlaminar stresses, FED, or by matrix crack induced delamination, MCID) and a flawless material (delamination caused either by FED or by matrix cracking once a transverse crack has been formed, TC-MCID).

The multi-level methodology proposed in this paper, divides the problem into four different steps, as shown in Fig. 2.3. Firstly, the initial population of lay-ups is generated by means of combinatorics as a result of the manageable size of the considered domains. Secondly, a first selection of candidates is accomplished using the rules imposed on the ply sequence such as maximum ply clustering or the angle-ply architecture in bi-angle configurations. Following that, a third level of the analysis applies a model using Classical Laminate Theory (CLT) and a set of failure criteria to delete those lay-ups which do not satisfy a reference tensile loading (strain). It is worth mentioning that the point of applying these constraints is to reduce the number of

cases to be analyzed by the finite element model used in the next step. Finally, the resulting lay-ups are evaluated using the free-edge cohesive zone model (FE-CZM) and the failure criteria proposed in paper B. At this point of the analysis, the strain for edge delamination is assessed for any of the damage mechanisms considered and the optimal lay-ups with the maximum strains are obtained.

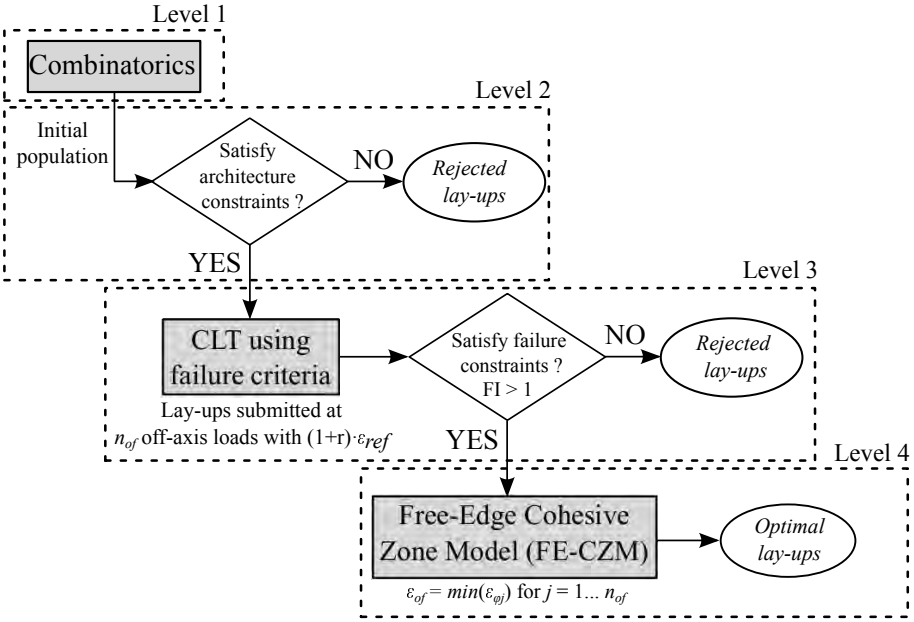

Fig. 2.3: Flowchart of the multi-level optimization methodology.

Although this methodology is specifically devoted to solving cases with stress singularities, many other similar geometries fall into this category such as open-holes, ply drop terminations, etc. Moreover, due to the well-known anisotropy of strength and failure mechanisms, even in elastically isotropic laminates, this study considers the full polar plot of off-axis loads.

Chapter 3

Results and discussion

This chapter summarizes the results of the papers as a whole and discusses them in accordance with five different building blocks: experimental observation of damage occurrence, transverse cracking prediction, edge delamination prediction, effect of the loading direction and design allowables for thin plies.

3.1 Experimental observation of damage occurrence

Experiments were performed on a quasi-isotropic thin-ply laminate under tensile loading and with two regions defined through the laminate thickness, as described in Chapter 2 (Fig. 2.1). By optically monitoring the laminate edge, three different damage mechanisms were observed: transverse cracking (TC), matrix crack induced delamination (MCID) and free-edge delamination (FED).

These damage mechanisms first occurred in the region where the thin-plies are clustered (THICK-ply region). TC occurred for the transverse plies oriented at 67.5° and 90° and then extensive delamination from these cracks (MCID) occurred for most of the lay-ups. Some plies also exhibited edge delamination as a result of high interlaminar stresses (FED), whereas the first-ply failure and the consequent delaminations (either by MCID or FED) in the region where plies are dispersed (THIN-ply region) occurred under larger strains. Fig. 3.1 illustrates the state of damage at the free-edge for each lay-up when a strain of 1.25% was applied and shows the extensive damage, in the form of matrix cracking and delamination, in the THICK region.

The critical strains of the three damage mechanisms considered for each lay-up and for each region are summarized in Fig. 3.2. This figure provides a visual depiction of the damage sequence for each laminate.

Fig. 3.1: Damage occurrence under an applied strain of 1.25% [55].

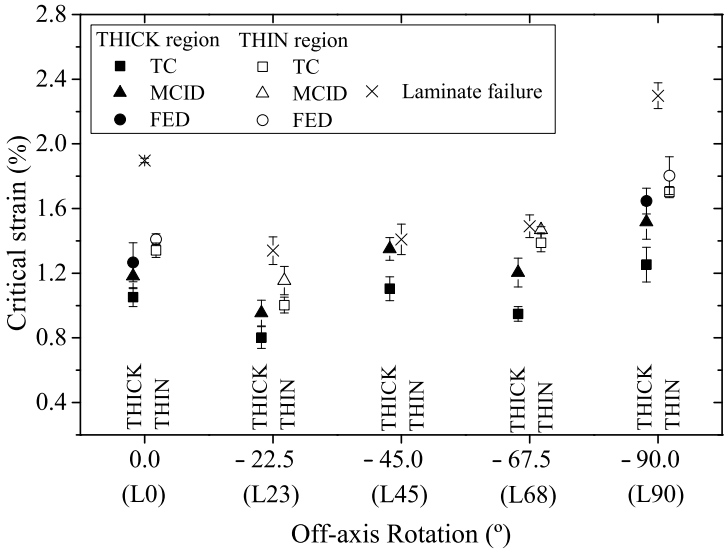

Fig. 3.2: Onset strain of damage mechanisms [55].

At the early stages of damage (initiation), the damage in one region does not affect the other region. Moreover, we also confirm that any bending/lateral displacement was observed during the experiments at this stage. However, close to the specimen's collapse, the damage at the free-edge became severe and failure mechanisms clearly interact between regions.

The experimental results provide evidence of the delay or even suppression of some damage mechanisms in the THIN-ply region, e.g., TC for lay-

ups L0, L23, L68 and L90 or the suppression of the three damage mechanisms for lay-up L45 (Fig. 3.2). Furthermore, lay-ups L0 and L90, which exhibited damage onset later than L23, L45 and L68, had the highest ultimate strengths. The differences among the lay-ups, resulting from the off-axis rotation, are discussed later in section 3.4.

3.2 Transverse cracking prediction

The differences in the onset strains for transverse cracking at each region can be explained by *in situ strength* theories [2]. These theories predict an increase in ply strength when ply thickness decreases. This effect is explained in detail in Paper B, where the onset of transverse cracking is predicted for both regions by means of a failure criterion [49] and classical lamination theory [57].

The comparison between the experimental results and the numerical predictions is summarized in Tab. 3.1. The predicted laminate stress for transverse cracking at the THICK region is lower than that of the THIN region. However, the predictions using the failure criteria over-estimate the experimental results. The most plausible explanation for this is that the proposed theoretical approach (CLT) does not take into account interlaminar stresses at free-edges, thus, it under-estimates the stresses in this region. In addition, the stress prediction using CLT depends only on the ply orientation and thus, lay-ups L0, L45 and L90 or lay-ups L23 and L68 result in the same laminate stress for transverse cracking.

Despite the aforementioned over-prediction, the in-situ strength ratio η_{is}°, exhibits a reasonable agreement between predictions and experiments: experiments show an increase in the onset strain for transverse cracking at the THIN region, with respect to that of the THICK region, of more than 24%, whereas for the predictions this value is around 38% (Tab. 3.1).

	THICK region		THIN region			
Ref.	Analytical σ_c° (MPa)	Experimental σ_c° (MPa)	Analytical σ_c° (MPa)	Experimental σ_c° (MPa)	Experimental η_{is}°	Predicted η_{is}°
L0	528.6	445	732.3	556	1.25	1.38
L23	521.4	319	729.6	394	1.24	1.40
L45	528.6	467	732.3	-	-	1.38
L68	521.4	399	729.6	566	1.42	1.40
L90	528.6	520	732.3	699	1.34	1.38

Table 3.1: Laminate stresses (σ_c°) and in situ laminate strength ratio (η_{is}°) for transverse cracking between regions [43].

However, further research into these theories should be carried out because they predict an asymptotic behavior when the ply thickness is significantly reduced. Moreover, further investigations should be pursued to assess

the effect of interlaminar stresses which may affect the onset of this damage mechanism at the free edge.

3.3 Edge delamination prediction

In this thesis edge delamination is predicted from two sources: delaminations triggered by matrix cracks (MCID) and free-edge delamination (FED) due to high interlaminar stressess. The models used here to predict these failure mechanisms are explained in detail in Paper B. The numerical predictions for the onset of both failure mechanisms along with the experimental observations are summarized in Tab. 3.2.

	Ultimate	THICK region				THIN region			
Ref.	failure [55]	Int.	Exp. [55]	Num. prediction	Dif. (%)	Int.	Exp. [55]	Num. prediction	Dif. (%)
L0	1.897	9	$1.181^{\dagger}$,1.267^{*}	1.586^{*}	+25	8	1.410^{*}	1.798^{*}	+28
L23	1.360	11,12	$0.953^{\dagger}$	$0.825^{\dagger}$	-13	1	$1.154^{\dagger}$	$1.110^{\dagger}$	-4
L45	1.389	11,12	$1.350^{\dagger}$	$1.750^{\dagger}$	+30	4	-	2.102^{*}	-
L68	1.491	9,12	$1.204^{\dagger}$	$1.140^{\dagger}$	-5	1,2	$1.468^{\dagger}$	$1.535^{\dagger}$	+5
L90	2.344	11,12	$1.516^{\dagger}$,1.647^{*}	$1.700^{\dagger}$	+12	2	1.803^{*}	2.200^{*}	+22

† MCID, * FED

Table 3.2: Delamination strains in (%) at THICK and THIN regions [43]

The predicted results follow the same trend as those observed in the experiments: the onset of MCID and FED at the THIN-ply region is delayed with respect to the THICK-ply region. Tab. 3.3 summarizes the increase in the onset strain for edge delamination measured at the THIN-ply region vs. the THICK region. The improvement in the onset of delamination triggered by matrix cracks at the THIN-ply region with respect to the THICK-ply has increased by approximately 20% (experiments) and 34% (predictions). With delaminations induced by high interlaminar stresses (FED), experiments show a minimum increase of 10% while the predictions are above 13%.

The aforementioned results indicate that the proposed models qualitatively capture the effect of the ply location and ply thickness on the damage occurrence. However, the quantitative values on the onset strain for edge delamination are reasonably predicted with differences below 31%, as shown in Tab. 3.2. The greater differences, e.g. lay-ups L0, L45 and L90, are attributed to the interaction among delaminations triggered by matrix cracks and the subsequent delaminations, delaminations originating from the interlaminar stresses induced by the free-edge effects. A strong interaction between both failure modes exists, and this interaction is not accounted for in the predictive models proposed in Paper B. If computational cost was not a concern, advanced models including progressive intralaminar and interlaminar damage could be considered to obtain more accurate predictions.

	Improvement over the THICK-ply region (%)	
Lay-up	Experiments	Predictions
L0*	11.3	13.3
L23†	21.1	34.5
L45	-	-
L68†	21.9	34.6
L90*	9.5	29.4

† MCID, *FED

Table 3.3: Improvement in the onset of delamination at the THIN region vs. the THICK region. Note that the improvement is quantified when the same damage mechanism is observed at both regions.

3.4 Effect of the loading direction

As a result of the differences in the damage occurrence caused by the ply thickness effect, the loading direction of the laminate also plays an important role in the onset of damage mechanisms and the consequent laminate failure. For instance, the non-crimp-fabric quasi-isotropic laminate studied in Papers A and B has been shown to be isotropic in in-plane stiffness but totally anisotropic in strength. Fig. 3.3 illustrates the crack growth for each lay-up resulting from the loading directions studied.

Fig. 3.3: Crack growth for each lay-up just before ultimate failure [43].

The lay-ups with plies aligned to the load (L0, L45 and L90) exhibited the highest onset strains and ultimate laminate strengths, see Fig. 3.2. Lay-up L45 was the only one whose strength was reduced due to the rapid and extensive damage growth in the THICK-ply region, see Fig. 3.3. The main

differences between these lay-ups was the position of the 0° plies: L0 has the 0° plies at the outer faces, L45 has these distributed through the ply thickness and in L90 these are located at the mid-plane. The experiments showed that those lay-ups with 0° plies located close to the mid-plane or at the outer faces, exhibited the highest laminate strengths. On the other hand, for the lay-ups loaded off-axis (none of the ply orientations matching the loading direction, L23 and L68), exhibited extensive crack growth in the form of transverse cracking and delamination until laminate failure.

In order to provide a qualitative explanation for the high anisotropy in strength between on-axis and off-axis lay-ups, Fig. 3.5 shows the deformed shapes at the free-edge for each lay-up which are obtained by the finite element model.

Based on the well-known anisotropy of strength observed in the experiments and captured well by the predictive models, even in elastically isotropic laminates, Paper C considers the full polar plot of off-axis loads for a $[\pm 45/0/90]_{2S}$ quasi-isotropic lay-up. In this case, the critical strain for delamination due to high interlaminar stresses (FED) is calculated for several loading directions between 0° and 180°, as shown in Fig. 3.4.

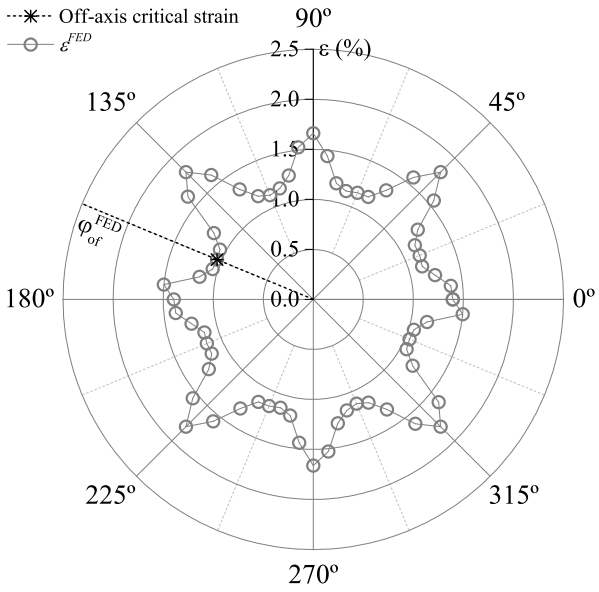

Fig. 3.4: Off-axis failure strains due to free-edge delamination (FED) for a $[\pm 45/0/90]_{2S}$ [56].

This polar representation demonstrates once again that the design of a stacking sequence for one loading direction can behave in an entirely different manner under another loading direction, even in elastically isotropic laminates.

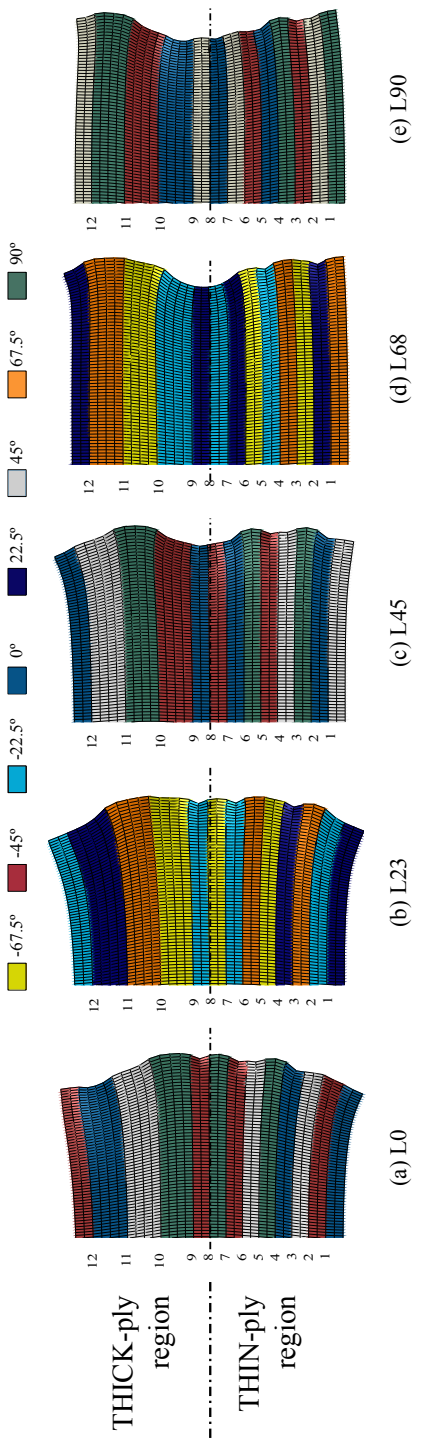

Fig. 3.5: Deformed shapes at the edge of each lay-up resulting from the load directions [43].

3.5 Design allowables for thin plies

The experimental and numerical results presented in Papers A and B, respectively, demonstrate the advantages of thin plies in delaying, or suppressing, the onset of damage mechanisms. Based on this, the material design allowables can be enhanced (larger allowable strain) when thin-ply based laminates are used. In a numerical study to find quasi-isotropic laminates with optimal edge delamination resistance (Paper C), several optimal lay-ups were obtained using two materials (standard-ply and thin-ply NCFs) and two quasi-isotropic ply configurations made of ply orientations multiples of $\pi/4$ and $\pi/8$. Tab. 3.4 summarizes the results obtained for all the case studies considered in [56].

	Domain	Flawless laminate, (FLAWLESS)	Laminate with flaws, (WFLAWS)
Baseline	QI4-UD	-	-
Standard-ply UD	QI4-UD	1.7	6.6
	QI8-UD	-	7.9
Thin-ply NCF	QI4-NCF	42.2	72.3
	QI8-NCF	39.3	72.5

Table 3.4: Improvements in % over the baseline lay-up for each case study.

In a first case study, the laminate was considered flawless, i.e. delamination can only occur due to high interlaminar stresses (FED) or once a matrix crack has been formed using the TC-MCID criterion [56]. The resulting optimal lay-ups made of standard plies show that the critical off-axis strain is barely improved with respect to a baseline lay-up, which is also made of the same plies. A mere 2% of improvement is obtained in the minimum off-axis strain for delamination, as shown in Tab. 3.4. On the contrary, when thin-ply based materials are used (thin-ply NCFs), the critical strain for edge delamination with respect to the baseline lay-up is significantly increased (by more than 40%), not only in the critical loading direction, but in the other directions as well (see Tab. 3.4). The polar representation of the critical strain for edge delamination from two optimal thin-ply based laminates is represented in Fig. 3.6 assuming a flawless material.

An interesting result from Fig. 3.6 is that the polar plot of the critical strain tends to be isotropic as the elastic behavior is. In this case, the tolerance for a shift in the direction of the load and the total safe area for design are greatly enlarged in comparison to standard plies.

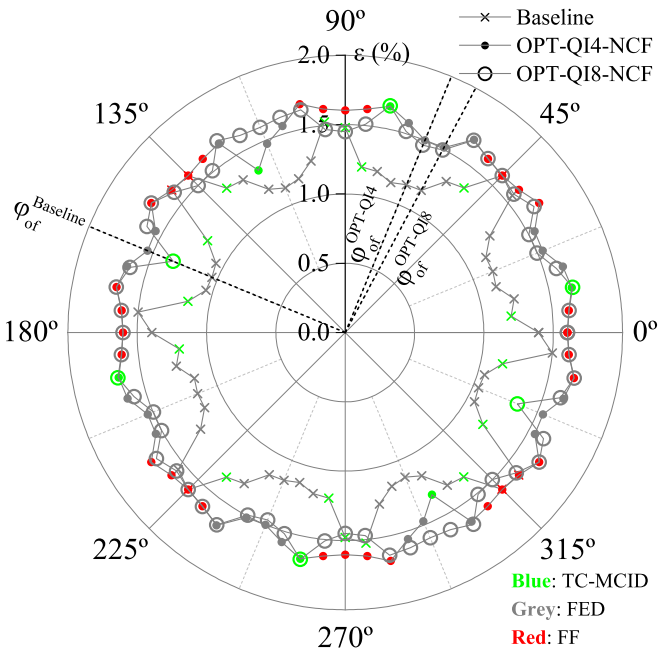

Fig. 3.6: Off-axis edge delamination strain for two optimal thin-ply lay-ups assuming a flawless laminate [56]. For the references to color in this figure legend, the reader is referred to the web version of this thesis or article.

In a second case study, the laminate was considered to contain flaws, i.e. delamination can appear at free-edges by matrix crack induced delamination (MCID) or by FED. The same trend is obtained with respect to the previous case study. The use of standard plies barely improves the baseline reference strain (only by 8%, see Tab. 3.4) while when using thin plies the critical delamination strain is increased up to 70% (Tab. 3.4). The polar representation of the critical strain for edge delamination from two optimal thin-ply based laminates is represented in Fig. 3.7 assuming a material with flaws. It is worth mentioning that this case study can be considered as the most conservative approach for predicting edge delamination because the MCID failure criterion becomes the dominant failure mechanism in most of the off-axis loading directions.

In general terms, small differences are obtained between quasi-isotropic conventional $\pi/4$ (QI4) and non-conventional $\pi/8$ (QI8) laminates for the case studies considered here. However, when the driven failure mechanism is FED (delamination originated by interlaminar normal and shear stresses) the conventional laminates outperform the non-conventional ones. This can be explained by the use of small step angles such as, $\pi/8$, which tend to increase the interlaminar stresses at the free edge.

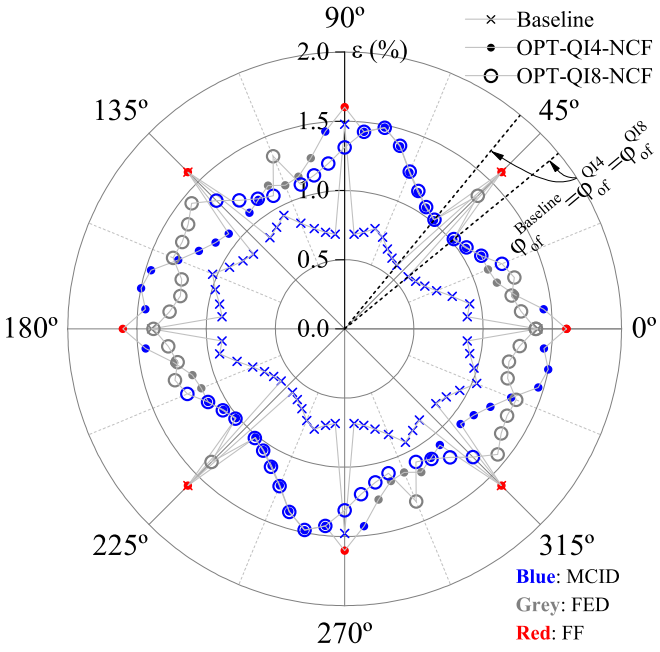

Fig. 3.7: Off-axis edge delamination strain for two optimal thin-ply lay-ups assuming a laminate with flaws [56]. For the references to color in this figure legend, the reader is referred to the web version of this thesis or article.

Furthermore, defects or manufacturing flaws are also responsible for a shift in the most critical failure mechanism for edge delamination. Without them, interlaminar normal and shear stresses are the more restrictive (Fig. 3.6), while when defects exist, delamination induced by flaws (equivalent to a matrix crack) is the most critical failure mechanism (Fig. 3.7).

Chapter 4

Concluding remarks

4.1 Conclusions

The initiation and development of damage mechanisms at the edge of a thin-ply non-crimp fabric (NCF) laminate under different loading directions was studied experimentally and numerically. Two models were developed for predicting edge delamination from two different sources: an analytical model using a failure criterion for predicting delamination triggered by matrix cracks (MCID) and a finite element model with cohesive elements for predicting free-edge delamination (FED) due to high interlaminar stresses. Then, a methodology was proposed for determining quasi-isotropic lay-ups with optimal edge delamination resistance under off-axis loading directions.

Based on the results obtained from this thesis the following conclusions can be drawn:

- A quasi-isotropic non-crimp-fabric thin-ply laminate under tensile loading has been shown to improve the critical strain for edge delamination by more than 10% by dispersing the thin plies instead of grouping them.
- In order to predict edge delamination, two different formulations are used: a failure criterion for predicting delamination induced by matrix cracks and a finite element model with cohesive elements for predicting delaminations due to high interlaminar stresses. The use of these simplified and rapid models provide a good balance between predictive capabilities and computational effort.
- Overestimated predictions for edge delamination are obtained, in particular for FED. The difficulties in obtaining accurate predictions may be minimized by including the interaction between both transverse cracking and delamination in the simulations.

- Lay-ups loaded on-axis (some ply orientations aligned to the loading direction) usually exhibit the highest onset strains for damage mechanisms and consequently, the highest ultimate laminate strengths. Whereas, lay-ups loaded off-axis (none of the ply orientations match with the loading direction) exhibit extensive crack growth in the form of transverse cracking and delamination until laminate failure.

- The representation of the critical delamination strain in a full polar plot shows that the onset of delamination appears at different load levels with respect to the orientation of the lay-up. Thus, the loading direction of the laminate plays an important role and may actually impair the strength of the laminate.

- In a numerical study, the domains of quasi-isotropic $\pi/4$ and $\pi/8$ lay-ups made of 16 standard-plies (0.182 mm) are explored in order to find those with optimal delamination resistance. Lay-ups with small step angles, such as $\pi/8$, tend to increase the interlaminar stresses at the free-edge and do not improve the delamination resistance of the traditional quasi-isotropic lay-ups with $\pi/4$ step angles.

- For the same domains of ply configurations, when the ply thickness is reduced to half of the standard-ply thickness, 0.091 mm plies (thin-ply NCFs), the critical off-axis strain (full polar plot) for edge delamination can be increased by more than 40% with respect to a baseline laminate made of standard plies.

- When thin plies are used, the polar plot of the critical strain tends to be isotropic as the elastic behavior is. As a consequence, the tolerance to the direction of the load and the total safe area for design are greatly enhanced in comparison to standard-ply laminates. In fact, by reducing the ply thickness, the free-edge delamination strain can be delayed until fiber failure, resulting in the previously mentioned isotropic behavior.

- Defects or manufacturing flaws are also responsible for a shift in the most critical failure mechanism for edge delamination. Without them, interlaminar normal and shear stresses are the most restrictive. In the presence of defects, delamination induced by flaws (equivalent to matrix cracks) is the most critical.

- The results obtained demonstrate the advantages of thin plies in delaying, or even suppressing, the onset of damage mechanisms and they bring to the fore the benefit of incorporating them into the structural design of laminated composites.

4.2 Perspectives and future work

During this Ph.D. thesis, progress into better understanding the delamination behavior of thin plies was made. During the work, problems yet to be solved were revealed which has led to the following suggestions for further research work.

- A non-conventional symmetric lay-up ($B_{ij} = 0$) with different ply thicknesses is studied under tensile loading in Papers A and B. The combination of thin and thick plies at the same lay-up should be re-examined in other types of loading conditions such as impact or bending.
- In Paper B, two available approaches have been challenged in order to predict the onset of edge delamination with respect to ply thickness. Using thinner plies has been shown to modify the sequence of damage events and the interaction between the plies is extremely important. The next step would be to develop a more detailed model able to account for both intralaminar and interlaminar damage in order to predict the whole sequence of damage. The onset, progression and the interaction between damage mechanisms will help to better understand the ply thickness's dependence on the failure of the laminate.
- Several quasi-isotropic $\pi/4$ and $\pi/8$ made of standard-ply and thin-ply materials are found to be optimal for edge delamination resistance in Paper C. The next step would be to perform an experimental test campaign to validate that the proposed lay-ups are more delamination resistant than the baseline lay-up.
- The role of the mismatch angle and the ply orientation from two consecutive plies on the matrix crack induced delamination should be investigated further. A detailed numerical and experimental study should be conducted in order to analyze the effect of the mismatch angle ranging from 0° (ply clustering) to 90° with different ply thicknesses in order to evaluate the damage occurrence and the delamination growth.

References

[1] S. Sihn, R. Kim, K. Kawabe, and S. W. Tsai, "Experimental studies of thin-ply laminated composites," *Composites Science and Technology*, vol. 67, no. 6, pp. 996–1008, 2007.

[2] P. P. Camanho, C. G. Dávila, S. T. Pinho, L. Iannucci, and P. Robinson, "Prediction of in situ strengths and matrix cracking in composites under transverse tension and in-plane shear," *Composites Part A: Applied Science and Manufacturing*, vol. 37, pp. 165–176, February 2006.

[3] F. W. Crossman, W. J. Warren, A. S. D. Wang, and G. E. Law Jr, "Initiation and Growth of Transverse Cracks and Edge Delamination in Composite Laminates Part 2. Experimental Correlation," *Journal of Composite Materials Supplement*, vol. 14, pp. 88–108, 1980.

[4] R. B. Pipes and N. J. Pagano, "Interlaminar stresses in composite laminates under uniform axial extension," *Journal of Composite Materials*, vol. 4, pp. 538–548, 1970.

[5] N. J. Pagano, "Stress Fields in Composite Laminates," *International Journal of Solids and Structures*, vol. 14, pp. 385–400, 1978.

[6] C. Mittelstedt and W. Becker, "Interlaminar Stress Concentrations in Layered Structures: Part I - A Selective Literature Survey on the Free-Edge Effect since 1967," *Journal of Composite Materials*, vol. 38, no. 12, pp. 1037–1062, 2004.

[7] F. W. Crossman and A. S. D. Wang, "The dependence of transverse cracking and delamination on ply thickness in graphite/epoxy laminates," in *Damage in Composite Materials* (K. Reifsnider, ed.), pp. 118–139, ASTM International, January 1982.

[8] T. Lorriot, G. Marion, R. Harry, and H. Wargnier, "Onset of free-edge delamination in composite laminates under tensile loading," *Composites Part B: Engineering*, vol. 34, pp. 459–471, July 2003.

[9] T. K. O'Brien, "Analysis of local delaminations and their influence on composite laminate behavior," tech. rep., National Aeronatiucs and Space Adminstration (NASA), Hampton, Virgina, USA, 1984.

[10] P. Johnson and F. Chang, "Characterization of Matrix Crack-Induced Laminate Failure-Part I: Experiments," *Journal of Composite Materials*, vol. 35, pp. 2009–2035, January 2001.

[11] D. Leguillon, G. Marion, R. Harry, and F. Lécuyer, "The onset of delamination at stress-free edges in angle-ply laminates - analysis of two criteria," *Composites Science and Technology*, vol. 61, pp. 0–5, 2001.

[12] L. Lagunegrand, T. Lorriot, R. Harry, H. Wargnier, and J. Quenisset, "Initiation of free-edge delamination in composite laminates," *Composites Science and Technology*, vol. 66, pp. 1315–1327, August 2006.

[13] E. Martin, D. Leguillon, and N. Carrère, "A twofold strength and toughness criterion for the onset of free-edge shear delamination in angle-ply laminates," *International Journal of Solids and Structures*, vol. 47, no. 9, pp. 1297–1305, 2010.

[14] E. F. Rybicki and M. F. Kanninen, "A finite element calculation of stress intensity factors by a modified crack closure integral," *Engineering Fracture Mechanics*, vol. 9, no. 4, pp. 931–938, 1977.

[15] J. C. J. Schellekens and R. De Borst, "A non-linear finite element approach for the analysis of mode-I free edge delamination in composites," *International Journal of Solids and Structures*, vol. 30, no. 9, pp. 1239–1253, 1993.

[16] A. Turon, P. P. Camanho, J. Costa, and C. G. Dávila, "A damage model for the simulation of delamination in advanced composites under variable-mode loading," *Mechanics of Materials*, vol. 38, pp. 1072–1089, November 2006.

[17] A. Turon, C. G. Dávila, P. P. Camanho, and J. Costa, "An engineering solution for mesh size effects in the simulation of delamination using cohesive zone models," *Engineering Fracture Mechanics*, vol. 74, pp. 1665–1682, July 2007.

[18] T. K. O'Brien, "Characterization of delamination onset and growth in a composite laminate," tech. rep., National Aeronatiucs and Space Adminstration (NASA), Hampton, Virgina, USA, January 1981.

[19] S. R. Hallett, W. G. Jiang, B. Khan, and M. R. Wisnom, "Modelling the interaction between matrix cracks and delamination damage in scaled quasi-isotropic specimens," *Composites Science and Technology*, vol. 68, pp. 80–89, January 2008.

[20] L. Zubillaga, A. Turon, J. Renart, J. Costa, and P. Linde, "An experimental study on matrix crack induced delamination in composite laminates," *Composite Structures*, vol. 127, pp. 10–17, 2015.

[21] P. Maimí, P. P. Camanho, J. A. Mayugo, and A. Turon, "Matrix cracking and delamination in laminated composites. Part I: Ply constitutive law, first ply failure and onset of delamination," *Mechanics of Materials*, vol. 43, pp. 169–185, April 2011.

[22] L. Zubillaga, A. Turon, P. Maimí, J. Costa, S. Mahdi, and P. Linde, "An energy based failure criterion for matrix crack induced delamination in laminated composite structures," *Composite Structures*, vol. 112, pp. 339–344, June 2014.

[23] A. S. D. Wang and F. W. Crossman, "Initiation and Growth of Transverse Cracks and Edge Delamination in Composite Laminates Part 1. An Energy Method," *Journal of Composite Materials Supplement*, vol. 14, pp. 71–87, 1980.

[24] F. P. Van Der Meer and L. J. Sluys, "Continuum Models for the Analysis of Progressive Failure in Composite Laminates," *Journal of Composite Materials*, vol. 43, no. 20, pp. 2131–2156, 2009.

[25] E. V. Iarve, M. R. Guvich, D. H. Mollenhauer, C. A. Rose, and C. G. Dávila, "Mesh-independent matrix cracking and delaminaiton modeling in laminated composites," *International Journal for Numerical Methods in Engineering*, vol. 88, no. February, pp. 749–773, 2011.

[26] A. Puck and H. Schürmann, "Failure analysis of FRP laminates by means of physically based phenomenological models," *Composites Science and Technology*, vol. 3538, no. 96, 1998.

[27] C. G. Dávila, P. P. Camanho, and C. A. Rose, "Failure Criteria for FRP Laminates," *Journal of Composite Materials*, vol. 39, pp. 323–345, February 2005.

[28] C. T. Herakovich, "Mechanics of composites: A historical review," *Mechanics Research Communications*, vol. 41, pp. 1–20, April 2012.

[29] R. Amacher, J. Cugnoni, J. Botsis, L. Sorensen, W. Smith, and C. Dransfeld, "Thin ply composites: Experimental characterization and modeling of size-effects," *Composites Science and Technology*, vol. 101, pp. 121–132, September 2014.

[30] K. Kawabe, T. Matsuo, and Z. Maekawa, "New Technology for Opening Various Reinforcing Fiber Tows," *Journal of the Society of Materials Science, Japan*, vol. 47, no. 7, pp. 727–734, 1998.

[31] R. G. Krueger, "Apparatus and method for spreading fibrous tows into linear arrays of generally uniform density and products made thereby," 2001.

[32] H. Uno, "Innovative technology for carbon and aramid," *JEC Composites Magazine*, no. 17, 2005.

[33] T. Roure and P. Sanial, "C-PLY, a new structural approach to multiaxials in composites," *JEC Composites Magazine*, pp. 53–54, October 2011.

[34] E. Shahidi, "C-Ply SP (thin-plies) usage for Aerospace applications: potential benefits," in *Franco-British Symposium on Composite Materials*, (London), 2015.

[35] S. K. Ha, "Innovative design procedures for large-scale wind turbine blades," *JEC Composites Magazine*, no. 70, pp. 39–45, 2012.

[36] S. W. Tsai and A. T. Nettles, "Representative test data on bi-angle thin-ply NCF," *JEC Composites Magazine*, pp. 62–63, October 2011.

[37] S. W. Tsai and M. Papila, "Homogenization made easy with bi-angle thin-ply NCF," *JEC Composites Magazine*, pp. 70–71, October 2011.

[38] T. Yokozeki, Y. Aoki, and T. Ogasawara, "Experimental characterization of strength and damage resistance properties of thin-ply carbon fiber/toughened epoxy laminates," *Composite Structures*, vol. 82, no. 3, pp. 382–389, 2008.

[39] T. Yokozeki, A. Kuroda, A. Yoshimura, T. Ogasawara, and T. Aoki, "Damage characterization in thin-ply composite laminates under out-of-plane transverse loadings," *Composite Structures*, vol. 93, pp. 49–57, December 2010.

[40] H. Saito, M. Morita, K. Kawabe, M. Kanesaki, H. Takeuchi, M. Tanaka, and I. Kimpara, "Effect of ply-thickness on impact damage morphology in CFRP laminates," *Journal of Reinforced Plastics and Composites*, vol. 30, pp. 1097–1106, August 2011.

[41] A. Arteiro, G. Catalanotti, J. Xavier, and P. P. Camanho, "Notched response of non-crimp fabric thin-ply laminates," *Composites Science and Technology*, vol. 79, pp. 97–114, April 2013.

[42] A. Arteiro, G. Catalanotti, J. Xavier, and P. P. Camanho, "Large damage capability of non-crimp fabric thin-ply laminates," *Composites Part A: Applied Science and Manufacturing*, vol. 63, pp. 110–122, 2014.

[43] G. Guillamet, A. Turon, J. Costa, and P. Linde, "A quick procedure to predict free-edge delamination in thin-ply laminates under tension," *Engineering Fracture Mechanics (article in press)*, 2016.

[44] A. Arteiro, G. Catalanotti, J. Xavier, and P. P. Camanho, "Notched response of non-crimp fabric thin-ply laminates: Analysis methods," *Composites Science and Technology*, vol. 88, pp. 165–171, November 2013.

[45] J. M. Whitney and R. J. Nuismer, "Stress Fracture Criteria for Laminated Composites Containing Stress Concentrations," *Journal of Composite Materials*, vol. 8, pp. 253–265, 1974.

[46] P. P. Camanho, G. H. Erçin, G. Catalanotti, S. Mahdi, and P. Linde, "A finite fracture mechanics model for the prediction of the open-hole strength of composite laminates," *Composites Part A: Applied Science and Manufacturing*, vol. 43, no. 8, pp. 1219–1225, 2012.

[47] S. T. Pinho, C. G. Dávila, P. P. Camanho, L. Iannucci, and P. Robinson, "Failure Models and Criteria for FRP Under In-Plane or Three-Dimensional Stress States Including Shear Non-Linearity," tech. rep., National Aeronatiucs and Space Adminstration (NASA), Hampton, Virgina, USA, February 2005.

[48] G. Catalanotti, P. P. Camanho, and A. T. Marques, "Three-dimensional failure criteria for fiber-reinforced laminates," *Composite Structures*, vol. 95, pp. 63–79, January 2013.

[49] P. P. Camanho, A. Arteiro, A. R. Melro, G. Catalanotti, and M. Vogler, "Three-dimensional invariant-based failure criteria for fibre-reinforced composites," *International Journal of Solids and Structures*, vol. 55, pp. 92–107, 2014.

[50] P. P. Camanho, A. Turon, J. Costa, G. Guillamet, A. Arteiro, and E. V. González, "Structural integrity of thin-ply laminates," *JEC Composites Magazine*, no. 71, pp. 49–50, 2012.

[51] H. Saito, H. Takeuchi, and I. Kimpara, "A study of crack suppression mechanism of thin-ply carbon-fiber-reinforced polymer laminate with mesoscopic numerical simulation," *Journal of Composite Materials*, vol. 48, no. 17, pp. 2085–2096, 2013.

[52] A. Arteiro, G. Catalanotti, A. R. Melro, P. Linde, and P. P. Camanho, "Micro-mechanical analysis of the in situ effect in polymer composite laminates," *Composite Structures*, vol. 116, pp. 827–840, 2014.

[53] H. Saito, H. Takeuchi, and I. Kimpara, "Experimental Evaluation of the Damage Growth Restraining in 90 Layer of Thin-ply CFRP Cross-ply Laminates," *Advanced Composite Materials*, vol. 21, pp. 57–66, 2012.

[54] Dassault Systèmes Simulia Corp., Providence, RI, USA, *Abaqus 6.12 Analysis User's Manual*, 2012.

[55] G. Guillamet, A. Turon, J. Costa, J. Renart, P. Linde, and J. A. Mayugo, "Damage occurrence at edges of Non-crimp-fabric thin-ply laminates under off-axis uniaxial loading," *Composites Science and Technology*, vol. 98, pp. 44–50, May 2014.

[56] G. Guillamet, A. Turon, J. Costa, J. A. Mayugo, and P. Linde, "In search of the quasi-isotropic laminate with optimal delamination resistance under off-axis loads . Effect of the ply sequence and of using thin-plies," *Submitted to Composites - Part A: Applied Science and Manufacturing*, 2016.

[57] C. T. Herakovich, *Mechanics of Fibrous Composites*. 1997.

PAPERS

Paper A

Damage occurrence at edges of non-crimp-fabric thin-ply laminates under off-axis uniaxial loading

G. Guillamet[a], A. Turon[a], J. Costa[a], J. Renart[a], P. Linde[b], J.A. Mayugo[a]

[a] AMADE, Polytechnic School, Universitat de Girona, Campus Montilivi s/n, 17071 Girona, Spain

[b] Airbus Operations GmbH, Kreetslag 10, 21129 Hamburg, Germany

The paper has been published in
Composite Science and Technology Vol. 98 (2014), pp.44-50, 2014.

Composites Science and Technology 98 (2014) 44–50

Contents lists available at ScienceDirect

Composites Science and Technology

journal homepage: www.elsevier.com/locate/compscitech

Damage occurrence at edges of non-crimp-fabric thin-ply laminates under off-axis uniaxial loading

G. Guillamet [a], A. Turon [a], J. Costa [a,*], J. Renart [a], P. Linde [b], J.A. Mayugo [a]

[a] AMADE, Polytechnic School, Universitat de Girona, Campus Montilivi s/n, 17071 Girona, Spain
[b] Airbus Operations GmbH, Kreetslag 10, 21129 Hamburg, Germany

ARTICLE INFO

Article history:
Received 11 February 2014
Received in revised form 14 April 2014
Accepted 18 April 2014
Available online 4 May 2014

Keywords:
A. Thin-ply laminates
A. Carbon fibres
B. Delamination
B. Matrix cracking

ABSTRACT

Thin-ply based laminates are a promising development in composite materials and are expected in the near future to outperform conventional laminates in mechanical performance. A rational design with thin plies requires understanding the effect of ply thickness on each damage mechanism. This paper presents an experimental investigation into damage occurrence in a quasi-isotropic laminate made from thin-ply, bi-axial, Non-Crimp-Fabric (NCF), under different off-axis uniaxial loadings. The NCF layers are positioned through the laminate thickness creating two regions, namely THICK and THIN (with and without ply clustering). Then, the onset and progress of three damage mechanisms (transverse matrix cracking, matrix crack induced delamination and free-edge delamination) for both regions are analyzed by monitoring the specimen's free-edge. The results show that the critical region where damage occurs is that with ply clustering (THICK), whereas delamination originating from matrix cracks or free edge effects are delayed or even suppressed in the THIN region.

1. Introduction

New manufacturing technologies for composite laminates are emerging and producing thinner than conventional plies [1,2]. One example is the *spread tow thin-ply technology*, which produces flat, straight plies until a dry ply thickness as low as 0.02 mm is reached [3].

Recent research publications report on the advantages of using thin-ply laminates. One pioneering work was carried out by Sihn et al. [2], who performed an experimental campaign comparing the mechanical properties of conventional laminates to so-called thin-ply laminates. In this study they observed that, without special resins, the thin-ply laminate composites suppress micro-cracking, delamination and splitting damage for static, fatigue and impact loadings. Another interesting work by González et al. [4], focused on the effect of ply clustering in low-velocity impact loading. In this experimental study, the authors concluded that ply clustering (thicker plies), reduces the damage resistance of a structure. More recently, a numerical study by Camanho et al. [5] analyzed the influence of ply thickness on the *in situ strengths* [6], as well as on the free-edge delamination onset of a specimen under tension. The numerical results showed a significant improvement in transverse cracking and delamination resistance when using thin-ply based laminates.

For a given total thickness of the laminate, the use of thin-plies in the design entails, as opposed to conventional plies, a higher number of plies. Therefore, thin-ply Non-Crimp Fabrics (NCFs), which group two to four plies together [3], have been proposed as an alternative to conventional unidirectional (UD) tapes and crimp textile configurations. NCF provides numerous benefits for laminate design, such as easy laminate homogenization and simpler ply stacking, a reduction in processing time, cost, waste and stacking errors [7,8].

Few published works make reference to the mechanical response of thin-ply NCF's. However, the potential contribution of this new material has been highlighted, for instance Tsai et al. [9] demonstrated a remarkable improvement in stiffness and strength of NCF thin-ply laminates for open-hole and compression after impact (CAI) tests. More recently, Arteiro et al. [10] carried out a fully experimental campaign of plain strength, center-notched, open-hole and bearing tests in thin-ply NCF laminates which demonstrated the ability of thin-ply laminates to suppress or delay some damage mechanisms and increase the strength of the laminate. However, none of these research works focused on the onset of damage mechanisms at the free-edge or their subsequent development. Thus, in order to achieve a comprehensive and solid understanding of the mechanical behavior of these

* Corresponding author. Tel.: +34 972419663; fax: +34 972418098.
E-mail address: josep.costa@udg.edu (J. Costa).

http://dx.doi.org/10.1016/j.compscitech.2014.04.014
0266-3538/

materials, which is a requirement to reach an optimum mechanical design, further experimental research is necessary.

As advanced composites are frequently used in strength-critical applications which must withstand loads in different directions, several studies which analyze the occurrence of damage in composite laminates using different off-axis loadings have been published. For instance, Sun and Zhou [11] found that due to the edge effects, a quasi-isotropic laminate (elastically isotropic in the laminate in-plane) is highly anisotropic in strength. Other authors, such as Varna et al. [12], studied the off-axis problem from a different angle. They analyzed the occurrence of damage in a lay-up by examining various orientations of a particular ply without changing the orientation of the others. They found that matrix cracking was observed in the ply under transverse tension stresses and that the laminate elastic moduli underwent changes with the crack density. On the other hand, compression stresses normal to the fiber direction altered the elastic moduli, even though matrix cracking was not observed. Nevertheless, the development of damage mechanisms and the strength of thin-ply NCF laminates with different off-axis loadings have not yet been investigated.

The objective of this work is to conduct an experimental campaign analyzing damage development in a quasi-isotropic laminate made of thin-ply NCF under different off-axis loads. The laminate studied has a specific stacking sequence, consisting of two regions or sub-laminates with and without ply clustering, identified in this paper as THICK and THIN regions, respectively. Damage occurrence and its evolution for both regions is analyzed utilizing optical monitoring of the specimen's free-edge. Moreover, the same laminate is tested with different off-axis loads to evaluate the strength of the laminate in each direction.

The content of this paper is structured as follows. Firstly, the methodology of the experimental campaign is presented together with a brief description of the material, the specimen characteristics and the test procedure. Then, the results of the stress–strain relations are presented along with the occurrence of damage mechanisms at the free-edge of the specimen. Finally, the results are discussed in light of the influence of the ply clustering and the direction of the off-axis loading.

2. Experimental

2.1. Material and manufacturing

The material investigated in this study is carbon T700 made up of two layers, 0° and −45° and commercialized by Chomarat: T700 C-Ply™ [0/−45] NCF. This material is manufactured with the *spread tow thin-ply technology* resulting in a total areal weight of 150 g/m^2 per bi-angle layer (2×75 g/m^2). The material was pre-impregnated by Aldila using the epoxy system AR2527. The elastic ply properties are $E_1 = 110$ GPa for the longitudinal modulus of elasticity, $E_2 = 7.4$ GPa for the transverse modulus, $G_{12} = 4.2$ GPa for the in-plane shear modulus and $v_{12} = 0.3$ for the longitudinal Poisson's ratio [10].

The stacking sequence is a $\pi/4$ quasi-isotropic configuration $[(0/-45)/(45/0)/(90/45)/(-45/90)]_s$. This lay-up is composed of 16 unidirectional plies (8 bi-angle layers) with a nominal ply thickness of 0.08 mm and a nominal laminate thickness of 1.3 mm. Note that, the ply configuration is not symmetric in terms of unidirectional plies, but symmetric in terms of a bi-angle layer of [0/−45]. This lay-up has no shear-extension coupling ($A_{16} = A_{26} = 0$) and the terms of the coupling matrix are zero ($B_{ij} = 0$).

The panel was manufactured at VX Aerospace using vacuum bagging. The specimens were obtained by cutting the panel with a diamond-coated disk at Airborne Composites.

2.2. Specimen characteristics

Specimens were cut from the panel in five different directions, as shown in Fig. 1, where the longitudinal direction of each specimen was the loading direction during the tests. Fifteen specimens, three specimens per batch or off-axis loading, were tested.

Taking the specimen loading direction as the 0° orientation for each specimen results in five different ply stacking sequences. They are labeled as L0, L23, L45, L68 and L90, which are rotated respectively over the panel 0°, −22.5°, −45°, −67.5° and −90°. The corresponding stacking sequences for each one are shown in Fig. 2. Two regions, or sub-laminates through the laminate thickness, are defined. The first region, hereafter referred to as THICK, has a ply clustering of two plies for those layers from 10 to 15, while in the second region, hereafter referred to as THIN, there is no ply clustering. Additionally, the sequence of mismatch angles (angles between adjacent layers) remains the same for all the lay-ups [13]. It is worth noting that, the sequence of mismatch angles includes mismatch angles between the $[0/-45]$ bi-angle layers.

Using the polar method applied to the Classical Laminate Theory (CLT) [14,15], it can be demonstrated that all laminates are isotropic in in-plane stiffness, but they are not isotropic in flexural stiffness. The polar plot of the two engineering constants of the laminate for each off-axis direction rotated over the panel is shown in Fig. 3, where E^{lam} and E_f^{lam} are respectively the in-plane and flexural laminate moduli; which are calculated by using the material elastic properties [10]. The proposed lay-ups, L0, L23, L45, L68 and L90, correspond to the 0°, 337.5°, 315°, 292.5° and 270° directions on the polar plot.

2.3. Test set-up

All experimental tests were performed under uniaxial tension using a MTS 810 servo-hydraulic testing machine (250 kN). The cross head displacement rate was set to 0.5 mm/min under displacement control. During the test, a digital camera (Canon EOS 550D with a 100 mm macro lens) was located in front of the specimen's edge to monitor the different damage mechanisms occurring at the free-edges [16]. The working distance (defined as the distance from the specimen edge to the support of the camera) was set between 300 and 320 mm, which implies monitoring a specimen length of about 50 mm. Additionally, an axial extensometer with a 25 mm gage length was used to measure the strain of the specimen during the test. The camera shots and the value of the strain from the extensometer were acquired simultaneously with a user-defined software.

All tensile tests were based on ASTM D3039/D3039M-08 [17]. The specimens' edges were polished with silicon carbide paper to

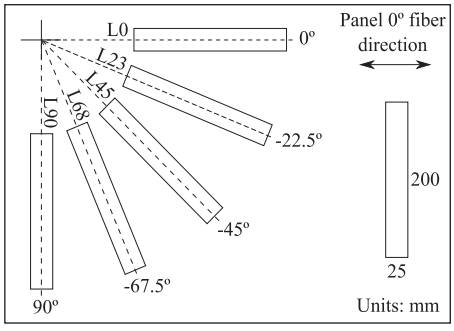

Fig. 1. Specimen cuts over the panel.

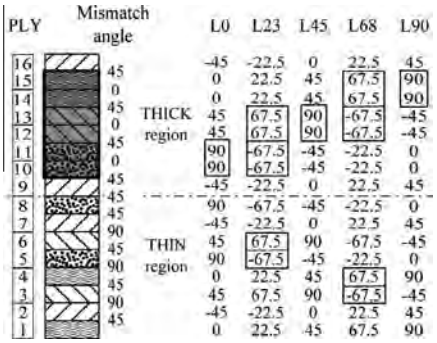

Fig. 2. Ply configuration for each off-axis loading.

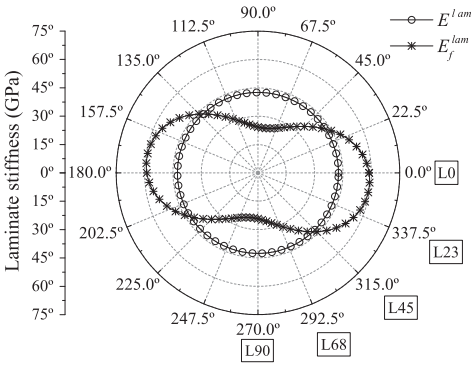

Fig. 3. Polar plot of laminate stiffness terms.

obtain a flat surface. This strategy was adopted to avoid premature damage from the edges [11].

3. Results and discussion

3.1. Stiffness and strength

The results of the stress–strain response for all the lay-ups are shown in Fig. 4. The laminate stress is obtained from the load measured by the load cell, and the applied strain is obtained from the axial extensometer. Each sub-figure shows the experimental results of three specimens (S1, S2 and S3) together with the linear response obtained from the CLT (Analytical) [14].

An excellent repeatability of the stress–strain response between the three specimens is observed. The lay-ups containing plies at 0° (L0, L45 and L90) have a linear response during the test (Fig. 4a, c, and e), while lay-ups L23 and L68 exhibit a smooth non-linear response before the peak load, (Fig. 4b and d). Additionally, lay-up L90 has a non-linear response at an advanced damage state, just before the specimen's failure.

The mean values and standard deviations of the ultimate tensile longitudinal strength (σ_T^L), the ultimate tensile longitudinal strain (ε_T^L) and the elastic laminate modulus (E^{lam}) of each laminate are summarized in Table 1.

As expected, Table 1 evidences that all the lay-ups exhibit a similar in-plane stiffness or laminate moduli. The calculated value of the analytical laminate modulus, 42.6 GPa, is in good agreement with the experimental measurements, with the relative error being between 0.5% and 5.0%. In spite of the concordance in stiffness,

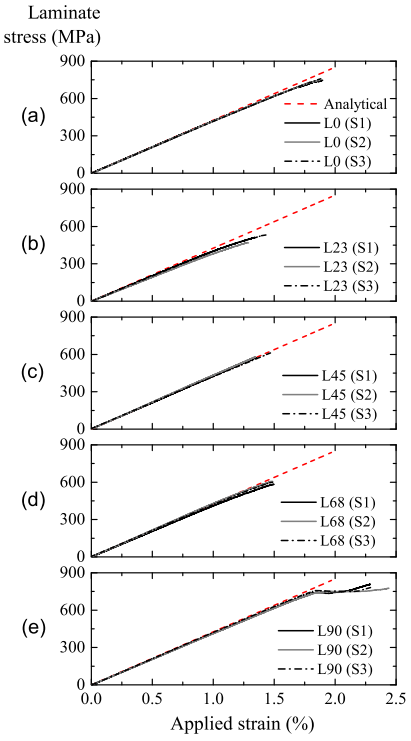

Fig. 4. Stress–strain response for each lay-up.

Table 1
Plain strength test results for each lay-up.

	$\sigma_T^L(MPa)$		$\varepsilon_T^L(\%)$		$E^{lam}(GPa)$	
Ref.	Mean	Std.	Mean	Std.	Mean	Std.
L0	751	4	1.897	0.014	41.9	0.3
L23	505	34	1.360	0.083	40.5	2.1
L45	591	24	1.389	0.073	42.4	0.9
L68	596	13	1.491	0.005	41.8	0.6
L90	790	16	2.344	0.084	41.6	0.7

there are substantial differences in the ultimate stresses and strains for each lay-up.

3.2. Onset of damage mechanisms

The different sequences of damage mechanisms between specimens as the load increases can explain the differences in laminate strength. The edge of a composite laminate is well-known to be a critical region where damage mechanisms are prone to occur [18]. Once the damage is initiated, laminate properties may deteriorate, leading to premature failure. In this work, the evolution of damage mechanisms were observed by optically monitoring the free-edge of the specimen. The following damage mechanisms were identified: transverse matrix cracking (TC), matrix crack induced delamination (MCID) [19] and free-edge delamination (FED), see Fig. 5.

During the tests, it was observed that the first ply failure occurs at those plies with orientations closer to transverse plies: oriented

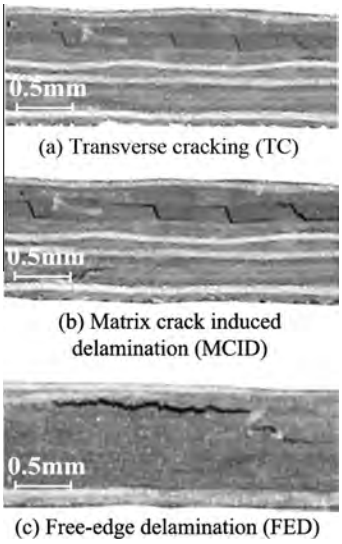

Fig. 5. Failure mechanisms observed at the free-edge.

at 90° and at ±67.5° . The distribution of these critical plies along the thickness for each lay-up is indicated in Fig. 2. The initiation and the propagation of damage at the free-edge of the specimen was mainly observed on, and next to, the indicated plies.

The results for the onset of the damage mechanisms TC, MCID and FED are summarized in Table 2. Each damage mechanism is addressed separately for the THICK and THIN regions of each lay-up. The critical strain is defined as the strain where the first crack is observed (in many cases a multiplicity of cracks appears simultaneously). Then, the critical onset strain for each damage mechanism is computed as the average critical strain for the three specimens of each batch. Regarding the crack density, it corresponds to the number of cracks observed for the critical onset strain in a length of 50 mm. As well as the critical strain, the value is computed as the average for the three specimens of each batch.

3.2.1. Transverse cracking

The first damage mechanism to appear in all the lay-ups is TC and it is observed in those layers oriented at 90° and ±67.5° (Fig. 2). As shown in Table 2, the critical strains in the THIN region for lay-ups L0, L23, L68 and L90 are higher than those for the THICK region (33% higher on average) and the number of cracks in the THIN region is lower than in the THICK region. For the case of lay-up L45, there is no evidence of TC in the THIN region before laminate failure. With regards the effect of the direction on the off-axis loading, lay-ups L23 and L68 exhibit earlier matrix cracking than lay-ups L0, L45 and L90. These results show that the onset of TC in the THIN region is delayed or even suppressed in comparison with the THICK region.

3.2.2. Matrix crack induced delaminations

Matrix crack induced delaminations or delaminations triggered by matrix cracks (MCID) can only occur once transverse cracking is initiated. Therefore, the critical plies for the onset of this damage mechanism are the same as for transverse cracking: plies oriented at 90° and ±67.5°. For instance, MCID for lay-ups L0, L45, and L90 (Table 2), is completely suppressed in the THIN region, whereas lay-ups L23 and L68 have MCID in this region with laminate strains close to the ultimate strains and are 21% higher than in the THICK region. These results show that MCID is strongly present during the damage development for all the lay-ups and that in some cases it is drastically reduced or suppressed in the THIN region.

3.2.3. Free-edge delaminations

The results of the critical strains and the number of free-edge delaminations are also summarized in Table 2. It is worth noting that, the presence of FED is only observed for lay-ups L0 and L90 which exhibit the highest ultimate strains. It can be observed that, the onset of FED in the THICK region takes place prior to the THIN region (10% higher strains in the THIN region), following the same previously described trend in the other damage mechanisms.

Fig. 6 summarizes the critical strains of the three damage mechanisms considered for each lay-up, and provides a visual depiction of the damage sequence for each laminate. A critical strain for each damage mechanism in the THICK and THIN region is provided for each lay-up. This figure evidences the delay or even suppression of some damage mechanisms in the THIN region (the delay in occurrence of TC for lay-ups L0, L23, L68 and L90 or the suppression of the three damage mechanisms for lay-up L45). Moreover,

Table 2
Critical strains for each failure mechanism.

		THICK region				THIN region			
Failure mechanism	Ref.	Num. of cracks in 50 mm	Std. (–)	Critical onset strain (%)	Std. (%)	Num. of cracks in 50 mm	Std. (–)	Critical onset strain (%)	Std. (%)
Transverse Cracking (TC)	L0	17	4	1.052	0.059	4	1	1.342	0.044
	L23	8	2	0.802	0.067	2	1	1.003	0.049
	L45	11	4	1.105	0.074	–	–	–	–
	L68	7	3	0.949	0.045	4	2	1.388	0.056
	L90	4	2	1.253	0.107	3	1	1.702	0.035
Matrix crack Induced Delamination (MCID)	L0	8	3	1.181	0.077	–	–	–	–
	L23	6	3	0.953	0.080	3	1	1.154	0.088
	L45	14	3	1.350	0.070	–	–	–	–
	L68	6	2	1.204	0.090	4	2	1.468	0.019
	L90	3	2	1.516	0.106	–	–	–	–
Free-edge Delamination (FED)	L0	3	2	1.267	0.121	3	1	1.410	0.033
	L23	–	–	–	–	–	–	–	–
	L45	–	–	–	–	–	–	–	–
	L68	–	–	–	–	–	–	–	–
	L90	4	1	1.647	0.080	3	1	1.803	0.117

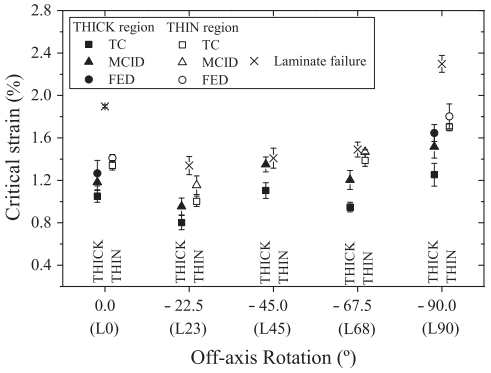

Fig. 6. Damage mechanisms onset strain: TC (Transverse Cracking), MCID (Matrix crack induced delamination), FED (Free-edge delamination). Onset strains are provided for the THIN and THICK region of each lay-up.

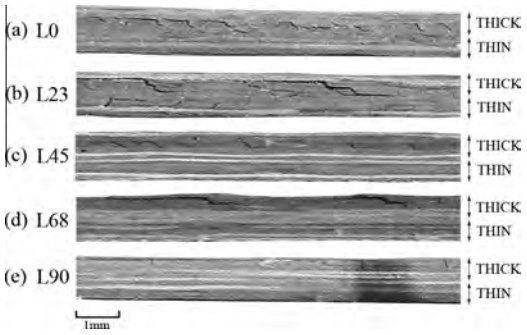

Fig. 7. Damage occurrence under an applied strain of 1.25%.

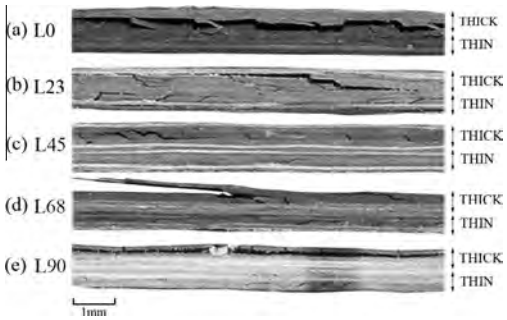

Fig. 8. Crack growth for each lay-up just before ultimate failure.

lay-ups L0 and L90, which exhibit a later onset of damage than L23, L45 and L68, have the highest ultimate strains.

3.3. Damage evolution

In spite of its in-plane isotropic elastic behavior, the damage progression strongly depends on the direction of the load. The

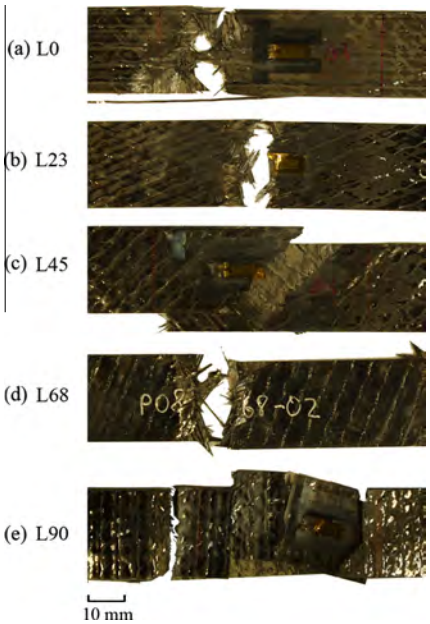

Fig. 9. Failure mode for each laminate after testing.

observation of the damage mechanisms of the specimens' edge supports this assertion. Fig. 7 corresponds to the damage state at the free-edge of each lay-up under an applied strain of 1.25%.

For each lay-up it is found that the cracks are mainly located in the THICK region (Fig. 7). The main damage mechanisms at this strain are TC and MCID, and they are located in the plies with orientations closer to the transverse directions, 90° and 67.5° (90° in L0, L45 and L90; 67.5° in L23 and L68). Note that, in L23 and L68 the transverse cracks span over more plies than in the rest of the lay-ups and, the crack density is also lower. This fact is related to the clustering of the critical plies in these lay-ups (Fig. 2): the two blocks of $+67.5^\circ$ and -67.5° plies, seem to behave as a block of four transverse plies. Therefore, these results suggest that the THICK region, where the ply clustering is present, contribute to higher interlaminar stress concentration in adjacent interfaces [5] and to lower in situ strengths [6], which trigger damage mechanisms such as premature matrix cracking and delamination.

The damage observed just before the laminate failure for each lay-up is shown in Fig. 8. Lay-ups L0, L23, L45 and L68 are strongly dominated by delaminations triggered by matrix cracks (MCID), whereas in lay-up L90 the origin of the dominant delamination is not clear (either FED or MCID). These observations highlight the importance of MCID in the generation and progress of damage. In any case, in most of the configurations, a dominant crack parallel to the specimens' midplane is the most visible form of damage before failure.

Finally, Fig. 9 depicts the broken specimens following testing where, in general, all lay-ups are strongly dominated by delaminations and matrix cracking. Plies in each specimen tend to fail following their transverse direction ($\pm45^\circ$ and 90° in L0, L45 and L90, and $\pm67.5^\circ$ in L23 and L68).

Delaminations with broken plies at $\pm45^\circ$ are observed for lay-ups L0, L45 and L90 which have 0° plies in the load direction. The 0° plies are the main load carrier plies and all three stacking

sequences include four of them. However, their location varies in each stacking sequence. In lay-up L0 they are located at the outer regions, in lay-up L45 they are distributed through the laminate thickness and in lay-up L90 they are located close to the mid-plane of the laminate. The most catastrophic response is observed in lay-up L90, which also exhibits the highest ultimate stress. In this lay-up, damage initiates at the outer plies, mainly in the THICK region, leaving the main core of the laminate intact until final failure. While lay-ups L0 and L45 have the same number of 0° plies as L90, they fail earlier (Fig. 4).

On the other hand, delaminations with broken plies at ±67.5° are observed for lay-ups L23 and L68. Both lay-ups have similar stacking sequences resulting in a similar failure section with broken plies at ±67.5°, in spite of the differences in strength (Table 1). The resulting failure response is less catastrophic than the rest of the lay-ups because of the lack of 0° layers in the load direction. Nevertheless, these lay-ups have the lowest ultimate strains, partly due to the presence of damage in both THICK and THIN sections (note the existence of ±67.5° plies at both regions (Fig. 2)).

4. Challenges for designing with thin-plies

The experimental results presented, demonstrate the advantages of thin plies in delaying, or suppressing, the onset of damage mechanisms and they raise the prospect of incorporating them into the structural design of laminated composites. However, for a given laminate thickness or laminate stiffness, the number of plies increases as the ply thickness decreases and, in consequence, the number of candidate stacking sequences increases. A proper optimization methodology is required to find the best solutions for a given load case, or set of load cases.

This work has shown that the strength and damage evolution under a uni-axial loading is strongly dependent on the loading direction and ply orientation, despite the laminate being elastically isotropic. Therefore, the optimization methodology claimed above, should rely on failure criteria at the ply level with refined capabilities. For instance, in addition to the ply properties, as the thickness and orientation of the reinforcement, the failure criteria should be sensitive to the location of the ply in the laminate. The effect of the thickness should be re-examined when dealing with thin plies, as current theories would predict and asymptotic ply strength as the thickness decreases. Moreover, the interaction between failure mechanisms (i.e. delamination induced in the vicinity of matrix cracks) should also be accounted for). The combination of the physical complexity under such failure mechanisms and the large number of potential stacking sequences with thin plies for a laminate of useful thickness, constitute a computational challenge for future. The prospect is there, however, to attain an expanded design space (larger allowable strain) by incorporating thin-ply based laminates.

5. Conclusions

The initiation and development of damage mechanisms in a thin-ply bi-axial non-crimp fabric laminate under different off-axis loadings were studied. The ply sequence was devised so that a THIN region could be distinguished from a THICK region (where plies were clustered). Specimens from the same panel, which was elastically isotropic in the laminate plane, were extracted following 5 different orientations (0°, 22.5°, 45°, 67.5° and 90°). Then, the specimens were tested under an uniaxial load while the damage mechanisms were investigated by optically monitoring the free-edge of the specimen. Strains for the onset of transverse matrix cracking (TC), of delaminations appearing from matrix cracks (MCIDs) and of free-edge delaminations (FEDs) were quantified, along with their initial density.

The experimental results provided evidence that the damage mechanisms in the THIN region are clearly delayed, if not suppressed, with respect to their occurrence in the THICK region. Specimens with clustered transverse plies were observed to exhibit earlier damage onset, in agreement with the in situ strength theories that predict decreasing ply strength as ply thickness increases.

Three of ply sequences analyzed contained the same number of 0° plies, but with a different distribution. Strength, damage progression and failure mode have been analyzed and discussed. The lay-up L90, where the 0° plies are close to the mid-plane of the laminate, exhibited the highest strength. In this case, the damage developed at the outer regions, and left the block of inner plies with almost no damage until failure.

A further conclusion from this work is that any potential optimization of the stacking sequence performed for one loading direction can have an entirely different effect under a different loading direction. Therefore, the dramatic enhancement of design freedom associated with the use of thin plies (and their combination with standard thickness plies) should be counterbalanced with improved design tools able to anticipate stacking sequence effects at any orientation.

Acknowledgements

The authors would like to acknowledge Chomarat (Ardèche, France) and Prof. S.W. Tsai (Stanford University, USA) for providing the material, Aldila (Poway, California, USA) for the epoxy system pre-preg and VX Aerospace (Leesburg, Virginia, USA) for manufacturing the panel. The authors also acknowledge the support of the Spanish government through the Ministerio de Economía y Competitividad under the contracts DPI2012-34465 and MAT2012-37552-C03-03. The first author especially acknowledges the support of the Generalitat de Catalunya with the pre-doctoral Grant FI-DGR (2013FI-B01062).

References

[1] Kawabe K, Matsuo T, Maekawa Z-i. New technology for opening various reinforcing fiber tows. J Soc Mater Sci Jpn 1998;47(7):727–34.
[2] Sihn S, Kim R, Kawabe K, Tsai S. Experimental studies of thin-ply laminated composites. Compos Sci Technol 2007;67(6):996–1008.
[3] Roure T, Sanial P. C-PLY, a new structural approach to multiaxials in composites. JEC Compos Mag 2011(68):53–4.
[4] González E, Maimí P, Camanho P, Lopes C, Blanco N. Effects of ply clustering in laminated composite plates under low-velocity impact loading. Compos Sci Technol 2011;71(6):805–17.
[5] Camanho P, Arteiro A, Turon A, Costa J, Guillamet G, González E. Structural integrity of thin-ply laminates. JEC Compos Mag 2012;49(71):91–2.
[6] Camanho PP, Dávila CG, Pinho ST, Iannucci L, Robinson P. Prediction of in situ strengths and matrix cracking in composites under transverse tension and in-plane shear. Compos Part A: Appl Sci Manuf 2006;37(2):165–76.
[7] Tsai S, Netteles A. Representative test data on bi-angle thin-ply NCF. JEC Compos Mag 2011(68):62–3.
[8] Tsai S, Papila M. Thin-ply NCF: design for deformation through anisotropy. JEC Compos Mag 2011(68):66–7.
[9] Tsai S, Papila M. Homogenization made easy with bi-angle thin-ply NCF. JEC Compos Mag 2011(68):70–1.
[10] Arteiro A, Catalanotti G, Xavier J, Camanho P. Notched response of non-crimp fabric thin-ply laminates. Compos Sci Technol 2013;79:97–114.
[11] Sun C, Zhou S. Failure of quasi-isotropic composite laminates with free edges. J Reinf Plast Compos 1988;7(6):515–57.
[12] Varna J, Akshantala NV, Talreja R. Damage in composite laminates with off-axis plies. Compos Sci Technol 1999;59:2139–47.
[13] Sebaey T, González E, Lopes C, Blanco N, Maimí P, Costa J. Damage resistance and damage tolerance of dispersed CFRP laminates: effect of the mismatch angle between plies. Compos Struct 2013;101:255–64.
[14] Herakovich C. Mechanics of fibrous composites; 1997.
[15] Tsai S. Strength and life of composites, composite design group. Stanford (CA): Department of Aeronautics & Astronautics; 2008.

[16] Sebaey T, Costa J, Maimí P, Batista Y, Blanco N, Mayugo J. Measurement of the in situ transverse tensile strength of composite plies by means of the real time monitoring of microcracking. Compos Part B: Eng 2014:1–7.
[17] ASTM. Standard test method for tensile properties of polymer matrix composite materials 1. ASTM D3039/D3039M-08, 2010. p. 1–13.
[18] Herakovich C. Free-edge effects in laminated composites: 1976–2006. In: 25th Technical conference of the American society for composites and 14th US–Japan conference on composite materials. handbook o ed., vol. 1. Dayton (OH, United States); 2010. p. 22–37.
[19] Zubillaga L, Turon A, Maimí P, Costa J, Mahdi S, Linde P. An energy based failure criterion for matrix crack induced delamination in laminated composite structures. Compos Struct 2014;112:339–44.

Paper B

A quick procedure to predict free-edge delamination in thin-ply laminates under tension

G. Guillamet[a], A. Turon[a], J. Costa[a], P. Linde[b]

[a]AMADE, Polytechnic School, Universitat de Girona, Campus Montilivi s/n, 17071 Girona, Spain

[b]Airbus Operations GmbH, Kreetslag 10, 21129 Hamburg, Germany

The paper has been published in the
Engineering Fracture Mechanics (article in press), 2016.

ARTICLE IN PRESS

Engineering Fracture Mechanics xxx (2016) xxx–xxx

Contents lists available at ScienceDirect

Engineering Fracture Mechanics

journal homepage: www.elsevier.com/locate/engfracmech

A quick procedure to predict free-edge delamination in thin-ply laminates under tension

G. Guillamet [a,*], A. Turon [a], J. Costa [a], P. Linde [b]

[a] AMADE, Polytechnic School, Universitat de Girona, Campus Montilivi s/n, 17071 Girona, Spain
[b] Airbus Operations GmbH, Kreetslag 10, 21129 Hamburg, Germany

ARTICLE INFO

Article history:
Received 21 April 2015
Received in revised form 12 January 2016
Accepted 13 January 2016
Available online xxxx

Keywords:
Thin-ply laminates
Free-edge delamination

ABSTRACT

Delaminations at the free-edges of a laminated composite under tension can be triggered by transverse cracks or by high interlaminar stresses. The capability for predicting these phenomena when the ply thickness is reduced (thin-ply laminates) is particularly challenging because damage mechanisms are delayed or even suppressed. In this work, an existing energy-based failure criterion and a simplified finite element model with cohesive elements are combined to develop a computationally inexpensive predictive tool. Its comparison with experimental data demonstrates that this approach captures the trends of the critical strain for delamination with respect to ply thickness and ply location and the quantitative agreement with the predictions is satisfactory.

1. Introduction

Thin-ply based laminates are rapidly gaining interest in the composite materials industry due to the advantages they offer over standard thickness plies in terms of first-ply-failure, ultimate strength and fatigue life [1–4]. The pioneering experimental work of Sihn et al. [1] showed that thin-ply laminates can delay or even suppress microcracking and delamination damage for static, fatigue and impact loadings. More recently, Amacher et al. [4] carried out a broader experimental campaign including coupons and bolted joints made of different ply thickness configurations, similar conclusions were obtained.

With thin-plies, a larger number of ply orientations for a given total thickness is required, which in turn enables the ply sequence to be tailored for an optimum behavior when confronting specific damage modes. Making a proper use of this extended design domain of ply sequences is a challenge. Furthermore, the processing costs involved in manufacturing such a large number of plies also increase. One alternative to reach a middle ground on this issue are thin-ply Non-Crimp-Fabrics (NCFs), which group two ore more Unidirectional (UD) plies together. In this case, the UD plies are mechanically stacked at two or more angles and then stitched together with thin non-structural fibers, thus eliminating the fabric waviness of woven fabrics [5].

While few experimental works deal with the mechanical performance of thin-ply NCFs, Arteiro et al. [2,6] carried out an experimental campaign of plain strength, center-notched, open-hole and bearing tests with thin-ply NCFs and then, they used analysis methods for predicting the open hole tensile and compression response. The results once again demonstrated the ability of thin-ply based laminates to suppress or delay some damage mechanisms and to increase the strength of the

* Corresponding author. Tel.: +34 972 418 817; fax: +34 972 418 098.
E-mail addresses: gerard.guillamet@udg.edu (G. Guillamet), albert.turon@udg.edu (A. Turon), josep.costa@udg.edu (J. Costa), peter.linde@airbus.com (P. Linde).

http://dx.doi.org/10.1016/j.engfracmech.2016.01.019
0013-7944/

Nomenclature

a	plate width
B	mixed mode delamination ratio
E_{11}, E_{22}, E_{33}	Young's moduli
G_{12}, G_{13}, G_{23}	shear moduli
G_{Ic}, G_{IIc}	critical fracture energy in mode I and mode II
G_I, G_{II}, G_{III}	energy release rate in mode I, II and III
G_{shear}	energy release rate for shear loading
G_T	total energy release rate
h	plate thickness
L	length of the plate
n	ply clustering
S_L	longitudinal shear strength
S_L^{is}	longitudinal in situ shear strength
S_T^{is}	transverse in situ shear strength
t	ply thickness
T_{cured}	cured temperature
T_{room}	room temperature
u, v, w	displacements of the front nodes
$\widetilde{u}, \widetilde{v}, \widetilde{w}$	displacements of the rear nodes
x, y, z	coordinates
X_i^{MD}, X_{ij}^{MD}	parameters failure criterion
Y_{BT}	biaxial tensile strength
Y_{BT}^{is}	biaxial in situ tensile strength
Y_T	transverse tensile strength
Y_T^{is}	transverse in situ tensile strength
$\alpha_{11}, \alpha_{22}, \alpha_{33}$	coefficients of thermal expansion
α_o	transverse compression fracture angle
β	shear response factor
ε_x	strain in x-direction
η_{B-K}	Benzeggagh–Kenane parameter
η_{is}°	in situ laminate strength ratio
$\nu_{12}, \nu_{13}, \nu_{23}$	Poisson's ratios
$\sigma_{11}, \sigma_{22}, \sigma_{12}$	in-plane lamina stresses
$\sigma_{zz}, \sigma_{xz}, \sigma_{yz}$	interlaminar stresses
σ_c°	laminate critical stress
τ_3	cohesive traction in mode I
τ_{13}, τ_{23}	cohesive tractions in shear mode
τ_3°	interface maximum strength in mode I
τ_{sh}°	interface maximum strength in shear mode

Acronyms

CLT	Classical Lamination Theory
FE-CZM	Free-Edge Cohesive Zone Model
FED	Free-Edge Delamination
MCID	Matrix Crack Induced Delamination
MCID-FC	Matrix Crack Induced Delamination Failure Criterion
NCF	Non-Crimp-Fabric
UD	Unidirectional

laminate. They also concluded that, when compared to traditional composites, thin-ply NCFs show an improved response to bolted-joint bearing loads, which is in agreement with the results in Ref. [4].

On the other hand, in a previous work [3], the current authors presented an experimental investigation focused on the onset of damage mechanisms at the free-edge of a thin-ply NCF lay-up under different on-axis and off-axis loads. In this case, the lay-up was devised to create two regions, or sub-laminates, with and without ply clustering. The authors concluded that:

Please cite this article in press as: Guillamet G et al. A quick procedure to predict free-edge delamination in thin-ply laminates under tension. Engng Fract Mech (2016), http://dx.doi.org/10.1016/j.engfracmech.2016.01.019

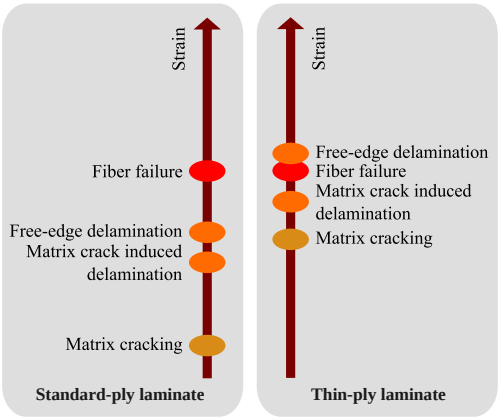

Fig. 1. Common sequence of damage mechanisms between standard- and thin-ply laminates.

(i) Transverse Cracking (TC) and Free-Edge Delamination (FED) were delayed or suppressed at the region without ply clustering; (ii) the laminate strength exhibited a heavy dependence on the direction of the off-axis load.

To synthesize the aforementioned experimental results, Fig. 1 provides a qualitative description of how thin-ply based laminates modify the sequence of damage events with respect to standard thickness plies.

The question arises whether current design procedures (failure criteria and progressive damage models) can capture the particular phenomenology of thin-ply composite materials, which is an obvious requirement if these new materials are to be introduced into an industrial context. Particularly challenging is predicting the sequence of damage events at free-edges in thin-ply laminates as different mechanisms can take place and interact due to the existing singular stresses [7]. These local stresses might lead to delamination and/or matrix cracking. If matrix cracks appear first, delaminations may be triggered around them [8,9].

With regards to matrix cracking, some failure criteria already take into account the effect of the ply thickness (in-situ strength phenomenon [10–12]. These methods are validated only with standard-ply laminates and for very low ply thicknesses they predict asymptotic behavior. In a recent micromechanical computational effort, Arteiro et al. [13] studied the in-situ effect for ultra-thin plies. Their results showed that thicker transverse laminae trigger cracks that suddenly propagate and lead to stress relaxation, whereas thinner transverse laminae show a gradual crack extension which do not completely penetrate through the thickness.

Delaminations at free-edges, in turn, may be triggered by matrix cracks or caused by interlaminar normal or shear stresses. A failure criterion to predict the delamination triggered by matrix cracks or also known as Matrix Crack Induced Delamination (MCID) was recently proposed by Zubillaga et al. [14]. This failure criterion compares the available energy release rate, due to the presence of a crack in the matrix, with the fracture toughness of the interface. Moreover, this criterion considers the mixed-mode delamination growth, which is evaluated at a ply level and is applicable to a general loading conditions. On the other hand, cohesive elements in a finite element framework have been shown to effectively reproduce the initiation and progression of delaminations at free-edges for standard-thickness plies [15–17].

Therefore, the objective of the present work is to evaluate the capability of two advanced design procedures (MCID criterion [14] and cohesive elements [15–17]) for predicting the experimental behavior of damage mechanisms observed at free-edges. Both approaches highlight two different phenomena that could either occur simultaneously or could interact (delaminations triggered by transverse cracks and delaminations generated by high interlaminar normal and shear stresses). However, for the sake of simplicity and quick response, this approach deals with both phenomena independently. The alternative, a progressive damage model with intra- and inter- ply damage laws, although feasible, would be computationally costly. Two case studies are proposed: one in which two similar lay-ups of standard-thickness and thin-plies are compared, and the other involving thin-ply based non-crimp-fabrics under different off-axis loads [3].

This paper first presents the methodology for predicting the occurrence of delamination at free-edges. Secondly, the two case studies mentioned above are analyzed and discussed.

2. Methodology

Delamination resistance at the free-edges of a prismatic specimen under tension (Fig. 2) is analyzed by means of two approaches: an energy-based Failure Criterion for predicting Matrix Crack Induced Delamination (MCID-FC) and a Free-Edge Cohesive Zone Model (FE-CZM).

Please cite this article in press as: Guillamet G et al. A quick procedure to predict free-edge delamination in thin-ply laminates under tension. Engng Fract Mech (2016), http://dx.doi.org/10.1016/j.engfracmech.2016.01.019

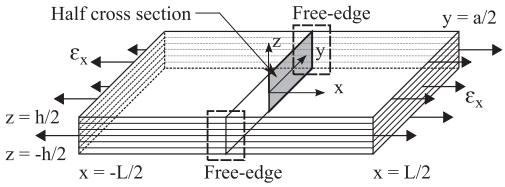

Fig. 2. Composite laminate under tension.

2.1. Failure Criterion for Matrix Crack Induced Delamination (MCID-FC)

An analytical model of a plate under tension is proposed for predicting the critical load for delaminations triggered by matrix cracks. The formulation combines the Classical Lamination Theory (CLT) [18] with the MCID-FC formulated by Zubillaga et al. [14]:

$$\left(\frac{\sigma_{11}}{X_1^{MD}}\right)^2+\left(\frac{\sigma_{22}}{X_2^{MD}}\right)^2+\left(\frac{\sigma_{12}}{X_6^{MD}}\right)^2+\frac{\sigma_{11}\sigma_{12}}{X_{16}^{MD}}+\frac{\sigma_{22}\sigma_{12}}{X_{26}^{MD}}+\frac{\sigma_{11}\sigma_{22}}{X_{12}^{MD}}=1 \tag{1}$$

where σ_{11}, σ_{22} and σ_{12} are the in-plane lamina stresses (obtained with the initial material stiffness); and X_i^{MD} and X_{ij}^{MD} are parameters which depend on the location of the ply within the laminate, the fracture toughness of the interface, the ply thickness and the laminate compliance before and after the presence of a matrix crack in a given ply. One of the advantages of this failure criterion is that it may consider a crack located close to the free-edge. The reader is referred to [14,19] for a complete description of the criterion and its validation.

2.2. Free-Edge Cohesive Zone Model (FE-CZM)

The stress state at free-edges of a composite laminate under tension (Fig. 2) is three-dimensional (3D) [7]. However, a full 3D model that takes into account all the potential interfaces for delamination would be computationally costly. Therefore, this study is based on a 3D generalized plane-strain model [20] (Fig. 3), but with a very low computational time. This 3D generalized plane-strain model can be run in about 30 min in a standard desktop computer. Typically, generalized plane-strain is used to simulate the cross-section of a long structure that is free to expand or that is subjected to a loading perpendicular to the cross-section. The simulated cross-section lies between two planes that can move with respect to each other, and hence, cause an uniform strain in the perpendicular direction that varies linearly with respect to the position in between the planes. Therefore, three-dimensional effects and out-of-plane stresses are reasonably accounted for.

The boundary conditions, which obey the typical generalized plane-strain models [21], are given by the following displacement field:

$$\begin{cases} u(x,y,z)=\widetilde{u}(y,z)+\varepsilon_x\cdot L \\ v(x,y,z)=\widetilde{v}(y,z) \\ w(x,y,z)=\widetilde{w}(y,z) \end{cases} \tag{2}$$

where u, v and w are the displacements in the three directions of nodes located on the front plane, whereas $\widetilde{u}$, $\widetilde{v}$ and $\widetilde{w}$ are the displacements of nodes located on the rear plane. Moreover, symmetry conditions with respect to x–z plane are applied ($v=0$) [22,23] and all of the displacements at the bottom-center node are constrained ($u=v=w=0$) in order to avoid any free body movement.

A parametric code implemented in Python™ programming language generates the finite element model in ABAQUS [24]. One row of eight-noded quadrilateral elements (C3D8I) with linear shape functions and eight integration points were used to model the half cross section of the composite plate. The parametric code adds cohesive elements at each ply interface in

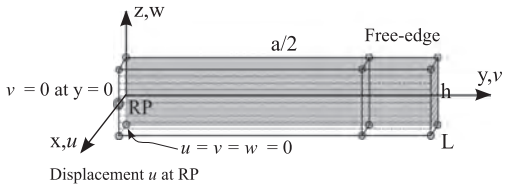

Fig. 3. Finite element model discretization (half cross section).

Please cite this article in press as: Guillamet G et al. A quick procedure to predict free-edge delamination in thin-ply laminates under tension. Engng Fract Mech (2016), http://dx.doi.org/10.1016/j.engfracmech.2016.01.019

order to predict free-edge delaminations. A cohesive zone model previously developed by the authors [15,17] is used in the simulations, implemented into ABAQUS by means of a user-written subroutine. This cohesive zone model predicts both delamination onset and propagation under mixed-mode loading conditions. The mixed-mode delamination ratio, B is defined as:

$$B = \frac{G_{shear}}{G_T} \tag{3}$$

where $G_T = G_I + G_{shear}$ is the energy release rate under mixed-mode loading conditions and $G_{shear} = G_{II} + G_{III}$ is the energy release rate for shear loading. The individual energy release rates are point-wise evaluated by computing the area under the cohesive law. The propagation criterion can be either a power law [25] or the Benzeggagh and Kenane [26]. For a more detailed description of the formulation, the reader is referred to [15].

It is worth to mention that a refined mesh is created at the free-edge in order to properly predict the onset and propagation [16].

2.2.1. Validation of the cohesive zone model

The validation of the FE-CZM has been performed by comparing its prediction with the experimental data and the analytical model proposed by O'Brien on a T300/5208 carbon reinforced composite [22]. In this study, a set of $[+45_n/-45_n/0_n/90_n]_S$ lay-ups with $n = 1, 2, 3$ resulting in 8-ply ($n = 1$), 16-ply ($n = 2$) and 24-ply ($n = 3$) laminates were loaded under tension and the critical load for free-edge delamination was determined. The elastic material properties as well as the interface properties of T300/5208 are summarized in Table 1. Assuming a mixed-mode power quadratic law criterion [25], the interface properties required by the cohesive zone model are: the critical fracture energies in mode I (G_{Ic}) and mode II (G_{IIc}); the maximum strengths in mode I (τ_3°) and shear (τ_{sh}°); and the penalty stiffness of the interface K (here taken as 10^6 N/mm^3 [16]). An element size of 0.01 mm in length and 2 elements through the ply thickness were used for each lay-up configuration.

With the aim of illustrating the effect on the interlaminar stresses when introducing cohesive elements at the interfaces, the results of two models, without (Fig. 4a) and with (Fig. 4b) cohesive elements, are compared. The interlaminar stresses ($\sigma_{zz}, \sigma_{xz}, \sigma_{yz}$) from the model without cohesive elements are compared to the cohesive tractions ($\tau_3, \tau_{13}, \tau_{23}$) from the model with cohesive elements. σ_{zz} and τ_3 are respectively delamination stress and traction in mode I; σ_{xz} and τ_{13} as well as σ_{yz} and τ_{23} are respectively delamination stresses and tractions in shear mode.

The observed stress singularities at the free-edges in Fig. 4a are relaxed through the use of cohesive elements (Fig. 4b) because of the generation of a failure process zone when the stresses overcome the interlaminar strength. An additional advantage of making use of cohesive elements is that they provide the mixed-mode delamination ratio. Results from O'Brien and the present FE-CZM indicate that the most critical interface for delamination is the 0/90 interface. Therefore, interlaminar stresses at this interface were determined for the three lay-ups ($n = 1, 2, 3$) so as to study the effect of the ply thickness (Fig. 5). The results follow a clear trend, because as the ply thickness increases the interlaminar stresses also increase, resulting in an early free-edge delamination when compared to thinner plies.

The critical strain for free-edge delamination for the three lay-up configurations is shown in Fig. 6. The experimental data and the analytical model proposed by O'Brien [22] are compared with the results of the proposed model. It can be observed that the results obtained by the FE-CZM are in good agreement with those of O'Brien. Moreover, it is worth noting that the FE-CZM, takes into account the delamination state at all interfaces of the lay-up in comparison to the O'Brien formulation which only takes into account one interface.

3. Free-edge delamination predictions

Once the proposed methodology has been validated, it is then applied to two case studies. The first case study deals with the effect of ply thickness (standard- and thin-plies) on the critical strain for free-edge delamination. The second case study consists of predicting the free-edge delamination in a thin-ply NCF lay-up under different off-axis loadings, corresponding to the experimental study previously published by the authors [3]. This lay-up was devised so that a THIN region could be differentiated from a THICK region, where plies were clustered.

3.1. Effect of the ply thickness in standard- and thin-ply laminates

3.1.1. Experimental results

Free-edge delamination was evaluated by optically monitoring the specimen at the free-edge. The standard-ply lay-up, $[90/\pm 45/90_2/\pm 45/90]_S$, was made up of 16 unidirectional plies of 0.187 mm resulting in a nominal total laminate thickness of 3 mm. The thin-ply lay-up, $[(90/45)/(-45/90)]_{6S}$, was made up of 24 bi-axial plies (48 unidirectional plies) with a nominal ply thickness of 0.08 mm resulting in a total laminate thickness of 3.8 mm. It is important to point out that this lay-up is not symmetric in terms of unidirectional plies, but is symmetric in terms of bi-angle layers, see ply distribution in Fig. 8b. Despite of not being symmetric in terms of unidirectional plies the laminate coupling matrix is null ($B_{ij} = 0$). Two different materials were used for each lay-up, unidirectional prepreg with carbon/epoxy system T800S/M21 (standard-ply

Please cite this article in press as: Guillamet G et al. A quick procedure to predict free-edge delamination in thin-ply laminates under tension. Engng Fract Mech (2016), http://dx.doi.org/10.1016/j.engfracmech.2016.01.019

Table 1
Material properties for T300/5208 [22].

Elastic	E_{11} (GPa) 138	$E_{22} = E_{33}$ (GPa) 15	$\nu_{12} = \nu_{13} = \nu_{23}$ (–) 0.21	$G_{12} = G_{13} = G_{23}$ (GPa) 5.90
Interface	G_{Ic} (kJ/m^2) 0.088[b]	G_{IIc} (kJ/m^2) 0.154[b]	τ_3° (MPa) 40.7	τ_{sh}° (MPa) 53.81[a]

[a] Calculated base on the relations in [17].
[b] Ref. [27].

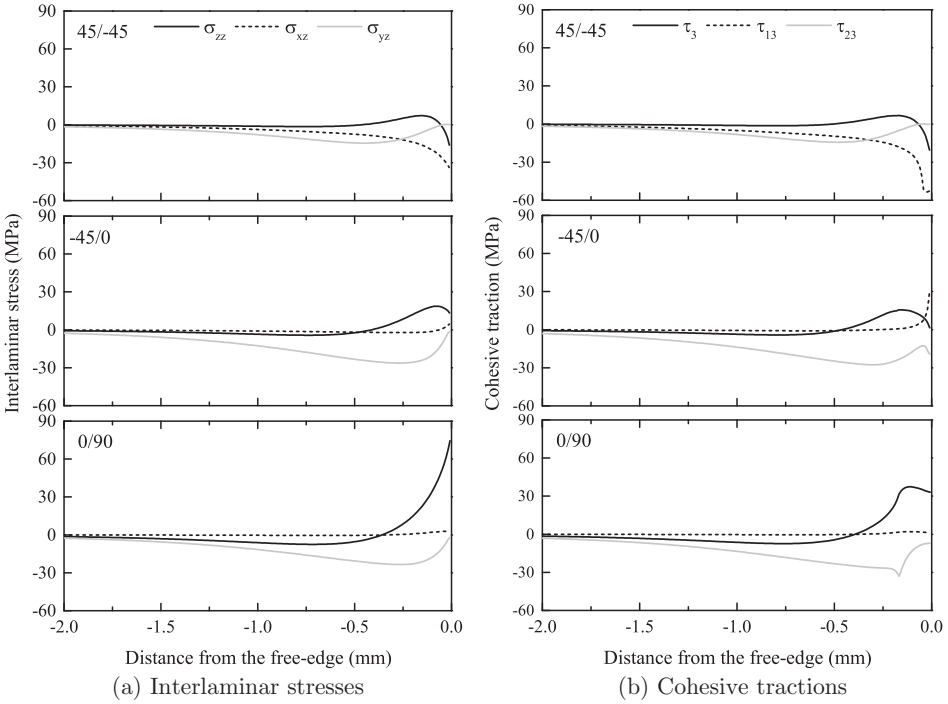

Fig. 4. Stress state at each interface for 8-ply lay-up $n = 1$ (applied strain 0.5%).

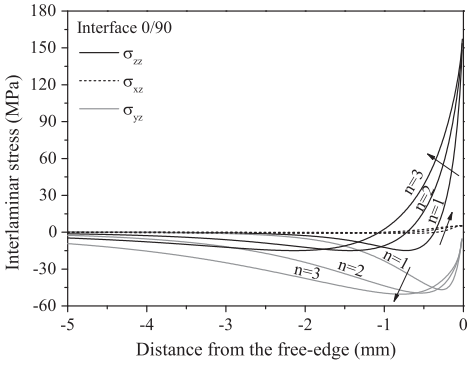

Fig. 5. Interlaminar stresses at 0/90 interface with an applied strain of 1.0%.

Please cite this article in press as: Guillamet G et al. A quick procedure to predict free-edge delamination in thin-ply laminates under tension. Engng Fract Mech (2016), http://dx.doi.org/10.1016/j.engfracmech.2016.01.019

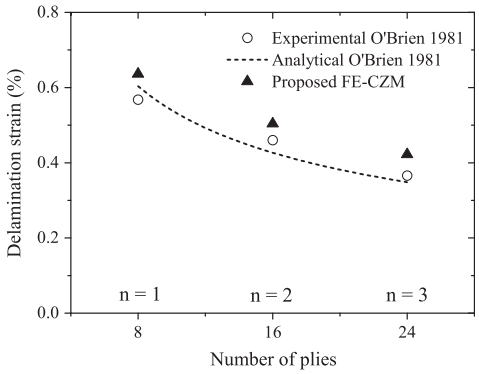

Fig. 6. Free-edge delamination prediction compared with $[+45_n/-45_n/0_n/90_n]_s$ (n = 1, 2, 3) data.

layup) provided by Hexcel and C-ply Non-Crimp-Fabric (NCF) T700/AR-2527 (thin-ply lay-up) provided by Chomarat. The properties of each material are summarized in Tables 2 and 3. Although they are not the same materials, nor do they have the same laminate thickness, they provide an insight into free-edge delamination response as a function of the ply thickness and, overall, this case represents a good benchmark case for the methodology presented.

The damage occurrence at the edge of both lay-ups is represented in Fig. 7 at different strain loads. First of all, matrix cracking occurs at clustered plies oriented at 90_2 for both configurations (more easily observable in the standard-ply laminate). This occurs at different strains in each material. Indeed, transverse cracking is clearly visible at 1.5% strain in the standard-ply laminate, whereas at this strain level there is no evidence for the thin-ply laminate, Fig. 7. The interfaces adjacent to the 90_2 clustered plies seems to behave as the most critical interfaces for delamination (it is observable at 2.12%). Regarding the thin-ply laminate, the critical delamination occurs at the outermost clustered ply of 90_2, see Fig. 8 for the ply distribution. Although interfaces in the thin-ply lay-up are difficult to identify on this scale, the most critical ones are located at the top of the lay-up, see Fig. 7b. Therefore, these results suggest that MCID is the main source of delamination for both ply configurations, i.e. clustered plies oriented at 90° trigger delaminations at the adjacent interfaces.

3.1.2. Predictions

The free-edge delamination in these two lay-ups was evaluated using the FE-CZM and the MCID-FC. According to the curing temperature of each material (Tables 2 and 3) a thermal jump of −156° and −123° was respectively applied to the standard-ply and thin-ply lay-ups prior to any mechanical load, in order to model the effect of residual stresses from the manufacturing process. The numerical prediction, as well as the experimental results from both configurations, are summarized in Table 4.

The FE-CZM and the MCID-FC predict that delamination will occur at the interfaces adjacent to 90_2 cluster for both lay-ups, in agreement with the experimental results. The influence of the ply clustering and/or ply thickness is captured by both models and the maximum difference between the numerical prediction and the experimental value is 3% for the standard-ply lay-up and lower than 18% for the thin-ply lay-up.

The FE-CZM predicts a mixed mode ratio of around 100% for both lay-up configurations, indicating that delamination takes place under a pure shear mode (Table 4). This fact is consistent with the deformed shape at the free-edge for both lay-ups (Fig. 8).

3.2. Thin-ply NCF lay-up under off-axis loading

A lay-up designed to have two regions through the laminate thickness, namely THICK and THIN regions (with and without ply clustering) is analyzed in this section. The lay-up is a $\pi/4$ quasi-isotropic laminate $[(0/-45)/(45/0)/(90/45)/(-45/90)]_S$ composed of 16 unidirectional plies (8 bi-angle layers) with a nominal ply thickness of 0.08 mm and a total nominal laminate thickness of 1.3 mm. Once again, the ply configuration is not symmetric in terms of unidirectional plies, but is symmetric in terms of each bi-angle layer. Despite of not being symmetric in terms of unidirectional plies, see Table 5, the laminate coupling matrix is also null ($B_{ij} = 0$). The material properties of this lay-up are summarized in Table 3. Moreover, the effect of the off-axis loading on the tensile strength of the lay-up is also analyzed. Five off-axis loads under tension are studied by rotating the specimen over the panel at 0°, −22.5°, −45°, −67.5°, and 90°, resulting in five different ply sequences, as shown in Table 5.

The experimental results, which were reported by the authors in a previous paper [3], focused on the damage occurrence and damage progression at the free-edge.

Please cite this article in press as: Guillamet G et al. A quick procedure to predict free-edge delamination in thin-ply laminates under tension. Engng Fract Mech (2016), http://dx.doi.org/10.1016/j.engfracmech.2016.01.019

Table 2
Material properties for T800S/M21 [28].

Elastic	E_{11} (GPa)	$E_{22} = E_{33}$ (GPa)	$G_{12} = G_{13}$ (GPa)	G_{23} (GPa)	$\nu_{12} = \nu_{13}$ (–)	ν_{23} (–)
	134.7	7.7	4.2	2.5	0.369	0.45
Interface	G_{Ic} (kJ/m^2)	G_{IIc} (kJ/m^2)	τ_3° (MPa)	τ_{sh}° (MPa)	η_{B-K} (–)	
	0.246	0.742	41.43[b]	68.68[a]	1.7	
Thermal	α_{11} (°C^{-1})	$\alpha_{22} = \alpha_{33}$ (°C^{-1})	T_{cured} (°C)	T_{room} (°C)		
	-0.308×10^{-6}	31.8×10^{-6}	180	24		

[a] Calculated base on equations in [17].
[b] Assumed as equal as Y_T.

Table 3
Material properties for T700/AR-2527 [6].

Elastic	E_{11} (GPa)	$E_{22} = E_{33}$ (GPa)	$G_{12} = G_{13}$ (GPa)	G_{23} (GPa)	$\nu_{12} = \nu_{13}$ (–)	ν_{23} (–)
	110	7.4	4.2	2.6	0.3	0.45
Strength	Y_T (MPa)	Y_{BT} (MPa)	S_L (MPa)	α_o (°)	β (–)	
	66	41[c]	93	53	5×10^{-8}	
Interface	G_{Ic} (kJ/m^2)	G_{IIc} (kJ/m^2)	τ_3° (MPa)	τ_{sh}° (MPa)	η_{B-K} (–)	
	0.227	0.636	66.0[b]	110.5[a]	1.3	
Thermal	α_{11} (°C^{-1})	$\alpha_{22} = \alpha_{33}$ (°C^{-1})	T_{cured} (°)	T_{room} (°)		
	-0.23×10^{-6}[d]	38.7×10^{-6}[d]	143	20		

[a] Calculated base on equations in [17].
[b] Assumed as equal as Y_T.
[c] Assumed based on [29].
[d] Assumed based on [30].

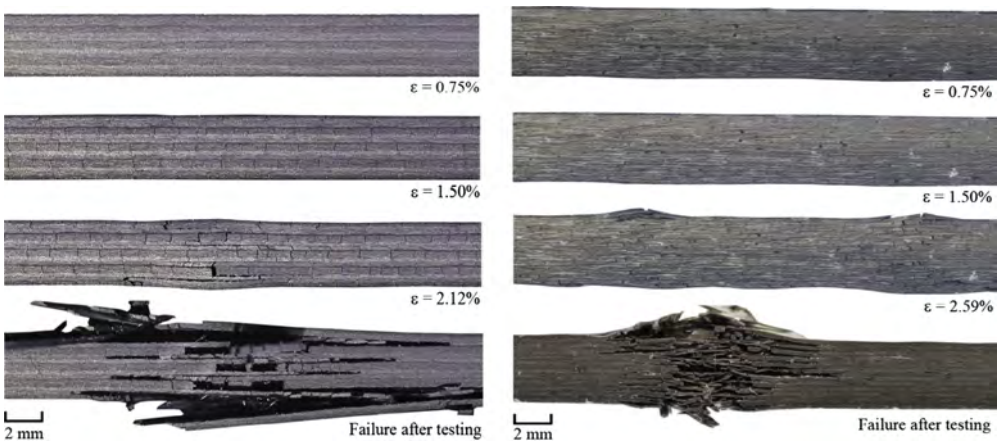

(a) Standard-ply laminate (b) Thin-ply laminate

Fig. 7. Free-edge damage of standard- and thin-ply laminates.

3.2.1. In situ strength effect

In order to illustrate the effect of ply thickness in a given lay-up, the in situ strength theories [10], which predict a decrease on the ply strength as ply thickness increases, are used as a preliminary analysis. In situ strengths are calculated for the two ply regions of the lay-up using material properties in Table 3: thin embedded plies (THIN-region) and thick embedded plies (THICK-region) (Table 6). The calculated in situ strengths are: the transverse strength Y_T^{is}; the longitudinal and transverse shear strengths S_L^{is} and S_T^{is} ; and the bi-axial transverse strength Y_{BT}^{is}. Note that, only strengths for transverse tension are taken into account because this is the predominant failure mode when the lay-up is loaded under tension.

The critical stress of the laminate (σ_c°) for which matrix cracking is first observed is presented in Table 7. σ_c° is calculated using Classical Lamination Theory (CLT) [18] together with a recent failure criteria formulated by Camanho et al. [29,32] that

Please cite this article in press as: Guillamet G et al. A quick procedure to predict free-edge delamination in thin-ply laminates under tension. Engng Fract Mech (2016), http://dx.doi.org/10.1016/j.engfracmech.2016.01.019

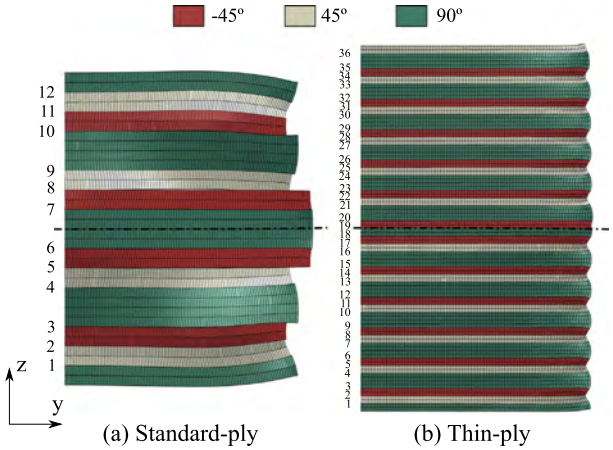

Fig. 8. Ply distribution and lay-up deformed shapes with an applied strain of 1.6% (deformed scale factor of 15).

Table 4
Laminate strains for free-edge delamination at adjacent interfaces of 90_2 ply.

Lay-up	Experimental			Prediction				
	MCID strain (%)	FED strain (%)	Ultimate failure strain (%)	MCID-FC strain (%)	Difference (%)	Mixed mode ratio (%)	FE-CZM strain (%)	Difference (%)
Standard-ply	1.65	2.08	2.12	1.70	+3	100	2.01	−3
Thin-ply	2.20	2.20	2.59	2.42	+10	98	2.58	+17

Table 5
Laminate stacking sequences for each off-axis loading. In bold ply clustered plies considered as the THICK-region of the lay-up.

Ref.	Rot. (°)	Laminate stacking sequence with respect to the load direction
L0	0	[(0/ − 45)/(45/0)/(90/45)/(−45/90)/(−45/**90**)/(**90**/**45**)/(**45**/**0**)/(**0**/ − 45)]
L23	−22.5	[(22.5/ − 22.5)/(67.5/22.5)/(−67.5/67.5)/(−22.5/ − 67.5)/(−22.5/ − **67.5**)/(−**67.5**/**67.5**)/(**67.5**/**22.5**)/(**22.5**/ − 22.5)]
L45	−45	[(45/0)/(90/45)/(−45/90)/(0/ − 45)/(0/ − **45**)/(−**45**/**90**)/(**90**/**45**)/(**45**/0)]
L68	−67.5	[(67.5/22.5)/(−67.5/67.5)/(−22.5/ − 67.5)/(22.5/ − 22.5)/(22.5/ − **22.5**)/(−**22.5**/ − **67.5**)/(−**67.5**/**67.5**)/(**67.5**/22.5)]
L90	90	[(90/45)/(−45/90)/(0/ − 45)/(45/0)/(45/**0**)/(**0**/ − **45**)/(−**45**/**90**)/(**90**/45)]

Table 6
Calculated in situ strengths for T700/AR-2527.

Ply configuration	Y_T^{is} (MPa)[a]	S_L^{is} (MPa)[a]	S_T^{is} (MPa)[b]	Y_{BT}^{is} (MPa)[b]
Thin embedded ply	164.0	122.1	187.4	94.5
Thick embedded ply (2t)	116.0	113.1	138.3	65.8

[a] Ref. Camanho et al. (2006) and Maimí et al. (2013) [10,31].
[b] Ref. Camanho et al. (2015) [32] considering a shear response factor $\beta = 5 \times 10^{-10}$.

Table 7
Laminate stresses (σ_c°) and in situ laminate strength ratio (η_{is}°) for transverse cracking between regions.

Ref.	THICK region		THIN region		Experimental η_{is}°	Predicted η_{is}°
	Analytical σ_c° (MPa)	Experimental σ_c° (MPa)	Analytical σ_c° (MPa)	Experimental σ_c° (MPa)		
L0	528.6	445	732.3	556	1.25	1.38
L23	521.4	319	729.6	394	1.24	1.40
L45	528.6	467	732.3	–	–	1.38
L68	521.4	399	729.6	566	1.42	1.40
L90	528.6	520	732.3	699	1.34	1.38

Please cite this article in press as: Guillamet G et al. A quick procedure to predict free-edge delamination in thin-ply laminates under tension. Engng Fract Mech (2016), http://dx.doi.org/10.1016/j.engfracmech.2016.01.019

takes into account the effect of the ply thickness and ply location at lamina level. In order to show the increase in strength between the two regions, the in situ laminate strength ratio (η_{is}°) is calculated as the quotient of the laminate stress at THIN region divided by the laminate stress at THICK region.

First of all, the predicted stress for transverse cracking at the THICK region is lower than that of the THIN region (Table 7), which is in agreement with the experimental results [3]. However, the predictions of the failure criteria over-predict the experimentally observed stress for transverse cracking. The fact that CLT does not take into account the stress distribution at free-edges, thus underestimates the stresses in this region, is the most plausible explanation [8]. In addition, the stress prediction for transverse cracking using CLT depends only on the ply orientation. Hence, lay-ups loaded on-axis (L0, L45 and L90) or lay-ups loaded off-axis (L23 and L68) result in the same laminate stress for transverse cracking.

Despite the aforementioned over-prediction on the onset stresses for transverse cracking at the free-edge, the in-situ strength ratio, η_{is}°, exhibits a reasonable agreement between predictions and experiments (Table 7).

3.2.2. Predictions

The critical strain for free-edge delamination, triggered by matrix cracks or due to interlaminar normal and shear stresses, has been calculated for each lay-up using the MCID-FC and the FE-CZM. The critical strain appearing in Table 8 was taken as the minimum value between both phenomena. The observed phenomenology is that when transverse cracking occurs and the adjacent interfaces have a significant shear delamination mode, it is MCID that is driving delamination growth. However, to the contrary, when the mode I component is significant, free-edge delamination caused by out-of-plane stresses is predominant (FED).

The results presented in Table 8 indicate that MCID is the predominant failure mechanism in most of the lay-ups, which means that delamination occurs in shear mode rather than mode I. The plies where delaminations first appear are correctly predicted by the failure criteria, e.g. interfaces of plies oriented at 90° and ±67.5° [3]. Mixed mode delamination ratios are also calculated for each lay-up at each interface using the FE-CZM, see Table 9. Note that, mixed mode ratios are calculated for a low applied strain (0.1%) at which cohesive elements are not damaged. Increasing the load, the mixed mode ratio may evolve due to the damage generated. These predicted ratios confirm that most of the interfaces are loaded in shear, so MCID failure mechanism is predominant over mode I FED, for the proposed lay-ups.

In agreement with the experimental observations, the numerical model predicts a delay on the free-edge delamination at the THIN region with respect to the THICK one. In the THICK region, where ply clustering is present, interlaminar stresses are higher in addition to the lower in situ strengths which, in turn, trigger damage mechanisms such as premature matrix cracking and delamination. In some cases, the prediction of the strain for free-edge delamination at THIN region is close to the ultimate failure of the lay-up (L0 and L90) or it is even above the experimental ultimate failure, that is, free-edge delamination is practically suppressed (L45 in Table 8).

The proposed numerical model quantitatively captures the effect of the ply location and ply thickness and reasonably predicts the onset strain for free-edge delamination, with differences below 31%. The greater differences (e.g. lay-ups L0, L45 or L90) can be attributed to the interaction among delaminations triggered by matrix cracks and the, next to appear, delaminations originated by mode I interlaminar stresses. It is timely to state that both phenomena are dealt with independently in the current theoretical approach. If the computational cost was not a concern, advanced models including progressive intralaminar and interlaminar damages could be considered to obtain more accurate predictions.

The effect of off-axis loads on the onset strain for free-edge delamination was also analyzed. The deformed shapes at the free-edge of each lay-up are presented in Fig. 9. It should be noted that the deformed shapes as well as the mixed mode ratios in Table 9, are calculated under the same applied strain. These shapes illustrate the differences in the free-edge behavior for the studied lay-ups and, in turn, provide a qualitative explanation for the high anisotropy in strength experimentally observed (Table 8).

Fig. 9 also shows that as the loading direction changes from 0° (L0) to 90° (L90), the shear delamination mode becomes more dominant throughout the interfaces. For instance, some interfaces of lay-ups L0, L23 and L45 exhibit mixed mode ratios

Table 8
Delamination strains in (%) at THICK and THIN regions.

Ref.	Ultimate failure [3]	THICK region				THIN region			
		Int.	Experimental [3]	Numerical prediction	Difference (%)	Int.	Experimental [3]	Numerical prediction	Difference (%)
L0	1.897	9	1.181†, 1.267*	1.586*	+25	8	1.410*	1.798*	+28
L23	1.360	11, 12	0.953†	0.825†	−13	1	1.154†	1.110†	−4
L45	1.389	11, 12	1.350†	1.750†	+30	4	–	2.102*	–
L68	1.491	9, 12	1.204†	1.140†	−5	1, 2	1.468†	1.535†	+5
L90	2.344	11, 12	1.516†,1.647*	1.700†	+12	2	1.803*	2.200*	+22

* FED.
† MCID.

Please cite this article in press as: Guillamet G et al. A quick procedure to predict free-edge delamination in thin-ply laminates under tension. Engng Fract Mech (2016), http://dx.doi.org/10.1016/j.engfracmech.2016.01.019

Table 9
Mixed mode ratios calculated at the free-edge for each interface (applied strain of 0.1%). In bold critical interfaces for delamination.

Ref./Int.	THIN region								THICK region			
	1	2	3	4	5	6	7	8	9	10	11	12
L0	89	93	100	75	78	99	81	**78**	**77**	73	100	100
L23	**100**	73	89	88	64	92	94	93	92	59	**78**	**100**
L45	100	78	84	**100**	86	82	100	100	100	77	**71**	**92**
L68	**100**	**100**	90	98	99	97	100	100	**100**	94	72	**85**
L90	100	**100**	96	91	100	100	100	100	100	100	**88**	**86**

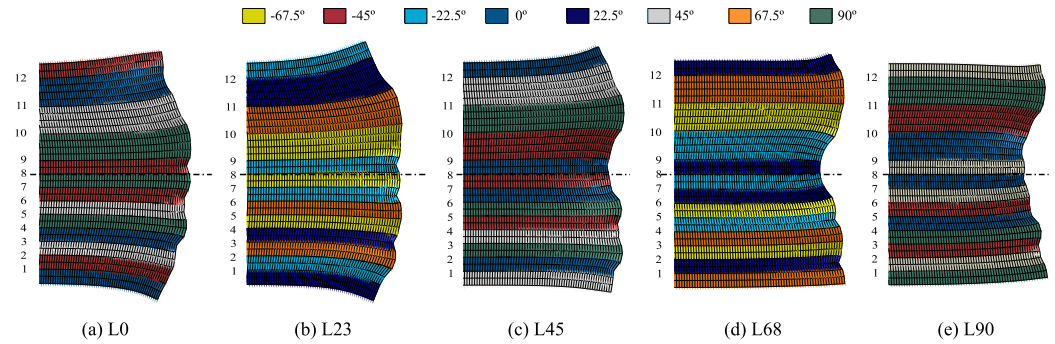

Fig. 9. Off-axis deformed shapes using an applied strain of 0.1% (deformed scale factor of 50).

close to 50%, resulting free-edge delaminations at both delamination modes. This behavior was also observed in the experimental results for both lay-ups. On the contrary, in the remaining lay-ups most of the interfaces have mixed mode delamination ratios close to 100%, resulting in free-edge delaminations originated in almost pure shear mode.

4. Conclusions

A numerical analysis of the free-edge delamination for thin-ply laminates is performed taking into account two sources of delaminations: Matrix Crack Induced Delaminations (MCID) and free-edge delaminations due to interlaminar normal or shear stresses (FED). The first delamination mechanism is accounted for by means of an analytical failure criterion (MCID-FC) and Classical Lamination Theory (CLT), whereas the second mechanism is dealt with using a Free-Edge Cohesive Zone Model (FE-CZM) in a finite element method framework.

This approach is first validated by making use of existing published results. Then, the free-edge delamination on two similar lay-ups of different ply thicknesses (standard and thin) demonstrates a significant improvement in delamination resistance at the free-edge in thin plies. The deviation in the numerical prediction of the critical strains for delamination with respect to the experimental results is 3% for the standard-ply laminate and below 18% for the thin-ply lay-up.

Then, a series of non-crimp fabric lay-ups under off-axis loads that had been experimentally investigated in a previous work, were analyzed by means of MCID and FED. The lay-ups were devised so that a THIN region could be distinguished from a THICK region (where plies are clustered). The numerical results show the same trend observed in the experimental results: a clear delay in the onset of free-edge delaminations at the THIN region with respect to the THICK region. The failure criteria for MCID and the numerical model for FED contribute to a better understanding of the effect of ply thickness and the effect of off-axis loads on the appearance of the mixed mode at the interfaces.

The difficulties in obtaining accurate predictions of free-edge delamination in thin-ply regions of the laminate arise from the fact that the two phenomena (transverse crack triggered delamination and delamination due to interlaminar normal and shear stresses) interact, however the theoretical approaches used consider them independently.

The present analysis is intended to support the understanding of the effect of ply thickness on free-edge behavior. It is demonstrated that the proposed models appear to be useful tools for quantitatively predicting the delamination at free-edges by taking into account the effect of the ply thickness, the ply location and the mixed mode ratio at interfaces. In addition, they provide a good equilibrium between predictive capabilities and computational effort.

Acknowledgements

The authors acknowledge the financial support of the Spanish government through the *Ministerio de Economía y Competitividad* under the contracts DPI2012-34465 and MAT2012-37552-C03-03, which is partially funded by the FEDER funds of

the EC. The first author acknowledges the support of the *Generalitat de Catalunya* with the pre-doctoral grant FI-DGR (2014FI_B1 00123). The company CHOMARAT (Ardèche, France) is acknowledged for providing the NCF material and Aldila (Poway, California, USA) for the epoxy system pre-preg. The company AIRBUS partially funded this work through the 2genCOMP project.

References

[1] Sihn S, Kim R, Kawabe K, Tsai S. Experimental studies of thin-ply laminated composites. Compos Sci Technol 2007;67(6):996–1008.
[2] Arteiro A, Catalanotti G, Xavier J, Camanho P. Notched response of non-crimp fabric thin-ply laminates. Compos Sci Technol 2013;79:97–114.
[3] Guillamet G, Turon A, Costa J, Renart J, Linde P, Mayugo J. Damage occurrence at edges of non-crimp-fabric thin-ply laminates under off-axis uniaxial loading. Compos Sci Technol 2014;98:44–50.
[4] Amacher R, Cugnoni J, Botsis J, Sorensen L, Smith W, Dransfeld C. Thin ply composites: experimental characterization and modeling of size-effects. Compos Sci Technol 2014;101:121–32.
[5] Roure T, Sanial P. C-PLY, a new structural approach to multiaxials in composites. JEC Compos Mag 2011;68:53–4.
[6] Arteiro A, Catalanotti G, Xavier J, Camanho P. Notched response of non-crimp fabric thin-ply laminates: analysis methods. Compos Sci Technol 2013;88:165–71.
[7] Herakovich C. Free-edge effects in laminated composites: 1976–2006. In: 25th Technical conference of the American society for composites and 14th US–Japan conference on composite materials, vol. 1. Dayton, OH, United States; 2010. p. 22–37.
[8] Johnson P, Chang FK. Characterization of matrix crack-induced laminate failure—Part I: Experiments. J Compos Mater 2001;35(22):2009–35.
[9] Hallett SR, Jiang WG, Khan B, Wisnom MR. Modelling the interaction between matrix cracks and delamination damage in scaled quasi-isotropic specimens. Compos Sci Technol 2008;68(1):80–9.
[10] Camanho PP, Dávila CG, Pinho ST, Iannucci L, Robinson P. Prediction of in situ strengths and matrix cracking in composites under transverse tension and in-plane shear. Compos Part A: Appl Sci Manuf 2006;37(2):165–76.
[11] Dávila CG, Camanho PP, Rose CA. Failure criteria for FRP laminates. J Compos Mater 2005;39(4):323–45.
[12] Catalanotti G, Camanho P, Marques A. Three-dimensional failure criteria for fiber-reinforced laminates. Compos Struct 2013;95:63–79.
[13] Arteiro A, Catalanotti G, Melro A, Linde P, Camanho P. Micro-mechanical analysis of the in situ effect in polymer composite laminates. Compos Struct 2014;116:827–40.
[14] Zubillaga L, Turon A, Maimí P, Costa J, Mahdi S, Linde P. An energy based failure criterion for matrix crack induced delamination in laminated composite structures. Compos Struct 2014;112:339–44.
[15] Turon A, Camanho P, Costa J, Dávila C. A damage model for the simulation of delamination in advanced composites under variable-mode loading. Mech Mater 2006;38(11):1072–89.
[16] Turon A, Dávila C, Camanho P, Costa J. An engineering solution for mesh size effects in the simulation of delamination using cohesive zone models. Engng Fract Mech 2007;74(10):1665–82.
[17] Turon A, Camanho P, Costa J, Renart J. Accurate simulation of delamination growth under mixed-mode loading using cohesive elements: definition of interlaminar strengths and elastic stiffness. Compos Struct 2010;92(8):1857–64.
[18] Herakovich C. Mechanics of fibrous composites; 1997.
[19] Zubillaga L, Turon A, Renart J, Costa J, Linde P. An experimental study on matrix crack induced delamination in composite laminates. Compos Struct 2015;127:10–7.
[20] Krueger R, Paris IL, Kevin O'Brien T, Minguet PJ. Comparison of 2D finite element modeling assumptions with results from 3D analysis for composite skin-stiffener debonding. Compos Struct 2002;57(1–4):161–8.
[21] Pipes R, Pagano N. Interlaminar stresses in composite laminates under uniform axial extension. J Compos Mater 1970;4:538.
[22] Kevin O'Brien T. Characterization of delamination onset and growth in a composite laminate. Tech rep. National Aeronautics and Space Administration (NASA), Hampton, Virgina, USA; 1981.
[23] Martin E, Leguillon D, Carrère N. A twofold strength and toughness criterion for the onset of free-edge shear delamination in angle-ply laminates. Int J Solids Struct 2010;47(9):1297–305.
[24] Abaqus 6.12 Analysis User's Manual, vol. I. Providence, RI, USA; 2012.
[25] Wu EM, Reuter Jr RC. Crack extension in fiberglass reinforced plastics, Report No. 275, University of Illinois; 1965.
[26] Benzeggagh ML, Kenane M. Measurement of mixed-mode delamination fracture toughness of unidirectional glass/epoxy composites with mixed-mode bending apparatus. Compos Sci Technol 1996;56(4):439–49.
[27] Ramkumar R. Performance of quantitative study of instability – related delamination growth. Tech rep. National Aeronautics and Space Administration (NASA), Hampton, Virgina, USA; 1983.
[28] Marín L, Trias D, Badalló P, Rus G, Mayugo J. Optimization of composite stiffened panels under mechanical and hygrothermal loads using neural networks and genetic algorithms. Compos Struct 2012;94(11):3321–6.
[29] Camanho P, Arteiro A, Melro A, Catalanotti G, Vogler M. Three-dimensional invariant-based failure criteria for fibre-reinforced composites. Int J Solids Struct 2014;55:92–107.
[30] Mulle M, Collombet F, Olivier P, Zitoune R, Huchette C, Laurin F, et al. Assessment of cure-residual strains through the thickness of carbon-epoxy laminates using FBGs. Part II: Technological specimen. Compos Part A: Appl Sci Manuf 2009;40(10):1534–44.
[31] Maimí P, González E, Camanho P. Comment to the paper 'Analysis of progressive matrix cracking in composite laminates II. First ply failure' by George J Dvorak and Norman Laws. J Compos Mater 2013;48(9):1139–41.
[32] Camanho P, Arteiro A, Catalanotti G, Melro A, Vogler M. Three-dimensional invariant-based failure criteria for transversely isotropic fibre-reinforced composites. In: Camanho P, Hallett S, editors. Numerical modelling of failure in advanced composite materials. Woodhead Publishing; 2015. p. 111–50 [chapter 5].

Please cite this article in press as: Guillamet G et al. A quick procedure to predict free-edge delamination in thin-ply laminates under tension. Engng Fract Mech (2016), http://dx.doi.org/10.1016/j.engfracmech.2016.01.019

Paper C

In search of the quasi-isotropic laminate with optimal delamination resistance under off-axis loads. Effect of the ply sequence and of using thin plies

G. Guillamet[a], J. Costa[a], A. Turon[a], J.A. Mayugo[a], P. Linde[b]
[a]AMADE, Polytechnic School, Universitat de Girona, Campus Montilivi s/n, 17071 Girona, Spain
[b]Airbus Operations GmbH, Kreetslag 10, 21129 Hamburg, Germany

The paper has been submitted to
Composites Part A: Applied Science and Manufacturing.

Embargoed until publication

G. Guillamet, J. Costa, A. Turon, J.A. Mayugo, P. Linde, ”In search of the quasi-isotropic laminate with optimal delamination resistance under off-axis loads. Effect of the ply sequence and of using thin plies”. Manuscript submitted for publication

Abstract

Delamination is one of the most feared failure modes in laminated composites and yet there is a lack of well established procedures to find the ply configuration with the highest delamination resistance for a given geometry of the component and a set of elastic and strength constraints. This paper presents a methodology for determining the quasi-isotropic ply sequence more resistant to delamination under off-axis uniaxial tension. Delamination is considered to be triggered by interlaminar stresses at free-edges or by matrix cracks. Two ply thicknesses (standard and thin) and two set of ply orientations (multiples of p/4 or p/8) are considered. The results show that the use of thin-plies enlarges the design domain by up to 70% and generates a practically isotropic safe space. The methodology presented is also suitable to optimize the delamination resistance of other load cases with stress singularities.

SUMMARY

The overall purpose of this Ph.D. thesis has been to demonstrate the potential benefits of thin-ply based laminates in terms of delamination resistance and to propose predictive tools for their design. The thesis is made up of three refereed journal papers:

Paper A analyses the occurrence and the sequence of damage mechanisms at the free-edge of a thin-ply based laminate by conducting an experimental campaign on tensile tests.

Paper B evaluates the capability of two current and advanced design procedures (a failure criterion for matrix crack induced delamination and cohesive elements) for predicting delamination at the free-edges of thin-ply laminates.

Paper C presents an optimization procedure for seeking quasi-isotropics lay-ups optimized in terms of free-edge delamination under different off-axis loading directions.

AMADE
ANALYSIS AND ADVANCED MATERIALS
FOR STRUCTURAL DESIGN